Mathematical modelling and analysis of unsteady poroelastohydrodynamics for an in-vivo type solid tumour

Meraj Alam[1*], Bibaswan Dey[2], Helen Byrne[3], G. P. Raja Sekhar[4]

[1*]Department of Mathematics, Mahindra University, Hyderabad, 500043, Telangana, India.
[2]University of North Bengal, Raja Rammohunpur, Darjeeling, 734013, West Bengal, India.
[3]Mathematical Institute, University of Oxford, Oxford, OX2 6GG, United Kingdom.
[4]Department of Mathematics, Indian Institute of Technology Kharagpur, Kharagpur, 721302, West Bengal, India.

*Corresponding author(s). E-mail(s): merajalam113@gmail.com;
Contributing authors: bibaswan287@gmail.com;
helen.byrne@maths.ox.ac.uk; rajas@iitkgp.ac.in;

Abstract

This study presents a mathematical model that describes the unsteady interstitial fluid percolation through a solid tumour and its surrounding healthy tissue, as well as the deformation of the cellular phase of the solid tumour and healthy tissue. The tumour and its healthy host are assumed to be connected via a smooth, fixed interface. Each of these tissue regions comprises interstitial fluid and solid constituents (i.e., tumour cells and extracellular matrix). The general mixture theory equations are adopted to represent conservation of mass and momentum in each tissue region. The fluid phase is modelled as an incompressible Newtonian fluid, and the solid phase as an isotropic deformable porous material. The governing equations are of mixed parabolic-hyperbolic type. We assume continuity of the interface fluid velocity (IFV), the solid-phase displacement (SPD), and the normal stress at the host-tumour interface, along with the Beavers-Joseph-Saffman condition. We establish well-posedness in a weak sense for the unsteady governing system using a Galerkin method and weak convergence. We then focus on calculating the system energy using the velocity fields of the fluid and solid components of the tumour and its host. The energy estimates in the context of

well-posedness yield the maximum system energy (MASE), and the minimum system energy is computed from the definitions of the $\boldsymbol{L^2}$ and $\boldsymbol{H^1}$ norms using the 1D solution of the governing equations. The system energy assists in ranking the viability of five types of tumours associated with five distinct carcinomas.

Keywords: Biphasic mixture theory, Weak formulation, Semi-discrete Galerkin method, System energies, Well-posedness

MSC Classification: 76Txx , 76Zxx , 35Q74 , 35D30 , 35C10

1 Introduction

Understanding how interstitial fluid (IF) flow and solid deformation in porous materials are coupled is a classical problem in geomechanics and soft tissue mechanics [1, 2, 5]. Several recent studies have used the theory of mixtures to study dynamic transport processes associated with interstitial fluid percolation and the solid phase (cells, Extracellular Matrix (ECM), etc.) deformation inside solid tumours [3–6, 11]. In this study, we focus on the mathematical modelling and analysis of the coupled problem of interstitial fluid flow and deformation of cell populations and the extracellular matrix (ECM) in the context of solid tumours.

The internal structure of tumours is complex and becomes a critical character of the type of tumour and its impact. Typically, living, functioning cancer cells within a tumour that are capable of metabolizing, proliferating, and potentially spreading indicate the viability of a tumour. Hence, any estimates of these internal activities would provide useful insights, reduce the number of animal experiments, and identify new experimental programs and improved treatment strategies [12]. To achieve this goal, we model tumour dynamics using mixture-theory-based governing equations, where the interstitial fluid flow constitutes one phase and the solid tissue the other.

There is extensive literature focused on using multiphase mixture theory to model tumour dynamics [6, 13–16]. Within this framework, variations in the density of the constituent phases may be explained. The impact of phase interactions on the mechanical stresses that develop within biological tissues can be investigated [16]. In brief, there are two main types of continuum models based on mixture theory in the context of tumour biology. One approach focuses on situations where the tumour cell volume density evolves and the time scale of interest is long. On this timescale, the tumour constituents can be described as a fluid [14, 17, 18]. The second approach focuses on interstitial hydrodynamics, the transport of blood-borne solutes (e.g., nutrients and drug molecules) and their metabolism inside a tumour [5, 6, 19]. These processes typically act on short timescales (on the order of seconds). The cell population (CP) and the extracellular matrix (ECM) respond to hydrodynamic drag as an elastic material on short timescales. Therefore, the CP and ECM, together or separately, can be viewed as solid continua, whereas the interstitial fluid (IF) is viewed as a fluid continuum. The description above is similar to that of a deformable

porous material at the macroscopic scale. In this context, when studying interstitial fluid flow and the transport of blood-borne solutes *in vivo*, it is natural to view the tumour and healthy tissue as two distinct deformable porous media. Dey et. al. [6] studied transvascular and interstitial fluid transport inside a solid tumour surrounded by healthy tissue. They employed a linearised biphasic mixture theory to describe the steady poroelastohydrodynamics (interstitial hydrodynamics and the deformation of tissue material) inside both tissue regions. The interstitial permeability is found to vary widely in healthy tissue. As a result, the interstitial fluid can give rise to significant viscous shearing inside the healthy tissue. Other researchers have used Darcy's equation (which neglects viscous shearing) to describe interstitial fluid flow inside a solid tumour [17, 19, 20]. One can couple a linear elasticity model with an equation of momentum balance for fluid [19] to describe the deformation of the solid phase inside the tumour. As a result, the two momentum balance equations, one for fluid phase and one for solid phase, yield a system analogous to Biot's classical poroelasticity model [5].

The existence and uniqueness of steady-state solutions to Darcy-type models of deformable porous media ere studied in [21], and the time-dependent problem is considered in [22]. Weak solutions to time-dependent models coupling Stokes flow and linear elasticity are discussed in [23]. Further, the Navier-Stokes/Biot system is investigated numerically in [24, 25]. The existence and uniqueness of weak solutions to the coupled Navier-Stokes equations with poroelasticity (Biot's) terms are developed in [26] via a semi-discrete Galerkin method. We note that the literature on the existence and uniqueness of solutions for biphasic mixture models in the context of tumours is limited. Alam et al. [3, 4] develop well-posedness, some regularity results in $2D$ and $3D$, and some closed-form solutions corresponding to a linear poroelastohydrodynamic model of fluid flow in an isolated (in-vitro) solid tumour (1D radially symmetric model). In separate studies, Alam et al. [27, 28] use a nonlinear poroelastohydrodynamics model to describe *in-vivo* and *in-vitro* fluid flow in solid tumours. The nonlinearities arose from the deformation-dependent hydraulic resistivity. By applying fixed-point theorems and the Galerkin method, they established well-posedness results in the weak sense.

This study considers a solid tumour within a healthy tissue (see Fig. 1). We are interested in unsteady poroelastohydrodynamics inside the solid tumour and surrounding host tissue. We note that in many mathematical models, tumour growth induces movement of the interface between the tumour and the surrounding tissue. However, in this study, we assume the interface is fixed. In practice, the fluids and blood-borne solutes from the tumour and host tissue are exchanged across the tumour-host interface. In the first part of this article (sections 2–3), we establish results regarding the existence, uniqueness, and continuous dependence in a weak sense of a poroelastohydrodynamic model of a tumour that mimics *in-vivo* conditions. In Sections 4-7, we construct a closed-form solution for simplified, 1D Cartesian geometry. We use this explicit solution to calculate the stress at the tumour-host interface and the system

energy of the solid tumour. This serves as a tool for characterizing tumour viability. The system energy depends on the velocity of interstitial fluid percolation and the movement of the cells within the tumour. Hence, variation in the system energy predicts an individual's contribution to the viability of a tumour [3, 4]. We start our analysis by introducing biphasic mixture theory.

2 Problem Definition

We suppose that $\Omega \subset \mathbb{R}^d$ $(d = 2,\ 3)$, denotes a bounded Lipschitz domain with two disjoint components Ω_1 and Ω_2 such that Ω_2 represents a tumour which is surrounded by normal tissue Ω_1. We denote by $\partial\Omega$ the boundary of Ω, and $\partial\Omega_{\rm i}$, ${\rm i} \in \{1, 2\}$ the boundary of $\Omega_{\rm i}$. We let $\Gamma_I = \partial\Omega_1 \cap \partial\Omega_2$ be the common interface between Ω_1 and Ω_2 and let $\Gamma_1 = \partial\Omega_1 \backslash \Gamma_I$, and $\Gamma_2 = \partial\Omega_2 \backslash \Gamma_I$, respectively denote the boundary of the tumour and healthy tissue excluding the interface Γ_I. We denote by $\mathbf{V}_{\rm i}^f$ and $\mathbf{V}_{\rm i}^s$ (for ${\rm i} \in \{1, 2\}$) the velocities of the extracellular fluid and solid constituents (cells and extracellular matrix) of $\Omega_{\rm i}$, respectively. The apparent densities and volume fractions of the fluid and solid phases are denoted by $\tilde{\rho}_{\rm i}^f$ and $\tilde{\rho}_{\rm i}^s$, and $\varphi_{\rm i}^f$ and $\varphi_{\rm i}^s$ respectively. The mass balance equations for the healthy host tissue region (Ω_1) are:

$$\frac{\partial}{\partial t}(\tilde{\rho}_{\rm i}^f \varphi_{\rm i}^f) + \nabla \cdot \left[(\tilde{\rho}_{\rm i}^f \varphi_{\rm i}^f)\mathbf{V}_{\rm i}^f\right] = \tilde{\rho}_{\rm i}^f S_{\rm i}^f, \tag{1}$$

$$\frac{\partial}{\partial t}(\tilde{\rho}_{\rm i}^s \varphi_{\rm i}^s) + \nabla \cdot [(\tilde{\rho}_{\rm i}^s \varphi_{\rm i}^s)\mathbf{V}_{\rm i}^s] = \tilde{\rho}_{\rm i}^s S_{\rm i}^s, \tag{2}$$

$i \in \{1, 2\}$. Here, S_i^f *and* S_i^s denote the corresponding source terms for the fluid and solid phase, respectively. Typically, the fluid source $S_{\rm i}^f({\rm x}, t)$ is assumed to be driven by the average transmural pressure so that [5, 19],

$$S_{\rm i}^f = -\left\{ L_{\rm bv}\left(\frac{A_{\rm bv}}{V}\right) + L_{\rm lv}\left(\frac{A_{\rm lv}}{V}\right)\right\}_{\rm i} (P_{\rm i} - P_{F_{\rm i}}), \quad {\rm i} \in \{1,\ 2\}, \tag{3}$$

where $L_{\rm bv}$ and $L_{\rm lv}$ are the wall conductivities of the blood and lymph vessels, respectively. The ratios $A_{\rm bv}/V$ and $A_{\rm lv}/V$ represent the surface areas per unit volume of vessels for the exchange of solute/fluid across the walls of the blood and lymph vessels, respectively. The first term in the second bracket of Equation (3) represents the distributed solute source through the blood vessels. The second term corresponds to the drainage of solutes from the interstitial space through the lymphatic vessels. $P_{F_{\rm i}}$ is the weighted vascular pressure within the $i^{\rm th}$ region (for more details, see [5], [6]). For simplcity, we assume constant pressure $P_{F_{\rm i}} = P_F$ for ${\rm i} \in \{1,\ 2\}$. Further, the volume fractions $\varphi_{\rm i}^f$ and $\varphi_{\rm i}^s$ satisfy the following saturation assumption

$$\varphi_{\rm i}^f + \varphi_{\rm i}^s = 1, \quad \text{for} \quad {\rm i} \in \{1, 2\} \tag{4}$$

The fluid momentum balance equations can be written as follows

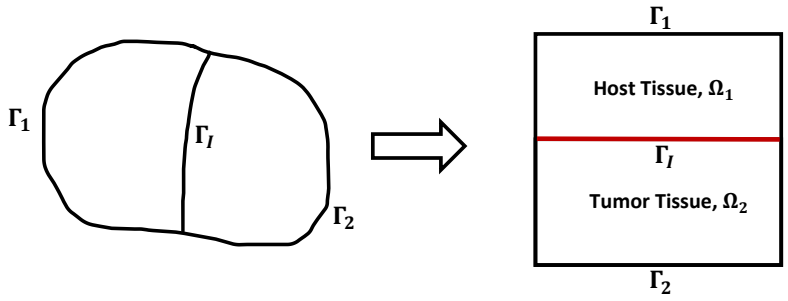

Fig. 1: Geometry of the problem

$$\rho_i^{\mathrm{j}}\left(\frac{\partial \mathbf{V}_{\mathrm{i}}^{\mathrm{j}}}{\partial t}+(\mathbf{V}_{\mathrm{i}}^{\mathrm{j}}\cdot\nabla)\mathbf{V}_{\mathrm{i}}^{\mathrm{j}}\right)=\nabla\cdot\mathbf{T}_{\mathrm{i}}^{\mathrm{j}}+\mathbf{b}_{\mathrm{i}}^{\mathrm{j}}+\mathbf{\Pi}_{\mathrm{i}}^{\mathrm{j}},\ \text{for j}\in\{f,s\},\ \mathrm{i}\in\{1,\ 2\},\tag{5}$$

where $\mathbf{T}_{\mathrm{i}}^{\mathrm{j}}$ denotes the stress tensor for the j^{th} phase in the i^{th} tissue sub-domain. Similarly, we denote by $\mathbf{b}_{\mathrm{i}}^{\mathrm{j}}$ any body force acting on phase j in region i. We suppose further that there is a drag force $\mathbf{\Pi}_{\mathrm{i}}^{\mathrm{j}}$ between the fluid and solid phases due to their relative motion, and that $-\mathbf{\Pi}_{\mathrm{i}}^{s}=\mathbf{\Pi}_{\mathrm{i}}^{f}$ by Newton's third law. We suppose that the constitutive relations for the stress tensor $\mathbf{T}_{\mathrm{i}}^{\mathrm{j}}$ and drag force $\mathbf{\Pi}_{\mathrm{i}}^{\mathrm{j}}$ are given by [5, 6, 13, 14],

$$\mathbf{T}_{\mathrm{i}}^{f}=-(\varphi_{\mathrm{i}}^{f})P_{\mathrm{i}}\mathbf{I}+\lambda^{f}(\nabla\cdot\mathbf{V}_{\mathrm{i}}^{f})\mathrm{I}+\mu^{f}\left(\nabla\mathbf{V}_{\mathrm{i}}^{f}+(\nabla\mathbf{V}_{\mathrm{i}}^{f})^{t_r}\right),\tag{6}$$

$$\mathbf{T}_{\mathrm{i}}^{s}=-\left[(\varphi_{\mathrm{i}}^{s}P_{\mathrm{i}})+\Xi_{\mathrm{i}}^{s}(\varphi_{\mathrm{i}}^{s})+\chi_{\mathrm{i}}^{s}(\varphi_{\mathrm{i}}^{s})(\nabla\cdot\mathbf{U}_{\mathrm{i}}^{s})\right]\mathbf{I}+\mu_{\mathrm{i}}^{s}\left(\varphi_{\mathrm{i}}^{s}\right)(\nabla\mathbf{U}_{\mathrm{i}}^{s}+(\nabla\mathbf{U}_{\mathrm{i}}^{s})^{t_r}),\tag{7}$$

$$-\mathbf{\Pi}_{\mathrm{i}}^{s}=\mathbf{\Pi}_{\mathrm{i}}^{f}=\mathbf{K}_{\mathrm{i}}\left(\mathbf{V}_{\mathrm{i}}^{s}-\mathbf{V}_{\mathrm{i}}^{f}\right)-(\nabla\varphi_{\mathrm{i}}^{s})\,P_{\mathrm{i}},\tag{8}$$

where t_r denotes the transpose of a matrix and $\mathbf{K}_{\mathrm{i}}=\mu^{f}\mathbf{k}_{\mathrm{i}}^{-1}$ denotes the drag coefficient (hydraulic conductivity) which accounts for deformation of the solid phase of the porous medium. We denote by $\mathbf{k}_i$ and P^i the permeability and hydrodynamic pressure of the i^{th} tissue region. The constants λ^f and μ^f are the first and second coefficients of the dynamic viscosity of the interstitial fluid. The constants χ_{i}^{s} and μ_{i}^{s} denote the Lame coefficient and shear modulus, respectively, of the solid phase. We denote by Ξ_{i}^{s} cell-cell interactions [6] and by $\mathbf{U}_{\mathrm{i}}^{s}$ and $\mathbf{V}_{\mathrm{i}}^{s}=\partial\mathbf{U}_{\mathrm{i}}^{s}/\partial t$ the displacement and velocity of the solid phase. The elastic moduli χ_{i}^{s} and μ_{i}^{s} can be expressed in terms of the Young's modulus ($\mathcal{Y}_{\mathrm{i}}^{s}$) and Poisson ratio ($\nu_{\mathrm{i}}^{s}$) as

$$\chi_{\mathrm{i}}^{s}=\frac{\nu_{\mathrm{i}}^{s}\mathcal{Y}_{\mathrm{i}}^{s}}{(1+\nu_{\mathrm{i}}^{s})(1-2\nu_{\mathrm{i}}^{s})},\quad \mu_{\mathrm{i}}^{s}=\frac{\mathcal{Y}_{\mathrm{i}}^{s}}{2(1+\nu_{\mathrm{i}}^{s})}.$$

We define the deformation and rate of deformation tensors $\mathbb{D}^s$ and $\mathbb{D}^f$ as follows:

$$\mathbb{D}^{s}(\mathbf{U}^{s})=\frac{1}{2}\left(\nabla\mathbf{U}^{s}+(\nabla\mathbf{U}^{s})^{t_r}\right),\qquad \mathbb{D}^{f}(\mathbf{V}^{f})=\frac{1}{2}\left(\nabla\mathbf{V}^{f}+(\nabla\mathbf{V}^{f})^{t_r}\right).$$

It is common in the literature to assume that $\mathbf{k}_i$ is isotropic and constant [14, 19, 20]. However, the supply of fluids and macromolecules within a tumour can be highly heterogeneous due to the non-uniform distribution of blood and lymph vessels. Consequently, the physiological transport parameters (e.g., hydraulic conductivity or permeability) should depend on space and deformation [8, 29]. Also, some biological tissues exhibit anisotropic permeability [30]. For example, articular cartilage is known to be anisotropic [31]. In the present work, we assume that the hydraulic conductivity $\mathbf{K}_i$ is an anisotropic matrix.

2.1 Assumptions on the present model

- In general, tumour growth depends on the percolation of interstitial fluid (containing nutrients) from the interstitial space to the tumour cells. Within a solid tumour, the permeability and elastic parameters (e.g., Ξ_i^s, χ_i^s and μ_i^s.) may depend on the solid volume fraction [6, 14], which may vary with spatial position and time. It is difficult to analyse tumour growth and fluid transport simultaneously. Therefore, in this section, we specialise our model to describe fluid transport within a fixed-size solid tumour surrounded by healthy tissue. Under this assumption, all elastic parameters can be viewed as positive constants.
- Perfusion and percolation of fluid containing nutrients occur on much shorter timescales than the timescale for tumour cell growth. Accordingly, we view the tumour as a static perfused domain. On the short timescale associated with fluid percolation within the tumour, cell death and proliferation are negligible. Therefore, we fix $S_{\mathrm{i}}^s = 0$ in the tumour and normal tissue regions. Further on the timescale of interest, the volume fraction φ_{i}^s of the solid phase remains constant in both regions. For simplicity, we assume that φ_{i}^s is independent of both spatial position and time. Also, in the absence of cell growth, cell-cell interactions can be ignored so that $\Xi_{\mathrm{i}}^s = 0$ [5, 6].
- Cell movement and interstitial fluid flow are slow so that inertial terms can be neglected in the momentum balance equations for both phases [14, 32].

Under the above assumptions, Equations (1)-(8) reduce to the following system of equations for $(\mathbf{V}_1^f, P_1, \mathbf{U}_1^s)$ in $\Omega_1 \times (0,T)$:

$$(M_{1a}) \begin{cases} \rho^f \frac{\partial \mathbf{V}_1^f}{\partial t} - \nabla \cdot [2\mu^f \mathbb{D}^f(\mathbf{V}_1^f) + (\lambda^f \nabla \cdot \mathbf{V}_1^f - \varphi_1^f P_1)\mathbf{I}] + \mathbf{K}_1(\mathbf{V}_1^f - \mathbf{V}_1^s) = \mathbf{b}_1^f, \\ \rho_1^s \frac{\partial \mathbf{V}_1^s}{\partial t} - \nabla \cdot [2\mu_1^s \mathbb{D}^s(\mathbf{U}_1^s) + (\chi_1^s \nabla \cdot \mathbf{U}_1^s - \varphi_1^s P_1)\mathbf{I}] - \mathbf{K}_1(\mathbf{V}_1^f - \mathbf{V}_1^s) = \mathbf{b}_1^s, \\ \nabla \cdot \left(\varphi_1^f \mathbf{V}_1^f + \varphi_1^s \mathbf{V}_1^s\right) - L_{\mathrm{bv}} \left(\frac{A_{\mathrm{bv}}}{V}\right)_1 \{1 + (L_{\mathrm{lv}} A_{\mathrm{lv}})/(L_{\mathrm{bv}} A_{\mathrm{bv}})_1\} (P_1 - P_F) = 0, \end{cases}$$

and for $(\mathbf{V}_2^f, P_2, \mathbf{U}_2^s)$ in $\Omega_2 \times (0,T)$:

$$(M_{1b}) \begin{cases} \rho^f \frac{\partial \mathbf{V}_2^f}{\partial t} + \nabla \cdot \left(\varphi_2^f P_2 \mathbf{I}\right) + \mathbf{K}_2 \left(\mathbf{V}_2^f - \mathbf{V}_2^s\right) = \mathbf{b}_2^f, \\ \rho_2^s \frac{\partial \mathbf{V}_2^s}{\partial t} - \nabla \cdot \left(2\mu_2^s \mathbb{D}^s(\mathbf{U}_2^s) + (\chi_2^s \nabla \cdot \mathbf{U}_2^s - \varphi_2^s P_2)\,\mathbf{I}\right) - \mathbf{K}_2 \left(\mathbf{V}_2^f - \mathbf{V}_2^s\right) = \mathbf{b}_2^s, \\ \nabla \cdot (\varphi_2^f \mathbf{V}_2^f + \varphi_2^s \mathbf{V}_2^s) - L_{\rm bv} \left(\frac{A_{\rm bv}}{V}\right)_2 \left\{1 + (L_{\rm lv} A_{\rm lv})/(L_{\rm bv} A_{\rm bv})_2\right\} (P_2 - P_F) = 0, \end{cases}$$

We assume $0 < T < T_{\max} < \infty$ so that the upper bound for time $T_{\max}$ is finite. To close the above equations, we must impose suitable initial, boundary, and interface conditions. We assume an interface separates the Brinkman-Darcy porous media. Guided by the literature [33, 34], we impose the following conditions on the interface Γ_I that separates Ω_1 and Ω_2.

Interface Conditions:

$$\mathbf{V}_1^f \cdot \mathbf{n}_1 + \mathbf{V}_2^f \cdot \mathbf{n}_2 = 0, \tag{9a}$$

$$-\beta \left(\mathbf{n}_1 . \mathbf{T}_1^f \cdot \mathbf{t}\right) = \mathbf{V}_1^f \cdot \mathbf{t}, \tag{9b}$$

$$-\left(\mathbf{n}_1 \cdot \mathbf{T}_1^f \cdot \mathbf{n}_1\right) = \varphi_2^f P_2, \tag{9c}$$

$$\mathbf{U}_1^s = \mathbf{U}_2^s, \tag{9d}$$

$$\mathbf{T}_1^s \cdot \mathbf{n}_1 + \mathbf{T}_2^s \cdot \mathbf{n}_2 = 0, \tag{9e}$$

where $\mathbf{n}_1$, $\mathbf{n}_2$ denote the outward unit normal vectors of Ω_1 and Ω_2, respectively, and $\mathbf{n}_I$ is the unit normal vector on the interface Γ_1, pointing from Ω_1 to Ω_2. Hence $\mathbf{n}_I = \mathbf{n}_1|_{\Gamma_I} = -\mathbf{n}_2|_{\Gamma_I}$. The unit vector $\mathbf{t}$ lies on the tangent plane to Γ_I. Equation (9a) ensures continuity of the normal component of the fluid phase velocity, and Equation (9b) is the Beavers-Joseph-Saffman slip condition for the tangential component of the fluid phase velocity. In Equation (9b), $\beta = 1/\left(s_c \sqrt{\mu^f K_0}\right)$, where s_c is the slip coefficient, K_0 is the constant hydraulic resistivity at the interface Γ_I so that $1/\beta$ denotes the resistance in the tangential direction. Equation (9c) ensures that the normal component of the stress in the fluid phases is continuous across the interface Γ_I. Equations (9d) and (9e) guarantee continuity of the displacement of the solid phase and the normal component of stress in the solid phase.

Boundary conditions: We assume that there is no displacement of the solid phase on the domain boundaries and that the healthy tissue is subject to an externally applied normal stress $\mathbf{T}_\infty^f$, so that

$$\mathbf{T}_1^f \cdot \mathbf{n}_1 = \mathbf{T}_\infty^f,\ \mathbf{U}_1^s = 0 \text{ on } \Gamma_1 \times (0,T),\ \mathbf{U}_2^s = 0,\ \mathbf{V}_2^f \cdot \mathbf{n}_2 = 0 \text{ on } \Gamma_2 \times (0,T). \tag{10}$$

Initial conditions: We suppose that initially the velocity and displacement are identically zero, so that

$$\mathbf{V}_1^f(\mathrm{x},0) = 0,\ \mathbf{V}_2^f(\mathrm{x},0) = 0,\ \mathbf{U}_1^s(\mathrm{x},0) = 0,\ \mathbf{U}_2^s(\mathrm{x},0) = 0,\ \dot{\mathbf{U}}_1^s(\mathrm{x},0) = 0,\ \dot{\mathbf{U}}_2^s(\mathrm{x},0) = 0. \tag{11}$$

2.2 Non-dimensionalization

We denote by L the length of the d-cube in which Ω is contained and introduce the following dimensionless variables and parameters.

$$\hat{\mathbf{x}} = \frac{\mathbf{x}}{L},\ \hat{t} = \left(\frac{\mu^f}{L^2\rho^f}\right)t,\ \hat{\nabla} = L\,\nabla,\ \hat{\mathbb{D}}^f = L\,\mathbb{D}^f,\ \hat{\mathbb{D}}^s = L\,\mathbb{D}^s,\ \hat{\mathbf{K}}_i = \frac{\mathbf{K}_i}{K_d},\ \hat{K}_0 = \frac{K_0}{K_d},$$
$$\hat{P}_i = \frac{P_i}{P_F},\ \hat{\mathbf{V}}_i^f = \left(\frac{LK_d}{P_F}\right)\mathbf{V}_i^f,\ \hat{\mathbf{U}}_i^s = \left(\frac{\mu^f K_d}{LP_F\rho^f}\right)\mathbf{U}_i^s \text{ for } i = 1,\ 2.$$

Here L is the characteristic length, K_d is the hydraulic conductivity of the tumour in the absence of deformation. Pressures, velocities, and displacements are non-dimensionalised as stated above. Under the above rescaling equations in $(M_{1a})-(M_{1b})$ and the interface, boundary and initial conditions (9a)-(11) reduce to give ("$\hat{}$" is dropped for convenience)

$$d_a\dot{\mathbf{V}}_1^f - \nabla\cdot\mathbf{T}_1^f + \mathbf{K}_1(\mathbf{V}_1^f - \dot{\mathbf{U}}_1^s) = \mathbf{b}_1^f \ \text{ in } \ \Omega_1\times(0,T), \tag{12}$$
$$d_a\rho_{\mathrm{R}_1}\ddot{\mathbf{U}}_1^s - \nabla\cdot\mathbf{T}_1^s - \mathbf{K}_1(\mathbf{V}_1^f - \dot{\mathbf{U}}_1^s) = \mathbf{b}_1^s \ \text{ in } \ \Omega_1\times(0,T), \tag{13}$$
$$\nabla\cdot(\varphi_1^f\mathbf{V}_1^f + \varphi_1^s\dot{\mathbf{U}}_1^s) + \alpha_1^2(P_1 - 1) = 0 \ \text{ in } \ \Omega_1\times(0,T), \tag{14}$$
$$d_a\dot{\mathbf{V}}_2^f + \varphi_2^f\nabla P_2 + \mathbf{K}_2(\mathbf{V}_2^f - \dot{\mathbf{U}}_2^s) = \mathbf{b}_2^f \ \text{ in } \ \Omega_2\times(0,T), \tag{15}$$
$$d_a\rho_{\mathrm{R}_2}\ddot{\mathbf{U}}_2^s - \nabla\cdot\mathbf{T}_l^s - \mathbf{K}_2(\mathbf{V}_2^f - \dot{\mathbf{U}}_2^s) = \mathbf{b}_2^s \ \text{ in } \ \Omega_2\times(0,T), \tag{16}$$
$$\nabla\cdot(\varphi_2^f\mathbf{V}_2 + \varphi_2^s\dot{\mathbf{U}}_2^s) + \alpha_2^2(P_2 - 1) = 0 \ \text{ in } \ \Omega_2\times(0,T), \tag{17}$$

where

$$\dot{\mathbf{V}}_1^f = \frac{\partial\mathbf{V}_1^f}{\partial t},\ \dot{\mathbf{U}}_i^s = \frac{\partial\mathbf{U}_i^s}{\partial t},\ \ddot{\mathbf{U}}_i^s = \frac{\partial^2\mathbf{U}_i^s}{\partial t^2},$$

$$\mathbf{T}_1^f = \left[2d_a\mathbb{D}^f(\mathbf{V}_1^f) + (\lambda d_a\nabla\cdot\mathbf{V}_1^f - \varphi_1^f P_1)\mathbf{I}\right],$$

and

$$\mathbf{T}_l^s = \left[2\gamma_l^s\mathbb{D}^s(\mathbf{U}_l^s) + (\delta_l^s(\nabla\cdot\mathbf{U}_l^s) - \varphi_l^s P_l)\,\mathbf{I}\right],$$

where $\gamma_l^s = \varrho_l^s/2(1+\nu_l^s)$, $\delta_l^s = \nu_l^s\varrho_l^s/(1+\nu_l^s)(1-2\nu_l^s)$, $l\in\{1,2\}$.

$$\mathbf{T}_1^f\cdot\mathbf{n}_1 = \mathbf{T}_\infty^f, \quad \mathbf{U}_1^s = 0 \ \text{ on } \ \Gamma_1\times(0,T), \ \ \mathbf{V}_2^f\cdot\mathbf{n}_2 = 0, \quad \mathbf{U}_2^s = 0 \ \text{ on } \ \Gamma_2\times(0,T). \tag{18}$$

$$\mathbf{V}_1^f(\mathrm{x},0) = 0,\ \mathbf{V}_2^f(\mathrm{x},0) = 0,\ \mathbf{U}_1^s(\mathrm{x},0) = 0,\ \mathbf{U}_2^s(\mathrm{x},0) = 0,\ \dot{\mathbf{U}}_1^s(\mathrm{x},0) = 0,\ \dot{\mathbf{U}}_2^s(\mathrm{x},0) = 0 \tag{19}$$

for all $x \in \Omega$.

$$\mathbf{V}_1^f \cdot \mathbf{n}_1 + \mathbf{V}_2^f \cdot \mathbf{n}_2 = 0, \qquad \mathbf{U}_1^s = \mathbf{U}_2^s \text{ on } \Gamma_I \times (0,T) \tag{20}$$

$$\beta^* \mathbf{V}_1^f \cdot \mathbf{t} = -(\mathbf{T}_1^f \cdot \mathbf{n}_1) \cdot \mathbf{t}, \quad -(\mathbf{T}_1^f \cdot \mathbf{n}_1) \cdot \mathbf{n}_1 = \varphi_2^f P_2, \quad \mathbf{T}_1^s \cdot \mathbf{n}_1 + \mathbf{T}_2^s \cdot \mathbf{n}_2 = 0 \text{ on } \Gamma_I \times (0,T) \tag{21}$$

In Equations (12)-(21) we have introduced the following dimensionless parameter groupings:

- $\alpha_1 = L\sqrt{K_d\left(\left(L_{\text{bv}}\frac{A_{\text{bv}}}{V}\right)_1 + \left(L_{\text{lv}}\frac{A_{\text{lv}}}{V}\right)_1\right)}$, $\alpha_2 = L\sqrt{K_d\left(\left(L_{\text{bv}}\frac{A_{\text{bv}}}{V}\right)_2 + \left(L_{\text{lv}}\frac{A_{\text{lv}}}{V}\right)_2\right)}$: These parameters represent the resistance to interstitial fluid movement and transcapillary fluid exchange inside Ω_1 and Ω_2, respectively.

- $\lambda = \lambda^f/\mu^f$: The ratio of the first and second coefficients of dynamic viscosity of the interstitial fluid.

- $d_a = \mu^f/(L^2 K_d)$: Darcy number.

- $\varrho_1^s = \mathcal{Y}_1^s \rho^f/(\mu^f K_d)$, $\varrho_2^s = \mathcal{Y}_2^s \rho^f/(\mu^f K_d)$: Scaled Young's moduli for the host and tumour tissues respectively.

- $\beta^* = s_c\sqrt{d_a K_0}$: Slip coefficient.

- $\rho_{\text{R}_1} = \rho_1^s/\rho^f$, $\rho_{\text{R}_2} = \rho_2^s/\rho^f$: the ratios of the solid and fluid densities in Ω_1 and Ω_2, respectively.

3 Well-posedness

Constructing analytical solutions to systems of partial differential equations (PDEs) is generally challenging. In such cases, it is important to verify fundamental questions relating to the well-posedness (existence, uniqueness, and continuous dependence) of the governing equations, in the sense of Hadamard. We outline below the steps we follow to establish well-posedness of Equations (12)-(21) in the weak sense.

• Step-1: Identify the solution and test function spaces.

• Step-2: Define a weak formulation (WF) in infinite-dimensional spaces, and call it the infinite-dimensional weak formulation (IDWF).

• Step-3: Prove the existence, uniqueness, and continuous dependence of a solution via relevant mathematical arguments.

• In step 3, we typically use Galerkin and weak convergence results, which can be

summarised as follows.

▷ Step-(a) Construct the finite-dimensional (FD) subspaces of the infinite-dimensional space under consideration.

▷ Step-(b) Project the IDWF onto the FD subspaces.

▷ Step-(c) Establish the well-posedness of the FDWF.

▷ Step-(d) Derive necessary estimates (or a priori bounds).

▷ Step-(e) Use the weak convergence method to pass to the limit in the FD WF.

3.1 Weak Formulation

Notation: Henceforth, for mathematical convenience, we omit the superscripts f, s from the functions $\mathbf{V}_i^f$, $\mathbf{U}_i^s$, $(i = \{1, 2\})$ and denote them by $\mathbf{V}_i$, $\mathbf{U}_i$.

Assumptions on the given data: We assume that all non-dimensional parameters listed in Sub-section-2.2 are known real positive constants. We assume that the hydraulic resistivity $\mathbf{K}_i \in \mathbb{L}^\infty(\Omega_i)$ is a time-independent, uniformly bounded, positive definite matrix. Accordingly, there exist $K^i_{\min}$, $K^i_{\max} > 0$ such that

$$\forall\ \mathbf{x} \in \Omega,\ K^i_{\min}\mathbf{x}\cdot\mathbf{x} \leq \mathbf{K}_i\mathbf{x}\cdot\mathbf{x} \leq K^i_{\max}\mathbf{x}\cdot\mathbf{x}.$$

For $i \in \{1, 2\}$ and $j \in \{f, s\}$, $\mathbf{b}_i^j \in L^2(0, T; \mathbf{L}^2(\Omega_i))$, $\mathbf{T}^f_\infty \in L^2(0, T; \mathbf{L}^2(\Gamma_1))$.

Weak Formulation:[1]. The triplets $(\mathbf{V}_1, P_1, \mathbf{U}_1) \in L^2(0, T; \mathbf{H}^1(\Omega_1)) \times L^2(0, T; L^2(\Omega_1)) \times L^2(0, T; \mathbf{H}^1_{0,\Gamma_1}(\Omega_1))$, and $(\mathbf{V}_2, P_2, \mathbf{U}_2) \in L^2(0, T; \mathbf{H}_{0,\Gamma_2}(\mathrm{div}; \Omega_2)) \times L^2(0, T; L^2(\Omega_2)) \times L^2(0, T; \mathbf{H}^1_{0,\Gamma_2}(\Omega_2))$, with $\dot{\mathbf{V}}_1 \in L^2(0, T; (\mathbf{H}^1(\Omega_1))^*)$, $\dot{\mathbf{V}}_2 \in L^2(0, T; \mathbf{L}^2(\Omega_2))$, $\dot{\mathbf{U}}_i \in L^2(0, T; \mathbf{L}^2(\Omega_i))$, $\ddot{\mathbf{U}}_i \in L^2(0, T; (\mathbf{H}^1_{0,\Gamma_1}(\Omega_i))^*)$,

[1] For function spaces and preliminary results, see Appendix Sub-section A.1 and [4]

$\nabla \cdot \dot{\mathbf{U}}_i \in L^2(0,T;\mathbf{L}^2(\Omega_i))$ are said to be a weak solution of (12)-(21) if

$$
(A_w)\begin{cases}
d_a\langle \dot{\mathbf{V}}_1(t),\boldsymbol{\eta}_1\rangle_{\Omega_1} + 2d_a(\mathbb{D}^f(\mathbf{V}_1(t)),\mathbb{D}^f(\boldsymbol{\eta}_1))_{\Omega_1} + \lambda d_a(\nabla\cdot\mathbf{V}_1(t),\nabla\cdot\boldsymbol{\eta}_1)_{\Omega_1}\\
-\varphi_1^f(P_1(t),\nabla\cdot\boldsymbol{\eta}_1)_{\Omega_1} + (\mathbf{K}_1\mathbf{V}_1(t),\boldsymbol{\eta}_1)_{\Omega_1} - (\mathbf{K}_1\dot{\mathbf{U}}_1(t),\boldsymbol{\eta}_1)_{\Omega_1}\\
+\beta^*(\mathbf{V}_1\cdot\hat{\mathbf{t}},\boldsymbol{\eta}_1\cdot\hat{\mathbf{t}})_{\Gamma_I} + d_a\rho_{R_1}\langle\ddot{\mathbf{U}}_1(t),\boldsymbol{\xi}_1\rangle_{\Omega_1} + 2\gamma_1^s(\mathbb{D}^s(\mathbf{U}_1(t)),\mathbb{D}^s(\boldsymbol{\xi}_1))_{\Omega_1}\\
+\delta_1^s(\nabla\cdot\mathbf{U}_1(t),\nabla\cdot\boldsymbol{\xi}_1)_{\Omega_1} - \varphi_1^s(P_1(t),\nabla\cdot\boldsymbol{\xi}_1)_{\Omega_1} - (\mathbf{K}_1\mathbf{V}_1(t),\boldsymbol{\xi}_1)_{\Omega_1}\\
+(\mathbf{K}_1\dot{\mathbf{U}}_1(t),\boldsymbol{\xi}_1)_{\Omega_1} + d_a\rho_{R_2}\langle\ddot{\mathbf{U}}_2(t),\boldsymbol{\xi}_2\rangle_{\Omega_2} + 2\gamma_2^s(\mathbb{D}^s(\mathbf{U}_2(t)),\mathbb{D}^s(\boldsymbol{\xi}_2))_{\Omega_2}\\
+\delta_2^s(\nabla\cdot\mathbf{U}_2(t),\nabla\cdot\boldsymbol{\xi}_2)_{\Omega_2} - \varphi_2^s(P_2(t),\nabla\cdot\boldsymbol{\xi}_2)_{\Omega_2} - (\mathbf{K}_2\mathbf{V}_2(t),\boldsymbol{\xi}_2)_{\Omega_2}\\
+(\mathbf{K}_2\dot{\mathbf{U}}_2(t),\boldsymbol{\xi}_2)_{\Omega_2} + d_a(\dot{\mathbf{V}}_2(t),\boldsymbol{\eta}_2)_{\Omega_2} - \varphi_2^f(P_2(t),\nabla\cdot\boldsymbol{\eta}_2)_{\Omega_2}\\
+(\mathbf{K}_2\mathbf{V}_2(t),\boldsymbol{\eta}_2)_{\Omega_2} - (\mathbf{K}_2\dot{\mathbf{U}}_2(t),\boldsymbol{\eta}_2)_{\Omega_2} + (\nabla\cdot(\varphi_1^f\mathbf{V}_1(t)\\
+\varphi_1^s\dot{\mathbf{U}}_1(t)),w)_{\Omega_1} + \alpha_1^2(P_1(t),w)_{\Omega_1} + (\nabla\cdot(\varphi_2^f\mathbf{V}_2(t) + \varphi_2^s\dot{\mathbf{U}}_2(t)),q)_{\Omega_2}\\
+\alpha_2^2(P_2(t),q)_{\Omega_2} = (\mathbf{b}_1^f(t),\boldsymbol{\eta}_1)_{\Omega_1} + (\mathbf{T}_\infty^f(t),\boldsymbol{\eta}_1)_{\Gamma_1} + (\mathbf{b}_1^s(t),\boldsymbol{\xi}_1)_{\Omega_1}\\
+(\mathbf{b}_2^f(t),\boldsymbol{\eta}_2)_{\Omega_2} + (\mathbf{b}_2^s(t),\boldsymbol{\xi}_2)_{\Omega_2} + (\alpha_1^2,w)_{\Omega_1} + (\alpha_2^2,q)_{\Omega_2}
\end{cases}
$$

holds for all test functions $\boldsymbol{\eta}_1 \in \mathbf{H}^1(\Omega_1)$, $\boldsymbol{\eta}_2 \in \mathbf{H}_{0,\Gamma_2}(\mathrm{div};\Omega_2)$, $\boldsymbol{\xi}_1 \in \mathbf{H}^1_{0,\Gamma_1}(\Omega_1)$, $\boldsymbol{\xi}_2 \in \mathbf{H}^1_{0,\Gamma_2}(\Omega_2)$, $w \in L^2(\Omega_1)$, and $q \in L^2(\Omega_2)$ respectively[2] and for a.e. $t \in (0,T)$ with

$$\mathbf{V}_1(0) = 0,\ \mathbf{U}_1(0) = 0,\ \dot{\mathbf{U}}_1(0) = 0,\ \text{a.e. in } \Omega_1, \tag{22}$$

$$\mathbf{U}_2(0) = 0,\ \ \dot{\mathbf{U}}_2(0) = 0,\ \mathbf{V}_2(0) = 0,\ \ \text{a.e. in } \Omega_2. \tag{23}$$

Theorem 1. *(Equivalence of the weak formulation). Let the data satisfy the assumptions listed in the previous section. Then any solution* $(\mathbf{V}_1,P_1,\mathbf{U}_1) \in L^2(0,T;\mathbf{H}^1(\Omega_1)) \times L^2(0,T;L^2(\Omega_1)) \times L^2(0,T;\mathbf{H}^1_{0,\Gamma_1}(\Omega_1))$, *and* $(\mathbf{V}_2,P_2,\mathbf{U}_2) \in L^2(0,T;\mathbf{H}_{0,\Gamma_2}(div;\Omega_2)) \times L^2(0,T;L^2(\Omega_2)) \times L^2(0,T;\mathbf{H}^1_{0,\Gamma_2}(\Omega_2))$, *with* $\dot{\mathbf{V}}_1 \in L^2(0,T;(\mathbf{H}^1(\Omega_1))^*)$, $\dot{\mathbf{V}}_2 \in L^2(0,T;\mathbf{L}^2(\Omega_2))$, $\dot{\mathbf{U}}_i \in L^2(0,T;\mathbf{L}^2(\Omega_i))$, $\ddot{\mathbf{U}}_i \in L^2(0,T;(\mathbf{H}^1_{0,\Gamma_i}(\Omega_i))^*)$, $\nabla\cdot\dot{\mathbf{U}}_i \in L^2(0,T;\mathbf{L}^2(\Omega_i))$, *($i = \{1,2\}$) of the system of equations (12)-(21) is also a solution of the weak formulation* (A_w) *and conversely, in distribution sense.*

Proof: The proof of this theorem relies on standard arguments, which we omit for brevity (see [35] for details).

[2]We assume the test functions $\boldsymbol{\xi}_1$, $\boldsymbol{\xi}_2$ and $\boldsymbol{\eta}_1$, $\boldsymbol{\eta}_2$ satisfy the continuity condition at the interface i.e., $\boldsymbol{\xi}_1 = \boldsymbol{\xi}_2$ and $\boldsymbol{\eta}_1\cdot\mathbf{n}_1 = \boldsymbol{\eta}_2\cdot\mathbf{n}_1$ at Γ_I in order to implement the interface conditions (21). Further, $\langle\ ,\ \rangle_\Omega$ represents the duality pairing between a Banach space (let $\mathbf{X}$) and its dual ($\mathbf{X}^*$).

3.2 Main Results

Before presenting our main results, we introduce the following time-dependent functions:

$$[G_1(t)]^2 = ||\mathbf{b}_1^f(t)||^2_{\Omega_1} + \frac{\alpha_3\alpha_4}{\min\{2d_a, K^1_{\min}\}}||\mathbf{T}^f_\infty(t)||^2_{\Gamma_1} + \frac{1}{2K^1_{\min}}||\mathbf{b}_1^f(t)||^2_{\Omega_1} + \alpha_1^2|\Omega_1| + \frac{1}{2K^2_{\min}}||\mathbf{b}_2^s(t)||^2_{\Omega_2} + \frac{1}{2K^2_{\min}}||\mathbf{b}_2^f(t)||^2_{\Omega_2} + \alpha_2^2|\Omega_2| \quad (24)$$

$$[G_2(t)]^2 = ||\dot{\mathbf{b}}_1^f(t)||^2_{\Omega_1} + \frac{1}{2K^1_{\min}}||\dot{\mathbf{b}}_1^s(t)||^2_{\Omega_1} + \frac{1}{2K^2_{\min}}||\dot{\mathbf{b}}_s^{in}(t)||^2_{\Omega_2} + \frac{1}{2K^2_{\min}}||\dot{\mathbf{b}}_f^{in}(t)||^2_{\Omega_2} + \frac{\alpha_3\alpha_4}{\min\{2d_a, K^1_{\min}\}}||\dot{\mathbf{T}}^f_\infty(t)||^2_{\Gamma_1} \quad (25)$$

and constants

$$||\mathbf{b}(0)||_\Omega = \left(||\dot{\mathbf{b}}_1^f(0)||^2_{\Omega_1} + ||\dot{\mathbf{b}}_1^s(0)||^2_{\Omega_1} + ||\dot{\mathbf{b}}_2^s(0)||^2_{\Omega_2} + ||\dot{\mathbf{b}}_2^f(0)||^2_{\Omega_2} + \alpha_1^4|\Omega_1| + \alpha_2^4|\Omega_2|\right)^{1/2}, \quad (26)$$

$$\beta_0 = \frac{1}{\rho_{\min}d_a}\exp\left(\frac{\mu}{\rho_{\min}d_a}T\right),\ \beta_1 = \left\{1 + \frac{T}{\rho_{\min}d_a}\left[1 + 4(K^1_{\max} + K^2_{\max})\right]\exp\left(\frac{\mu}{\rho_{\min}d_a}T\right)\right\}, \quad (27)$$

$$\beta_2 = \left[\frac{\rho_{\max}}{d_a\alpha^2}||\mathbf{b}(0)||^2_\Omega + ||G_2||^2_{L^2(0,T)}\right],\ \rho_{\min} = \min\{1, \rho_{R_1}, \rho_{R_2}\},\ \rho_{\max} = \max\{1, \rho_{R_1}, \rho_{R_2}\}, \quad (28)$$

$$\mu = \max\{(1 + 2K^1_{\max}), 2K^2_{\max}\},\ \alpha = \min\{1, \rho_{R_1}, \rho_{R_2}, \alpha_1^2/d_a, \alpha_2^2/d_a\}. \quad (29)$$

Theorem 2. *Assume that* $\mathbf{b}_i^j \in L^2(0,T;\mathbf{L}^2(\Omega_i))$, $i \in \{1,2\}$, $j \in \{f,s\}$, $\mathbf{T}^f_\infty \in \mathbf{L}^2(0,T;L^2(\Gamma_1))$. *Then the weak formulation* (A_w) *has at least one solution* $(\mathbf{V}_1, P_1, \mathbf{U}, \mathbf{V}_2, P_2)$ *that satisfies the following a priori estimates*[3]

$$||\mathbf{V}_1||^2_{L^\infty(0,T;\mathbf{L}^2(\Omega_1))} + ||\dot{\mathbf{U}}||^2_{L^\infty(0,T;\mathbf{L}^2(\Omega))} + ||\mathbf{V}_2||^2_{L^\infty(0,T;\mathbf{L}^2(\Omega_2))} \leq \beta_0||G_1||^2_{L^2(0,T)}, \quad (30)$$

[3]Here $\mathbf{U}$ is an auxiliary function defined as

$$\mathbf{U} = \begin{cases} \mathbf{U}_1, & \text{in } \Omega_1 \times (0,T) \\ \mathbf{U}_2, & \text{in } \Omega_2 \times (0,T), \end{cases}$$

with $\mathbf{U}_1 = \mathbf{U}_2$ on $\Gamma_I \times (0,T)$, and $\mathbf{U}_i \in L^2(0,T;\mathbf{H}^1_{0,\Gamma_i}(\Omega_i))$, for $i \in \{1,2\}$, hence $\mathbf{U} \in L^2(0,T;\mathbf{H}^1_0(\Omega))$.

and

$$(E_1)\begin{cases}\frac{\min\{2d_a,K^1_{\min}\}}{\alpha_3}||\mathbf{V}_1||^2_{L^2(0,T;\mathbf{H}^1(\Omega_1))}+2\lambda d_a||\nabla\cdot\mathbf{V}_1||^2_{L^2(0,T;\mathbf{L}^2(\Omega_1))}+2\beta^*||\mathbf{V}_1\cdot\hat{\mathbf{t}}||^2_{L^2(0,T;\mathbf{L}^2(\Gamma_I))}\\ +2\gamma_1^s||\mathbb{D}^s(\mathbf{U})||^2_{L^\infty(0,T;\mathbf{L}^2(\Omega_1))}+\delta_1^s||\nabla\cdot\mathbf{U}||^2_{L^\infty(0,T;\mathbf{L}^2(\Omega_1))}+2\gamma_2^s||\mathbb{D}^s(\mathbf{U})||^2_{L^\infty(0,T;\mathbf{L}^2(\Omega_2))}\\ +\delta_2^s||\nabla\cdot\mathbf{U}||^2_{L^\infty(0,T;\mathbf{L}^2(\Omega_2))}+\alpha_1^2||P_1||^2_{L^2(0,T;L^2(\Omega_1))}+\alpha_2^2||P_2||^2_{L^2(0,T;L^2(\Omega_2))}\leq\beta_1||G_1||^2_{L^2(0,T)}.\end{cases}$$

Further,

$$||\dot{\mathbf{V}}_1||^2_{L^\infty(0,T;\mathbf{L}^2(\Omega_1))}+||\ddot{\mathbf{U}}||^2_{L^\infty(0,T;\mathbf{L}^2(\Omega))}+||\dot{\mathbf{V}}_2||^2_{L^\infty(0,T;\mathbf{L}^2(\Omega_2))}\leq\beta_0\left[\frac{\rho_{\max}}{d_a\alpha^2}||\mathbf{b}(0)||^2_\Omega+||G_2||^2_{L^2(0,T)}\right], \tag{31}$$

$$(E_2)\begin{cases}\frac{\min\{2d_a,K^1_{\min}\}}{\alpha_3}||\dot{\mathbf{V}}_1||^2_{L^2(0,T;\mathbf{H}^1(\Omega_1))}+2\lambda d_a||\nabla\cdot\dot{\mathbf{V}}_1||^2_{L^2(0,T;\mathbf{L}^2(\Omega_1))}+2\beta^*||\dot{\mathbf{V}}_1\cdot\hat{\mathbf{t}}||^2_{L^2(0,T;\mathbf{L}^2(\Gamma_I))}\\ +2\gamma_1^s||\mathbb{D}^s(\dot{\mathbf{U}})||^2_{L^\infty(0,T;\mathbf{L}^2(\Omega_1))}+\delta_1^s||\nabla\cdot\dot{\mathbf{U}}||^2_{L^\infty(0,T;\mathbf{L}^2(\Omega_1))}+2\gamma_2^s||\mathbb{D}^s(\dot{\mathbf{U}})||^2_{L^\infty(0,T;\mathbf{L}^2(\Omega_2))}\\ +\delta_2^s||\nabla\cdot\dot{\mathbf{U}}||^2_{L^\infty(0,T;\mathbf{L}^2(\Omega_2))}+2\alpha_1^2||\dot{P}_1||^2_{L^2(0,T;L^2(\Omega_1))}+2\alpha_2^2||\dot{P}_2||^2_{L^2(0,T;L^2(\Omega_2))}\leq\beta_1\beta_2,\end{cases}$$

and

$$\varphi_2^f||\nabla\cdot\mathbf{V}_2(t)||_{\Omega_2}\leq\varphi_2^s||\nabla\dot{\mathbf{U}}_2(t)||_{\Omega_2}+\alpha_2^2||P_2(t)||_{\Omega_2}+\alpha_2^2|\Omega_2|^{1/2}. \tag{32}$$

Moreover,

$$\begin{aligned}||\dot{\mathbf{V}}_1||^2_{L^2(0,T;(\mathbf{H}^1(\Omega_1))^*)}\leq\frac{2}{d_a}\int_0^T[2d_a||\mathbb{D}^f(\mathbf{V}_1(\zeta))||^2_{\Omega_1}+\lambda d_a||\nabla\cdot\mathbf{V}_1(\zeta)||^2_{\Omega_1}+\varphi_1^f||P_1(\zeta)||^2_{\Omega_1}\\ +K^1_{\max}(||\mathbf{V}_1(\zeta)||^2_{\Omega_1}+||\dot{\mathbf{U}}(\zeta)||^2_{\Omega_1})+\alpha_4\beta^*||\mathbf{V}_1(\zeta)\cdot\hat{\mathbf{t}}||^2_{\Gamma_I}+||\mathbf{b}_1^f(\zeta)||^2_{\Omega_1}+\alpha_4||\mathbf{T}^f_\infty(\zeta)||^2_{\Gamma_1}]\,d\zeta\end{aligned} \tag{33}$$

and

$$\begin{aligned}||\ddot{\mathbf{U}}||_{L^2(0,T;\mathbf{H}^{-1}(\Omega))}\leq 2\int_0^T[2\gamma_1^s||\mathbb{D}^s(\mathbf{U}(\zeta))||^2_{\Omega_1}+\delta_1^s||\nabla\cdot\mathbf{U}(\zeta)||^2_{\Omega_1}+\varphi_1^s||P_1(\zeta)||^2_{\Omega_1}\\ +K^1_{\max}||\mathbf{V}_1(\zeta)||^2_{\Omega_1}+K^1_{\max}||\dot{\mathbf{U}}(\zeta)||^2_{\Omega_1}+2\gamma_2^s||\mathbb{D}^s(\mathbf{U}(\zeta))||^2_{\Omega_2}+\delta_2^s||\nabla\cdot\mathbf{U}(\zeta)||^2_{\Omega_2}\\ +\varphi_2^s||P_2(\zeta)||^2_{\Omega_2}+K^2_{\max}||\mathbf{V}_2(\zeta)||^2_{\Omega_2}+K^2_{\max}||\dot{\mathbf{U}}(\zeta)||^2_{\Omega_2}+||\mathbf{b}_1^s(\zeta)||^2_{\Omega_1}+||\mathbf{b}_2^s(\zeta)||^2_{\Omega_2}]\,d\zeta.\end{aligned} \tag{34}$$

Proof of Theorem 2: The proof of Theorem 2 involves of several steps. First, we project the weak formulation (A_w) onto a finite-dimensional problem, which we refer to as the Galerkin formulation (**GF**). Then, we use the semi-discrete Galerkin method to demonstrate the existence of a unique solution to (**GF**) (see Section 3.3). Finally, we derive a priori estimates (or energy estimates) (see Section 3.4) and use the method of weak convergence in the Hilbert space to pass to the limit in (**GF**) (see Section 3.5).

3.3 A semi-discrete Galerkin formulation

The spaces $\mathbf{H}^1(\Omega_1)$, $L^2(\Omega_1)$, $\mathbf{H}_0^1(\Omega)$, $\mathbf{H}_{0,\Gamma_2}(\mathrm{div};\Omega_2)$, $L^2(\Omega_2)$, are separable Hilbert. Thus, one can find a basis consisting of smooth functions $\{\mathbf{w}_1^i, q_1^i, \mathbf{\Psi}^i, \mathbf{w}_2^i, q_2^i\}$ of $\mathbf{Y} = \mathbf{H}^1(\Omega_1) \times L^2(\Omega_1) \times \mathbf{H}_0^1(\Omega) \times \mathbf{H}_{0,\Gamma_2}(\mathrm{div};\Omega_2) \times L^2(\Omega_2)$. Define $\mathbf{Y}_m = \mathrm{span}\{(\mathbf{w}_1^i, q_1^i, \Psi^i, \mathbf{w}_2^i, q_2^i),\ i = 1, \cdots, m\}$. Then a Galerkin approximation to the weak formulation (A_w) is the finite-dimensional problem which is defined as:
Find $(\mathbf{V}_1^m, P_1^m, \mathbf{U}^m, \mathbf{V}_2^m, P_2^m) \in L^2(0,T;\mathbf{Y}_m)$ with $\mathbf{V}_1^m \in H^1(0,T;\mathbf{L}^2(\Omega_1))$, $\mathbf{V}_2^m \in H^1(0,T;\mathbf{L}^2(\Omega_2))$ and $\mathbf{U}^m \in H^2(0,T;\mathbf{L}^2(\Omega))$ such that[4]

$$
(\mathbf{GF})\ \begin{cases}
d_a\langle\dot{\mathbf{V}}_1^m(t),\boldsymbol{\eta}_1\rangle_{\Omega_1} + 2d_a(\mathbb{D}^f(\mathbf{V}_1^m(t)),\mathbb{D}^f(\boldsymbol{\eta}_1))_{\Omega_1} + \lambda d_a(\nabla\cdot\mathbf{V}_1^m(t),\nabla\cdot\boldsymbol{\eta}_1)_{\Omega_1} \\
-\varphi_1^f(P_1^m(t),\nabla\cdot\boldsymbol{\eta}_1)_{\Omega_1} + (\mathbf{K}_1\mathbf{V}_1^m(t),\boldsymbol{\eta}_1)_{\Omega_1} - (\mathbf{K}_1\dot{\mathbf{U}}_1^m(t),\boldsymbol{\eta}_1)_{\Omega_1} \\
+\beta^*(\mathbf{V}_1^m\cdot\hat{\mathbf{t}},\boldsymbol{\eta}_1\cdot\hat{\mathbf{t}})_{\Gamma_I} + d_a\rho_{R_1}\langle\ddot{\mathbf{U}}_1^m(t),\boldsymbol{\xi}_1\rangle_{\Omega_1} + 2\gamma_1^s(\mathbb{D}^s(\mathbf{U}_1^m(t)),\mathbb{D}^s(\boldsymbol{\xi}_1))_{\Omega_1} \\
+\delta_1^s(\nabla\cdot\mathbf{U}_1^m(t),\nabla\cdot\boldsymbol{\xi}_1)_{\Omega_1} - \varphi_1^s(P_1^m(t),\nabla\cdot\boldsymbol{\xi}_1)_{\Omega_1} - (\mathbf{K}_1\mathbf{V}_1^m(t),\boldsymbol{\xi}_1)_{\Omega_1} \\
+(\mathbf{K}_1\dot{\mathbf{U}}_1^m(t),\boldsymbol{\xi}_1)_{\Omega_1} + d_a\rho_{R_2}\langle\ddot{\mathbf{U}}_2^m(t),\boldsymbol{\xi}_2\rangle_{\Omega_2} + 2\gamma_2^s(\mathbb{D}^s(\mathbf{U}_2^m(t)),\mathbb{D}^s(\boldsymbol{\xi}_2))_{\Omega_2} \\
+\delta_2^s(\nabla\cdot\mathbf{U}_2^m(t),\nabla\cdot\boldsymbol{\xi}_2)_{\Omega_2} - \varphi_2^s(P_2^m(t),\nabla\cdot\boldsymbol{\xi}_2)_{\Omega_2} - (\mathbf{K}_2\mathbf{V}_2^m(t),\boldsymbol{\xi}_2)_{\Omega_2} \\
+(\mathbf{K}_2\dot{\mathbf{U}}_2^m(t),\boldsymbol{\xi}_2)_{\Omega_2} + d_a(\dot{\mathbf{V}}_2^m(t),\boldsymbol{\eta}_2)_{\Omega_2} - \varphi_2^f(P_2^m(t),\nabla\cdot\boldsymbol{\eta}_2)_{\Omega_2} \\
+(\mathbf{K}_2\mathbf{V}_2^m(t),\boldsymbol{\eta}_2)_{\Omega_2} - (\mathbf{K}_2\dot{\mathbf{U}}_2^m(t),\boldsymbol{\eta}_2)_{\Omega_2} + (\nabla\cdot(\varphi_1^f\mathbf{V}_1^m(t) + \varphi_1^s\dot{\mathbf{U}}_1^m(t)),w)_{\Omega_1} \\
+\alpha_1^2(P_1^m(t),w)_{\Omega_1} + (\nabla\cdot(\varphi_2^f\mathbf{V}_2^m(t) + \varphi_2^s\dot{\mathbf{U}}_2^m(t)),q)_{\Omega_2} + \alpha_2^2(P_2^m(t),q)_{\Omega_2} \\
= (\mathbf{b}_1^f(t),\boldsymbol{\eta}_1)_{\Omega_1} + (\mathbf{T}_\infty^f(t),\boldsymbol{\eta}_1)_{\Gamma_1} + (\mathbf{b}_1^s(t),\boldsymbol{\xi}_1)_{\Omega_1} + (\mathbf{b}_2^f(t),\boldsymbol{\eta}_2)_{\Omega_2} \\
+(\mathbf{b}_2^s(t),\boldsymbol{\xi}_2)_{\Omega_2} + (\alpha_1^2,w)_{\Omega_1} + (\alpha_2^2,q)_{\Omega_2}
\end{cases}
$$

for a.e. $t \in (0,T)$, for all $(\boldsymbol{\eta}_1, \boldsymbol{\xi}, \boldsymbol{\eta}_2, w, q) \in \mathbf{Y}_m$ and

$$
\mathbf{V}_1^m(0) = 0,\ \mathbf{V}_2^m(0) = 0,\ \mathbf{U}_1^m(0) = 0,\ \mathbf{U}_2^m(0) = 0,\ \dot{\mathbf{U}}_1^m(0) = 0,\ \dot{\mathbf{U}}_2^m(0) = 0. \quad (35)
$$

Lemma 1. *For any $m \in \mathbb{N}$, the Galerkin formulation (**GF**) has a unique solution $(\mathbf{V}_1^m, P_1^m, \mathbf{U}^m, \mathbf{V}_2^m, P_2^m) \in L^2(0,T;\mathbf{Y}_m)$ with $\mathbf{V}_1^m \in H^1(0,T;\mathbf{L}^2(\Omega_1))$, $\mathbf{V}_2^m \in H^1(0,T;\mathbf{L}^2(\Omega_2))$ and $\mathbf{U}^m \in H^2(0,T;\mathbf{L}^2(\Omega))$ for all $t \in (0,T)$.*

[4] Here test function $\boldsymbol{\xi} \in H_0^1(\Omega)^d$ defined as

$$
\boldsymbol{\xi} = \begin{cases} \boldsymbol{\xi}_1, & \text{in } \Omega_1 \\ \boldsymbol{\xi}_2, & \text{in } \Omega_2 \end{cases}
$$

with $\boldsymbol{\xi}_1 = \boldsymbol{\xi}_2$ on Γ_I.

Proof: We show that the (**GF**) has a unique solution. We look for an approximation of the solution $(\mathbf{V}_1^m, P_1^m, \mathbf{U}^m, \mathbf{V}_2^m, P_2^m)$ in the following form

$$\mathbf{V}_1^m(x,t) = \sum_{j=1}^{m} a_j^m(t)\mathbf{w}_1^j(x),\ \mathbf{V}_2^m(x,t) = \sum_{j=1}^{m} b_j^m(t)\mathbf{w}_2^j(x), P_1(x,t) = \sum_{j=1}^{m} c_j^m(t)q_1^j(x),$$
$$P_2(x,t) = \sum_{j=1}^{m} d_j^m(t)q_2^j(x), \mathbf{U}^m(x,t) = \sum_{j=1}^{m} e_j^m(t)\mathbf{\Psi}^j(x),$$

where the coefficients a_j^m, b_j^m, c_j^m, d_j^m, and e_j^m are to be determined. With this form of approximate solution, the finite-dimensional problem (**GF**) yields the following system of autonomous second-order ordinary differential equations (ODEs) for the unknown coefficients a_j^m, b_j^m, c_j^m, d_j^m, and e_j^m

$$\mathbf{A}_1\frac{d\mathbf{a}}{dt} + \mathbf{A}_2\mathbf{a} - \mathbf{A}_3\mathbf{c} - \mathbf{A}_4\frac{d\mathbf{e}}{dt} = \mathbf{F}_1 \tag{36}$$

$$\mathbf{B}_1\frac{d^2\mathbf{e}}{dt^2} + \mathbf{B}_2\mathbf{e} - \mathbf{B}_6\mathbf{c} - \mathbf{B}_4\mathbf{a} + \mathbf{B}_3\frac{d\mathbf{e}}{dt} - \mathbf{B}_7\mathbf{d} - \mathbf{B}_5\mathbf{b} = \mathbf{F}_2 \tag{37}$$

$$\mathbf{A}_5\frac{d\mathbf{b}}{dt} - \mathbf{A}_6\mathbf{d} + \mathbf{A}_7\mathbf{b} - \mathbf{A}_8\frac{d\mathbf{e}}{dt} = \mathbf{F}_3 \tag{38}$$

$$\mathbf{A}_3\mathbf{a} + \mathbf{B}_6\frac{d\mathbf{e}}{dt} + \mathbf{Q}_1\mathbf{c} = \mathbf{F}_4 \tag{39}$$

$$\mathbf{A}_6\mathbf{b} + \mathbf{B}_7\frac{d\mathbf{e}}{dt} + \mathbf{Q}_2\mathbf{d} = \mathbf{F}_5 \tag{40}$$

$$\mathbf{a}(0) = 0,\ \mathbf{b}(0) = 0,\ \mathbf{e}(0) = 0,\ \dot{\mathbf{e}}(0) = 0,$$

where the expressions for the coefficient matrices $\mathbf{A}_i$, $i = 1, \ldots, 8$, $\mathbf{B}_i$, $i = 1, \ldots, 7$, $\mathbf{Q}_i$ $i = 1, 2$, and the functions $\mathbf{F}_i$, $i = 1, \ldots, 5$ on the right hand side are given in the Appendix section A.3.2. The unknown coefficients are:

$$\mathbf{a} = \begin{pmatrix} a_1^m(t) \\ \vdots \\ a_m^m(t) \end{pmatrix},\ \mathbf{b} = \begin{pmatrix} b_1^m(t) \\ \vdots \\ b_m^m(t) \end{pmatrix},\ \mathbf{c} = \begin{pmatrix} c_1^m(t) \\ \vdots \\ c_m^m(t) \end{pmatrix},\ \mathbf{d} = \begin{pmatrix} d_1^m(t) \\ \vdots \\ d_m^m(t) \end{pmatrix},\ \mathbf{e} = \begin{pmatrix} e_1^m(t) \\ \vdots \\ e_m^m(t) \end{pmatrix},$$

Introduce a vector $\boldsymbol{\theta}$ such that

$$\frac{d\mathbf{e}}{dt} = \boldsymbol{\theta} \tag{41}$$

and $\mathbf{A} = [\mathbf{a}, \mathbf{b}, \mathbf{e}, \boldsymbol{\theta}]^{t_r}$ (t_r : is abbreviated for transpose). From (39)-(40) we have $\mathbf{c} = \mathbf{Q}_1^{-1}(\mathbf{F}_4 - \mathbf{A}_3\mathbf{a} - \mathbf{B}_6\boldsymbol{\theta})$ and $\mathbf{d} = (\mathbf{F}_5 - \mathbf{A}_6\mathbf{b} - \mathbf{B}_7\boldsymbol{\theta})$. If we substitute for $\mathbf{c}$ and $\mathbf{d}$ in (36)-(38) then ODEs (36)-(38) and (41) reduce to the following, equivalent system

of autonomous first order ODEs in $\mathbf{A}(t)$:

$$\dot{\mathbf{A}} = -\mathbf{M}^{-1}\mathbf{N}\mathbf{A} + \mathbf{M}^{-1}\mathbf{F}, \quad \text{where } \mathbf{A}(0) \text{ is given,} \tag{42}$$

and

$$\mathbf{M} = \begin{pmatrix} \mathbf{A}_1 & \mathbf{0} & \mathbf{0} & \mathbf{0} \\ \mathbf{0} & \mathbf{A}_5 & \mathbf{0} & \mathbf{0} \\ \mathbf{0} & \mathbf{0} & \mathbb{I} & \mathbf{0} \\ \mathbf{0} & \mathbf{0} & \mathbf{0} & \mathbf{B}_1 \end{pmatrix},$$

$$\mathbf{N} = \begin{pmatrix} \mathbf{A}_2 + \mathbf{A}_3\mathbf{Q}_1^{-1}\mathbf{A}_3 & \mathbf{0} & \mathbf{0} & \mathbf{A}_3\mathbf{Q}_1^{-1}\mathbf{B}_6 - \mathbf{A}_4 \\ \mathbf{0} & \mathbf{A}_6\mathbf{Q}_2^{-1}\mathbf{A}_6 + \mathbf{A}_7 & \mathbf{0} & \mathbf{A}_6\mathbf{Q}_2^{-1}\mathbf{B}_7 - \mathbf{A}_8 \\ \mathbf{0} & \mathbf{0} & \mathbb{I} & -\mathbb{I} \\ \mathbf{B}_6\mathbf{Q}_1^{-1}\mathbf{A}_3 - \mathbf{A}_4 & \mathbf{B}_7\mathbf{Q}_2^{-1}\mathbf{A}_6 - \mathbf{B}_5 & \mathbf{B}_2 & \mathbf{B}_6\mathbf{Q}_2^{-1}\mathbf{B}_6 + \mathbf{B}_3 + \mathbf{B}_7\mathbf{Q}_2^{-1}\mathbf{B}_7 \end{pmatrix},$$

and $\mathbf{F} = \left(\mathbf{F}_1 + \mathbf{A}_3\mathbf{Q}_1^{-1}\mathbf{F}_4,\ \mathbf{F}_3 + \mathbf{A}_6\mathbf{Q}_2^{-1}\mathbf{F}_5,\ 0,\ \mathbf{F}_2 + \mathbf{B}_6\mathbf{Q}_1^{-1}\mathbf{F}_4 + \mathbf{B}_7\mathbf{Q}_2^{-1}\mathbf{F}_5 \right)^{\mathcal{T}}$.
We note as the basis functions are linearly independent, the matrices $\mathbf{A}_1$, $\mathbf{A}_5$, $\mathbf{B}_1$, $\mathbf{Q}_1$, $\mathbf{Q}_2$ are symmetric and invertible, being Gram matrices. Hence, the matrix $\mathbf{M}$ is also invertible. The matrices $\mathbf{M}$, $\mathbf{N}$ are $4m \times 4m$ and the vectors $\mathbf{A}$, $\mathbf{F}$ have length $4m$. In eq. (42), the right-hand side of the system of ODEs depends continuously (even Lipschitz) on the variables $\mathbf{a}$, $\mathbf{b}$, $\mathbf{e}$, $\boldsymbol{\theta}$ and time. Hence, the Cauchy-Lipschitz theorem implies that the Eq. (42) has a unique solution $(\mathbf{a}, \mathbf{b}, \mathbf{e}, \boldsymbol{\theta}) \in C^1(0,T;\mathbb{R}^m) \times C^1(0,T;\mathbb{R}^m) \times C^1(0,T;\mathbb{R}^m) \times C^1(0,T;\mathbb{R}^m)$, and $(\mathbf{c}, \mathbf{d}) \in C^1(0,T;\mathbb{R}^m) \times C^1(0,T;\mathbb{R}^m)$. Thus, the finite dimensional problem has a unique solution $(\mathbf{V}_1^m, P_1^m, \mathbf{U}^m, \mathbf{V}_2^m, P_2^m) \in L^2(0,T;\mathbf{Y}_m)$ with $\mathbf{V}_1^m \in H^1(0,T;\mathbf{L}^2(\Omega_1))$, $\mathbf{V}_2^m \in H^1(0,T;\mathbf{L}^2(\Omega_2))$ and $\mathbf{U}^m \in H^2(0,T;\mathbf{L}^2(\Omega))$. The next step is to find a prior bounds (or energy estimates) on the finite-dimensional solution $(\mathbf{V}_1^m, P_1^m, \mathbf{U}^m, \mathbf{V}_2^m, P_2^m)$.

3.4 Energy Estimates

Theorem 3. *Assume that* $b_i^j \in H^1(0,T;\mathbf{L}^2(\Omega_i))$, $i \in \{1,2\}$, $j \in \{f,s\}$, $\mathbf{T}_\infty^f \in H^1(0,T;\mathbf{L}^2(\Gamma_1))$, *and* $\mathbf{T}_\infty^f(x,0) = 0$. *Then the solution of the Galerkin formulation* $(\mathbf{V}_1^m, P_1^m, \mathbf{U}^m, \mathbf{V}_2^m, P_2^m) \in L^2(0,T;\mathbf{Y}_m)$ *with* $\mathbf{V}_1^m \in H^1(0,T;\mathbf{L}^2(\Omega_1))$, $\mathbf{V}_2^m \in H^1(0,T;\mathbf{L}^2(\Omega_2))$ *and* $\mathbf{U}^m \in H^2(0,T;\mathbf{L}^2(\Omega))$ *satisfies the following a priori bounds (or energy estimates) for all* $t \in [0,T]$:

$$||\mathbf{V}_1^m(t)||_{\Omega_1}^2 + ||\dot{\mathbf{U}}^m(t)||_{\Omega_1}^2 + ||\dot{\mathbf{U}}^m(t)||_{\Omega_2}^2 + ||\mathbf{V}_2^m(t)||_{\Omega_2}^2 \leq \beta_0 ||G_1||_{L^2(0,T)}^2 \tag{43}$$

$$(E_5) \begin{cases} \min\{2d_a, K_{\min}^1\} \int_0^t \left[||\mathbb{D}^f(\mathbf{V}_1^m(\zeta))||_{\Omega_1}^2 + ||\mathbf{V}_1^m(\zeta)||_{\Omega_1}^2 \right] d\zeta + \int_0^t \left[2\lambda d_a ||\nabla \cdot \mathbf{V}_1^m(\zeta)||_{\Omega_1}^2 \right. \\ \left. + 2\beta^* ||\mathbf{V}_1^m(\zeta) \cdot \hat{\mathbf{t}}||_{\Gamma_I}^2 \right] d\zeta + 2\gamma_1^s ||\mathbb{D}^s(\mathbf{U}^m(t))||_{\Omega_1}^2 + \delta_1^s ||\nabla \cdot \mathbf{U}^m(t)||_{\Omega_1}^2 + 2\gamma_2^s ||\mathbb{D}^s(\mathbf{U}^m(t))||_{\Omega_2}^2 \\ + \delta_2^s ||\nabla \cdot \mathbf{U}^m(t)||_{\Omega_2}^2 + \int_0^t \left[\alpha_1^2 ||P_1^m(\zeta)||_{\Omega_1}^2 + \alpha_2^2 ||P_2^m(\zeta)||_{\Omega_2}^2 \right] d\zeta \leq \beta_1 ||G_1||_{L^2(0,T)}^2. \end{cases}$$

Also,

$$||\dot{\mathbf{V}}_1^m(t)||^2_{\Omega_1}+||\ddot{\mathbf{U}}^m(t)||^2_{\Omega_1}+||\ddot{\mathbf{U}}^m(t)||^2_{\Omega_2}+||\dot{\mathbf{V}}_2^m(t)||^2_{\Omega_2} \leq \beta_0 \left[\frac{\rho_{\max}}{d_a\alpha^2}||\mathbf{b}(0)||^2_{\Omega}+||G_2||^2_{L^2(0,T)}\right], \tag{44}$$

$$(E_6)\begin{cases} \int_0^t \Big[\min\{2d_a, K^1_{\min}\}[||\mathbb{D}^f(\dot{\mathbf{V}}_1^m(\zeta))||^2_{\Omega_1}+||\dot{\mathbf{V}}_1^m(\zeta)||^2_{\Omega_1}]+2\lambda d_a||\nabla\cdot\dot{\mathbf{V}}_1^m(\zeta)||^2_{\Omega_1} \\ +2\beta^*||\dot{\mathbf{V}}_1^m(\zeta)\cdot\hat{\mathbf{t}}||^2_{\Gamma_I}\Big]\,d\zeta+2\gamma_1^s||\mathbb{D}^s(\dot{\mathbf{U}}^m(t))||^2_{\Omega_1}+\delta_1^s||\nabla\cdot\dot{\mathbf{U}}^m(t)||^2_{\Omega_1} \\ +2\gamma_2^s||\mathbb{D}^s(\dot{\mathbf{U}}^m(t))||^2_{\Omega_2}+\delta_2^s||\nabla\cdot\dot{\mathbf{U}}^m(t)||^2_{\Omega_2}+\int_0^t\Big[2\alpha_1^2||\dot{P}_1^m(t)||^2_{\Omega_1} \\ +2\alpha_2^2||\dot{P}_2^m(t)||^2_{\Omega_2}\Big]\,d\zeta \leq \beta_1\left[\frac{\rho_{\max}}{d_a\alpha^2}||\mathbf{b}(0)||^2_{\Omega}+||G_2||^2_{L^2(0,T)}\right], \end{cases}$$

and

$$\varphi_2^f||\nabla\cdot\mathbf{V}_2^m(t)||_{\Omega_2} \leq \varphi_2^s||\nabla\dot{\mathbf{U}}_2^m(t)||_{\Omega_2}+\alpha_2^2||P_2^m(t)||_{\Omega_2}+\alpha_2^2|\Omega_2|^{1/2}. \tag{45}$$

Moreover,

$$\begin{aligned} ||\dot{\mathbf{V}}_1^m||^2_{L^2(0,T;(\mathbf{H}^1(\Omega_1))^*)} \leq \frac{2}{d_a}\int_0^t\Big[2d_a||\mathbb{D}^f(\mathbf{V}_1^m(\zeta))||^2_{\Omega_1}+\lambda d_a||\nabla\cdot\mathbf{V}_1^m(\zeta)||^2_{\Omega_1} \\ +\varphi_1^f||P_1^m(\zeta)||^2_{\Omega_1}+K^1_{\max}||\mathbf{V}_1^m(\zeta)||^2_{\Omega_1}+K^1_{\max}||\dot{\mathbf{U}}^m(\zeta)||^2_{\Omega_1}+\alpha_4\beta^*||\mathbf{V}_1^m(\zeta)\cdot\hat{\mathbf{t}}||^2_{\Gamma_I} \\ +||\mathbf{b}_1^f(\zeta)||^2_{\Omega_1}+\alpha_4||\mathbf{T}^f_\infty(\zeta)||^2_{\Gamma_1}\Big]\,d\zeta \end{aligned} \tag{46}$$

and

$$\begin{aligned} ||\ddot{\mathbf{U}}^m||_{L^2(0,T;\mathbf{H}^{-1}(\Omega))} \leq 2\int_0^t\Big[2\gamma_1^s||\mathbb{D}^s(\mathbf{U}^m(\zeta))||^2_{\Omega_1}+\delta_1^s||\nabla\cdot\mathbf{U}^m(\zeta)||^2_{\Omega_1}+\varphi_1^s||P_1^m(\zeta)||^2_{\Omega_1} \\ +K^1_{\max}||\mathbf{V}_1^m(\zeta)||^2_{\Omega_1}+K^1_{\max}||\dot{\mathbf{U}}^m(\zeta)||^2_{\Omega_1}+2\gamma_2^s||\mathbb{D}^s(\mathbf{U}^m(\zeta))||^2_{\Omega_2}+\delta_2^s||\nabla\cdot\mathbf{U}^m(\zeta)||^2_{\Omega_2} \\ +\varphi_2^s||P_2^m(\zeta)||^2_{\Omega_2}+K^2_{\max}||\mathbf{V}_2^m(\zeta)||^2_{\Omega_2}+K^2_{\max}||\dot{\mathbf{U}}^m(\zeta)||^2_{\Omega_2}+||\mathbf{b}_1^s(\zeta)||^2_{\Omega_1}+||\mathbf{b}_s^{in}(\zeta)||^2_{\Omega_2}\Big]\,d\zeta. \end{aligned} \tag{47}$$

Remark 1.

- ***(i)*** *(43) implies* $\mathbf{V}_1^m$, $\dot{\mathbf{U}}^m$, *and* $\mathbf{V}_2^m$, *are bounded sequences in* $L^\infty(0,T;\mathbf{L}^2(\Omega_1))$, $L^\infty(0,T;\mathbf{L}^2(\Omega))$, *and* $L^\infty(0,T;\mathbf{L}^2(\Omega_2))$, *respectively.*
- ***(ii)*** (E_5) *implies the sequences* $\mathbf{V}_1^m$, $\mathbf{U}^m$, P_1^m *and* P_2^m *are bounded in* $L^2(0,T;\mathbf{H}^1(\Omega_1))$, $L^\infty(0,T;\mathbf{H}^1_0(\Omega))$, $L^2(0,T;L^2(\Omega_1))$ *and* $L^2(0,T;L^2(\Omega_2))$ *respectively.*
- ***(iii)*** *(44) implies* $\dot{\mathbf{V}}_1^m$, $\ddot{\mathbf{U}}^m$ *and* $\dot{\mathbf{V}}_2^m$ *are bounded in* $L^\infty(0,T;\mathbf{L}^2(\Omega_1))$, $L^\infty(0,T;\mathbf{L}^2(\Omega))$ *and* $L^\infty(0,T;\mathbf{L}^2(\Omega_2))$, *respectively.*
- ***(iv)*** (E_6) *implies the sequence* $\dot{\mathbf{V}}_1^m \in L^2(0,T;\mathbf{H}^1(\Omega_1))$, *and* $\dot{\mathbf{U}}^m \in L^\infty(0,T;\mathbf{H}^1_0(\Omega))$, $P_1 \in L^2(0,T;L^2(\Omega_1))$, $P_2 \in L^2(0,T;L^2(\Omega_2))$, *and are bounded.*
- ***(v)*** *(43), (45) imply* $\mathbf{V}_2^m$ *is bounded in* $\mathbf{H}_{0,\Gamma_2}(div;\Omega_2)$ *and (46) implies* $\dot{\mathbf{V}}_1^m$ *is bounded in* $L^2(0,T;(\mathbf{H}^1(\Omega_1))^*)$.

(vi) *(47) implies* $\ddot{\mathbf{U}}^m$ *is bounded in* $L^2(0,T;\mathbf{H}^{-1}(\Omega))$.

Proof of Theorem 3: We let $\boldsymbol{\eta}_1 = \mathbf{V}_1^m(t)$, $\boldsymbol{\eta}_2 = \mathbf{V}_2^m(t)$, $\boldsymbol{\xi} = \dot{\mathbf{U}}^m(t)$, $w = P_1^m(t)$, $q = P_2^m(t)$ in (**GF**) and using the Cauchy-Schwarz, trace, and Korn's inequalities and integrating with respect to 't' where $0 < t < T$, we get

$$(E_8)\begin{cases} d_a||\mathbf{V}_1^m(t)||^2_{\Omega_1} + \min\{2d_a, K^1_{\min}\}\int_0^t \left[||\mathbb{D}^f(\mathbf{V}_1^m(\zeta))||^2_{\Omega_1} + ||\mathbf{V}_1^m(\zeta)||^2_{\Omega_1}\right] d\zeta \\ + \int_0^t \left[2\lambda d_a||\nabla\cdot\mathbf{V}_1^m(\zeta)||^2_{\Omega_1} + 2\beta^*||\mathbf{V}_1^m(\zeta)\cdot\hat{\mathbf{t}}||^2_{\Gamma_I}\right] d\zeta + d_a\rho_{R_1}||\dot{\mathbf{U}}^m(t)||^2_{\Omega_1} \\ +2\gamma_1^s||\mathbb{D}^s(\mathbf{U}^m(t))||^2_{\Omega_1} + \delta_1^s||\nabla\cdot\mathbf{U}^m(t)||^2_{\Omega_1} + d_a\rho_{R_2}||\dot{\mathbf{U}}^m(t)||^2_{\Omega_2} \\ +2\gamma_2^s||\mathbb{D}^s(\mathbf{U}^m(t))||^2_{\Omega_2} + \delta_2^s||\nabla\cdot\mathbf{U}^m(t)||^2_{\Omega_2} + d_a||\mathbf{V}_2^m(t)||^2_{\Omega_2} \\ + \int_0^t \left[\alpha_1^2||P_1^m(\zeta)||^2_{\Omega_1} + \alpha_2^2||P_2^m(\zeta)||^2_{\Omega_2}\right] d\zeta \le \int_0^t \left[G_1(\zeta)\right]^2 d\zeta \\ + \int_0^t \left[2K^1_{\max}||\dot{\mathbf{U}}^m(\zeta)||^2_{\Omega_1} + (1+2K^1_{\max})||\mathbf{V}_1^m(\zeta)||^2_{\Omega_1} + 2K^2_{\max}||\dot{\mathbf{U}}^m(\zeta)||^2_{\Omega_{in}}\right. \\ \left. +2K^2_{\max}||\mathbf{V}_2^m(\zeta)||^2_{\Omega_2}\right] d\zeta. \end{cases}$$

Further, from (E_8) we deduce the following

$$(E_9)\begin{cases} ||\mathbf{V}_1^m(t)||^2_{\Omega_1} + ||\dot{\mathbf{U}}^m(t)||^2_{\Omega_1} + ||\dot{\mathbf{U}}^m(t)||^2_{\Omega_2} + ||\mathbf{V}_2^m(t)||^2_{\Omega_2} \le \frac{1}{\rho_{\min}d_a}||G_1||^2_{L^2(0,T)} \\ + \frac{\mu}{\rho_{\min}d_a}\int_0^t \left[||\dot{\mathbf{U}}^m(\zeta)||^2_{\Omega_1} + ||\mathbf{V}_1^m(\zeta)||^2_{\Omega_1} + ||\dot{\mathbf{U}}^m(\zeta)||^2_{\Omega_2} + ||\mathbf{V}_2^m(\zeta)||^2_{\Omega_2}\right] d\zeta. \end{cases}$$

where $\rho_{\min} = \min\{1, \rho_{R_1}, \rho_{R_1}\}$, $\mu = \max\{(1+2K^1_{\max}), 2K^2_{\max}\}$.
We define

$$\Phi(t) = ||\mathbf{V}_1^m(t)||^2_{\Omega_1} + ||\dot{\mathbf{U}}^m(t)||^2_{\Omega_1} + ||\dot{\mathbf{U}}^m(t)||^2_{\Omega_2} + ||\mathbf{V}_2^m(t)||^2_{\Omega_2}, \tag{48}$$

so that (E_9) can be rewritten as

$$\Phi(t) \le \frac{1}{\rho_{\min}d_a}||G_1||^2_{L^2(0,T)} + \frac{\mu}{\rho_{\min}d_a}\int_0^t \Phi(\zeta)\, d\zeta. \tag{49}$$

Applying the Gronwall integral inequality, we have that

$$||\mathbf{V}_1^m(t)||^2_{\Omega_1} + ||\dot{\mathbf{U}}^m(t)||^2_{\Omega_1} + ||\dot{\mathbf{U}}^m(t)||^2_{\Omega_2} + ||\mathbf{V}_2^m(t)||^2_{\Omega_2} \le \frac{1}{\rho_{\min}d_a}||G_1||^2_{L^2(0,T)}\exp\left(\frac{\mu}{\rho_{\min}d_a}T\right) \tag{50}$$

which proves (43). Further, using (50) and (E_8) we obtain (E_5).

Bounds on the sequences $\dot{\mathbf{V}}_1^m$, $\dot{\mathbf{V}}_2^m$, $\ddot{\mathbf{U}}^m$: Differentiate the Galerkin formulation (**GF**) with respect to 't' and let $\boldsymbol{\eta}_1 = \dot{\mathbf{V}}_1^m(t)$, $\boldsymbol{\eta}_2 = \dot{\mathbf{V}}_2^m(t)$, $\boldsymbol{\xi} = \ddot{\mathbf{U}}^m(t)$, $w = \dot{P}_1^m(t)$, $q = \dot{P}_2^m(t)$. Using the Cauchy-Schwarz, trace, and Korn's inequalities and integrating with respect to time $t \in (0,T)$ with zero initial conditions, we obtain

$$(E_{11}) \begin{cases} d_a||\dot{\mathbf{V}}_1^m(t)||^2_{\Omega_1} + \int_0^t \Big[\min\{2d_a, K^1_{\min}\}[||\mathbb{D}^f(\dot{\mathbf{V}}_1^m(\zeta))||^2_{\Omega_1} + ||\dot{\mathbf{V}}_1^m(\zeta)||^2_{\Omega_1}] \\ +2\lambda d_a||\nabla\cdot\dot{\mathbf{V}}_1^m(\zeta)||^2_{\Omega_1} + 2\beta^*||\dot{\mathbf{V}}_1^m(\zeta)\cdot\hat{\mathbf{t}}||^2_{\Gamma_I}\Big]\, d\zeta + d_a\rho_{R_1}||\ddot{\mathbf{U}}^m(t)||^2_{\Omega_1} \\ +2\gamma_1^s||\mathbb{D}^s(\dot{\mathbf{U}}^m(t))||^2_{\Omega_1} + \delta_1^s||\nabla\cdot\dot{\mathbf{U}}^m(t)||^2_{\Omega_1}] + d_a\rho_{R_2}||\ddot{\mathbf{U}}^m(t)||^2_{\Omega_2} \\ +2\gamma_2^s||\mathbb{D}^s(\dot{\mathbf{U}}^m(t))||^2_{\Omega_2} + \delta_2^s||\nabla\cdot\dot{\mathbf{U}}^m(t)||^2_{\Omega_2} + d_a||\dot{\mathbf{V}}_2^m(t)||^2_{\Omega_2} \\ +\int_0^t \Big[2\alpha_1^2||\dot{P}_1^m(t)||^2_{\Omega_1} + 2\alpha_2^2||\dot{P}_2^m(t)||^2_{\Omega_2}\Big]\, d\zeta \le \int_0^t [G_2(\zeta)]^2\, d\zeta \\ +\int_0^t \Big[(1+2K^1_{\max})||\dot{\mathbf{V}}_1^m(t)||^2_{\Omega_1} + (2K^1_{\max})||\ddot{\mathbf{U}}^m(t)||^2_{\Omega_1} + 2K^2_{\max}||\ddot{\mathbf{U}}^m(t)||^2_{\Omega_2} \\ +(2K^2_{\max})||\dot{\mathbf{V}}_2^m(t)||^2_{\Omega_2}\Big]\, d\zeta + d_a||\dot{\mathbf{V}}_1^m(0)||^2_{\Omega_1} + d_a\rho_{R_1}||\ddot{\mathbf{U}}^m(0)||^2_{\Omega_1} \\ +d_a\rho_{R_2}||\ddot{\mathbf{U}}^m(0)||^2_{\Omega_2} + d_a||\dot{\mathbf{V}}_2^m(0)||^2_{\Omega_2}. \end{cases}$$

In order to apply the Gronwall inequality in (E_{11}), we must find suitable bounds on $||\dot{\mathbf{V}}_1^m(0)||^2_{\Omega_1}$, $||\ddot{\mathbf{U}}^m(0)||^2_{\Omega_1}$, $||\ddot{\mathbf{U}}^m(0)||^2_{\Omega_2}$, $||\dot{\mathbf{V}}_2^m(0)||^2_{\Omega_2}$. If we let $\boldsymbol{\eta}_1 = \dot{\mathbf{V}}_1^m(0)$, $\boldsymbol{\eta}_2 = \dot{\mathbf{V}}_2^m(0)$, $\boldsymbol{\xi} = \ddot{\mathbf{U}}^m(0)$, $w = P_1^m(0)$, $q = P_2^m(0)$ in the finite-dimensional formulation, then (imposing zero initial conditions) we have that

$$(E_{12}) \begin{cases} d_a||\dot{\mathbf{V}}_1^m(0)||^2_{\Omega_1} + d_a\rho_{R_1}||\ddot{\mathbf{U}}^m(0)||^2_{\Omega_1} + d_a\rho_{R_2}||\ddot{\mathbf{U}}^m(0)||^2_{\Omega_2} + d_a||\dot{\mathbf{V}}_2^m(0)||^2_{\Omega_2} \\ +\alpha_1^2||P_1^m(0)||^2_{\Omega_1} + \alpha_2^2||P_2^m(0)||^2_{\Omega_2} \le (\dot{\mathbf{b}}_1^f(0), \dot{\mathbf{V}}_1^m(0))_{\Omega_1} + (\dot{\mathbf{b}}_1^s(0), \ddot{\mathbf{U}}^m(0))_{\Omega_1} \\ +(\dot{\mathbf{b}}_2^s(0), \ddot{\mathbf{U}}^m(0))_{\Omega_2} + (\dot{\mathbf{b}}_2^f(0), \dot{\mathbf{V}}_2^m(0))_{\Omega_2} + (\alpha_1^2, P_1^m(0))_{\Omega_1} + (\alpha_2^2, P_2^m(0))_{\Omega_2}. \end{cases}$$

Using the Cauchy-Schwarz inequality, we get

$$||\dot{\mathbf{V}}_1^m(0)||^2_{\Omega_1} + ||\ddot{\mathbf{U}}^m(0)||^2_{\Omega_1} + ||\ddot{\mathbf{U}}^m(0)||^2_{\Omega_2} + ||\dot{\mathbf{V}}_2^m(0)||^2_{\Omega_2} + ||P_1^m(0)||^2_{\Omega_1} + ||P_2^m(0)||^2_{\Omega_2} \le \frac{1}{d_a^2\alpha^2}||\mathbf{b}(0)||^2_{\Omega}, \qquad (51)$$

where $\alpha = \min\{1, \rho_{R_1}, \rho_{R_1}, \alpha_1^2/d_a, \alpha_2^2/d_a\}$. From (E_{11}) we have

$$(E_{13}) \begin{cases} ||\dot{\mathbf{V}}_1^m(t)||^2_{\Omega_1} + ||\ddot{\mathbf{U}}^m(t)||^2_{\Omega_1} + +||\ddot{\mathbf{U}}^m(t)||^2_{\Omega_2} + ||\dot{\mathbf{V}}_2^m(t)||^2_{\Omega_2} \\ \le \frac{\rho_{\max}}{d_a^2\alpha^2\rho_{\min}}||\mathbf{b}(0)||^2_{\Omega} + \frac{1}{\rho_{\min}d_a}\int_0^t [G_2(\zeta)]^2\, d\zeta + \frac{\mu}{\rho_{\min}d_a}\int_0^t \Big[||\dot{\mathbf{V}}_1^m(t)||^2_{\Omega_1} \\ +||\ddot{\mathbf{U}}^m(t)||^2_{\Omega_1} + ||\ddot{\mathbf{U}}^m(t)||^2_{\Omega_2} + ||\dot{\mathbf{V}}_2^m(t)||^2_{\Omega_2}\Big]\, d\zeta. \end{cases}$$

Now using the Gronwall integral inequality in (E_{13}) we obtain (44). Further, from (E_{11}) and (44), we obtain the estimate (E_6).
Next, we seek $\nabla \cdot \mathbf{V}_2^m(t) \in L^2(\Omega_2)$, $\dot{\mathbf{V}}_1^m \in L^2(0,T;(\mathbf{H}^1(\Omega_1))^*)$ and $\ddot{\mathbf{U}}^m \in L^2(0,T;\mathbf{H}^{-1}(\Omega))$ and are bounded. We have that (**GF**) holds for all test functions $(\boldsymbol{\eta}_1, \boldsymbol{\xi}, \boldsymbol{\eta}_2, w, q) \in \mathbf{Y}_m$, and it suffices to choose a suitable set of test functions. Choosing $\boldsymbol{\eta}_1 = 0,\ \boldsymbol{\xi} = 0,\ \boldsymbol{\eta}_2 = 0,\ w = 0,\ q = \nabla \cdot \mathbf{V}_2^m(t)$ and substituting in (**GF**) yields

$$\begin{aligned}\varphi_2^f ||\nabla \cdot \mathbf{V}_2^m(t)||_{\Omega_2}^2 = -\varphi_2^s(\nabla \dot{\mathbf{U}}_2^m(t), \nabla \cdot \mathbf{V}_2^m(t))_{\Omega_2} - \alpha_2^2(P_2^m(t), \nabla \cdot \mathbf{V}_2^m(t))_{\Omega_2} \\ +(\alpha_2^2, \nabla \cdot \mathbf{V}_2^m(t))_{\Omega_2}\end{aligned}$$

For $\nabla \cdot \mathbf{V}_2^m(t) \neq 0$ the Cauchy-Schwarz inequality gives (45).
Further[5], we choose a $\mathbf{W} \in \mathbf{H}^1(\Omega_1)$ such that $\mathbf{W} = \mathbf{W}_1 + \mathbf{W}_2$, where $\mathbf{W}_1 \in \mathbf{X}_m = \text{span}\{\mathbf{w}_1^i\}_{i=1}^m$ and $\mathbf{W}_2 \in \mathbf{X}_m^\perp$ (the orthogonal complement of $\mathbf{X}_m$). Clearly,

$$||\mathbf{W}_1||_{\mathbf{H}^1(\Omega_1)} \leq ||\mathbf{W}||_{\mathbf{H}^1(\Omega_1)}. \tag{52}$$

Substituting $\boldsymbol{\eta}_1 = \mathbf{W}_1$, $\boldsymbol{\xi} = 0$, $w = 0$, $q = 0$ in (**GF**), we obtain

$$\begin{aligned}d_a\langle \dot{\mathbf{V}}_1^m(t), \mathbf{W}\rangle_{\Omega_1} = d_a(\dot{\mathbf{V}}_1^m(t), \mathbf{W})_{\Omega_1} = d_a(\dot{\mathbf{V}}_1^m(t), \mathbf{W}_1)_{\Omega_1} \\ = -2d_a(\mathbb{D}^f(\mathbf{V}_1^m(t)), \mathbb{D}^f(\mathbf{W}_1))_{\Omega_1} - \lambda d_a(\nabla \cdot \mathbf{V}_1^m(t), \nabla \cdot \mathbf{W}_1)_{\Omega_1} + \varphi_1^f(P_1^m(t), \nabla \cdot \mathbf{W}_1)_{\Omega_1} \\ -(\mathbf{K}_1 \mathbf{V}_1^m(t), \mathbf{W}_1)_{\Omega_1} + (\mathbf{K}_1 \dot{\mathbf{U}}^m(t), \mathbf{W}_1)_{\Omega_1} - \beta^*(\mathbf{V}_1^m(t) \cdot \hat{\mathbf{t}}, \mathbf{W}_1 \cdot \hat{\mathbf{t}})_{\Gamma_I} \\ +(\mathbf{b}_1^f(t), \mathbf{w}_1^i)_{\Omega_1} + (\mathbf{T}_\infty^f(t), \mathbf{W}_1)_{\Gamma_1},\end{aligned}$$

Using the Cauchy-Schwarz, trace inequalities, and (52), we have

$$\begin{aligned}|d_a\langle \dot{\mathbf{V}}_1^m(t), \mathbf{W}\rangle_{\Omega_1}| \leq \Big[2d_a||\mathbb{D}^f(\mathbf{V}_1^m(t))||_{\Omega_1} + \lambda d_a||\nabla \cdot \mathbf{V}_1^m(t)||_{\Omega_1} + \varphi_1^f||P_1^m(t)||_{\Omega_1} \\ +K_{\max}^1||\mathbf{V}_1^m(t)||_{\Omega_1} + K_{\max}^1||\dot{\mathbf{U}}^m(t)||_{\Omega_1} + \alpha_4\beta^*||\mathbf{V}_1^m(t) \cdot \hat{\mathbf{t}}||_{\Gamma_I} + ||\mathbf{b}_1^f(t)||_{\Omega_1} \\ +\alpha_4||\mathbf{T}_\infty^f(t)||_{\Gamma_1}\Big]||\mathbf{W}||_{1,\Omega_1}\end{aligned} \tag{53}$$

Taking the supremum over non-zero $\mathbf{W} \in \mathbf{H}^1(\Omega_1)$ and integrating w.r.t $t \in (0,T)$, we obtain (46). Similarly, $\mathbf{W} \in \mathbf{H}_0^1(\Omega)$ is chosen such that $\mathbf{W} = \mathbf{W}_1 + \mathbf{W}_2$, where $\mathbf{W}_1 \in \mathbf{Z}_m = \text{span}\{\boldsymbol{\Psi}_1^i\}_{i=1}^m$ and $\mathbf{W}_2 \in \mathbf{Z}_m^\perp$ (the orthogonal complement of $\mathbf{Z}_m$). Clearly,

$$||\mathbf{W}_1||_{\mathbf{H}_0^1(\Omega)} \leq ||\mathbf{W}||_{\mathbf{H}_0^1(\Omega)}. \tag{54}$$

We introduce a weighted L^2 inner product on $\mathbf{H}_0^1(\Omega)$ via

$$[[\mathbf{U}, \boldsymbol{\xi}]]_\Omega = d_a\rho_{R_1}(\mathbf{U}, \boldsymbol{\xi})_{\Omega_1} + d_a\rho_{R_2}(\mathbf{U}, \boldsymbol{\xi})_{\Omega_2}, \quad \forall\ \mathbf{U},\ \boldsymbol{\xi} \in \mathbf{L}^2(\Omega). \tag{55}$$

[5] Here, we follow Salsa [36].

The norm induced on $\mathbf{H}_0^1(\Omega)$ via (55) is equivalent to the standard L^2 norm $||\cdot||_\Omega$. Substituting $\boldsymbol{\xi} = \mathbf{W}_1$, $\boldsymbol{\eta}_i = 0$, $w = 0$, $q = 0$ in (**GF**), we obtain

$$\begin{aligned}
d_a\rho_{R_1}\langle\ddot{\mathbf{U}}^m(t),\mathbf{W}\rangle_{\Omega_1} + d_a\rho_{R_2}\langle\ddot{\mathbf{U}}^m(t),\mathbf{W}\rangle_{\Omega_2} = d_a\rho_{R_1}(\ddot{\mathbf{U}}^m(t),\mathbf{W})_{\Omega_1} \\
+d_a\rho_{R_2}(\ddot{\mathbf{U}}^m(t),\mathbf{W})_{\Omega_2} = d_a\rho_{R_1}(\ddot{\mathbf{U}}^m(t),\mathbf{W}_1)_{\Omega_1} + d_a\rho_{R_2}(\ddot{\mathbf{U}}^m(t),\mathbf{W}_1)_{\Omega_2} \\
= -2\gamma_1^s(\mathbb{D}^s(\mathbf{U}^m(t)),\mathbb{D}^s(\mathbf{W}_1))_{\Omega_1} - \delta_1^2(\nabla\cdot\mathbf{U}^m(t),\nabla\cdot\mathbf{W}_1)_{\Omega_1} + \varphi_1^s(P_1^m(t),\nabla\cdot\mathbf{W}_1)_{\Omega_1} \\
+(\mathbf{K}_1\mathbf{V}_1^m(t),\mathbf{W}_1)_{\Omega_1} - (\mathbf{K}_1\dot{\mathbf{U}}^m(t),\mathbf{W}_1)_{\Omega_1} - 2\gamma_2^s(\mathbb{D}^s(\mathbf{U}^m(t)),\mathbb{D}^s(\mathbf{W}_1))_{\Omega_2} \\
-\delta_2^s(\nabla\cdot\mathbf{U}^m(t),\nabla\cdot\mathbf{W}_1)_{\Omega_2} + \varphi_2^s(P_2^m(t),\nabla\cdot\mathbf{W}_1)_{\Omega_2} + (\mathbf{K}_2\mathbf{V}_2^m(t),\mathbf{W}_1)_{\Omega_2} \\
-(\mathbf{K}_2\dot{\mathbf{U}}^m(t),\mathbf{W}_1)_{\Omega_2} + (\mathbf{b}_1^s(t),\mathbf{W}_1)_{\Omega_1} + (\mathbf{b}_2^s(t),\mathbf{W}_1)_{\Omega_2}.
\end{aligned}$$

Using the Cauchy-Schwarz inequality and (55), we obtain

$$\begin{aligned}
|[[\ddot{\mathbf{U}}^m(t),\mathbf{W}]]_\Omega| \leq \Big[2\gamma_1^s||\mathbb{D}^s(\mathbf{U}^m(t))||_{\Omega_1} + \delta_1^s||\nabla\cdot\mathbf{U}^m(t)||_{\Omega_1} + \varphi_1^s||P_1^m(t)||_{\Omega_1} \\
+K_{\max}^1||\mathbf{V}_1^m(t)||_{\Omega_1} + K_{\max}^1||\dot{\mathbf{U}}^m(t)||_{\Omega_1} + 2\gamma_2^s||\mathbb{D}^s(\mathbf{U}^m(t))||_{\Omega_2} + \delta_2^s||\nabla\cdot\mathbf{U}^m(t)||_{\Omega_2} \\
+\varphi_2^s||P_2^m(t)||_{\Omega_2} + K_{\max}^2||\mathbf{V}_2^m(t)||_{\Omega_2} + K_{\max}^2||\dot{\mathbf{U}}^m(t)||_{\Omega_2} + ||\mathbf{b}_1^s(t)||_{\Omega_1} \\
+||\mathbf{b}_2^s(t)||_{\Omega_2}\Big]||\mathbf{W}||_{1,\Omega}.
\end{aligned}$$

Taking the supremum over non-zero $\mathbf{W} \in \mathbf{H}_0^1(\Omega)$ and integrating with respect to $t \in (0,T)$, we obtain (47).

We have used energy estimates (see Theorem (3) and Remark (1)) and shown that the finite-dimensional solution $(\mathbf{V}_1^m, \mathbf{V}_2^m, \mathbf{U}^m, P_1^m, P_2^m)$ is bounded in some Hilbert space (say $\mathcal{H}$). Thus, there exists a subsequence, still denoted by the same symbol, and $(\mathbf{V}_1, \mathbf{V}_2, \mathbf{U}, P_1, P_2)$ in $\mathcal{H}$ such that

$$(\mathbf{V}_1^m, \mathbf{V}_2^m, \mathbf{U}^m, P_1^m, P_2^m) \rightharpoonup (\mathbf{V}_1, \mathbf{V}_2, \mathbf{U}, P_1, P_2), \tag{56}$$

and

$$(\dot{\mathbf{V}}_1^m, \dot{\mathbf{U}}^m, \ddot{\mathbf{U}}^m) \rightharpoonup (\mathbf{V}_1, \dot{\mathbf{U}}, \ddot{\mathbf{U}}) \tag{57}$$

converge weakly in $\mathcal{H}$. We use this weak convergence to pass to the limit in (**GF**).

3.5 Passing to the limits

Mathematically, the weak convergence results in (56) and (57) can be expanded to following

$$\mathbf{V}_1^m \rightharpoonup \mathbf{V}_1 \ \text{ in } \ L^2(0,T;H^1(\Omega_1)^d), \quad \dot{\mathbf{V}}_1^m \rightharpoonup \dot{\mathbf{V}}_1 \ \text{ in } \ L^2(0,T;L^2(\Omega_1)^d),$$

$$\begin{gathered}
\mathbf{V}_1^m \rightharpoonup \mathbf{V}_1 \ \text{ in } \ L^2(0,T;H^{1/2}(\partial\Omega_1)^d), \quad \mathbf{U}^m \rightharpoonup \mathbf{U} \ \text{ in } \ L^2(0,T;H^1(\Omega)^d) \\
\dot{\mathbf{U}}^m \rightharpoonup \dot{\mathbf{U}} \ \text{ in } \ L^2(0,T;L^2(\Omega)^d), \quad \ddot{\mathbf{U}}^m \rightharpoonup \ddot{\mathbf{U}} \ \text{ in } \ L^2(0,T;L^2(\Omega)^d), \\
P_1^m \rightharpoonup P_1 \ \text{ in } \ L^2(0,T;L^2(\Omega_1)), \quad \mathbf{V}_2^m \rightharpoonup \mathbf{V}_2 \ \text{ in } \ L^2(0,T;\mathbf{H}_{0,\Gamma_{in}}(\text{div};\Omega_2)),
\end{gathered}$$

$$P_2^m \rightharpoonup P_2 \ \text{ in } \ L^2(0,T;L^2(\Omega_2)), \quad \dot{\mathbf{V}}_2^m \rightharpoonup \dot{\mathbf{V}}_2 \ \text{ in } \ L^2(0,T;L^2(\Omega_2)^d).$$

Next, in order to pass to the limit as $m \to \infty$ in the finite-dimensional problem (**GF**), we fix $\boldsymbol{\eta}_1 \in L^2(0,T;\mathbf{H}^1(\Omega_1))$, $\boldsymbol{\eta}_2 \in L^2(0,T;\mathbf{H}_{0,\Gamma_2}(\mathrm{div};\Omega_2))$, $\boldsymbol{\xi} \in L^2(0,T;\mathbf{H}_0^1(\Omega))$, $w \in L^2(0,T;L^2(\Omega_1))$, and $q \in L^2(0,T;L^2(\Omega_1))$, such that

$$\boldsymbol{\eta}_1(t) = \sum_{k=1}^{\infty} a_k(t)\mathbf{w}_1^k, \quad \boldsymbol{\eta}_2(t) = \sum_{k=1}^{\infty} b_k(t)\mathbf{w}_2^k, \quad \boldsymbol{\xi}(t) = \sum_{k=1}^{\infty} e_k(t)\boldsymbol{\Psi}^k,$$
$$w(t) = \sum_{k=1}^{\infty} c_k(t)q_1^k, \quad q(t) = \sum_{k=1}^{\infty} d_k(t)q_1^k \tag{58}$$

where (58) converges in $\mathbf{H}^1(\Omega_1)$, $\mathbf{H}_{0,\Gamma_2}(\mathrm{div};\Omega_2)$, $\mathbf{H}_0^1(\Omega)$, $L^2(\Omega_1)$, and $L^2(\Omega_2)$ respectively, for a.e. $t \in (0,T)$. Let

$$\boldsymbol{\eta}_1^N(t) = \sum_{k=1}^{N} a_k(t)\mathbf{w}_1^k, \quad \boldsymbol{\eta}_2^N(t) = \sum_{k=1}^{N} b_k(t)\mathbf{w}_2^k, \quad \boldsymbol{\xi}^N(t) = \sum_{k=1}^{N} e_k(t)\boldsymbol{\Psi}^k,$$
$$w^N(t) = \sum_{k=1}^{N} c_k(t)q_1^k, \quad q^N(t) = \sum_{k=1}^{N} d_k(t)q_1^k. \tag{59}$$

For $m \geq N$, $\boldsymbol{\eta}_1^N \in L^2(0,T;span\{\mathbf{w}_1^k\}_{k=1}^m)$, $\boldsymbol{\eta}_2^N \in L^2(0,T;span\{\mathbf{w}_2^k\}_{k=1}^m)$, $\boldsymbol{\xi}^N \in L^2(0,T;span\{\boldsymbol{\Psi}^k\}_{k=1}^m)$, $w^N \in L^2(0,T;span\{q_1^k\}_{k=1}^m)$, and $q^N \in L^2(0,T;span\{q_2^k\}_{k=1}^m)$. Further, from (58) and (59) we have $\boldsymbol{\eta}_1^N(t) \to \boldsymbol{\eta}_1(t)$, $\eta_2^N(t) \to \boldsymbol{\eta}_2(t)$, $\xi^N(t) \to \boldsymbol{\xi}$, $w^N(t) \to w$, $q^N(t) \to q$ converge weakly in $\mathbf{H}^1(\Omega_1)$, $\mathbf{H}_{0,\Gamma_2}(\mathrm{div};\Omega_2)$, $\mathbf{H}_0^1(\Omega)$, $L^2(\Omega_1)$, and $L^2(\Omega_2)$ respectively. We let $\boldsymbol{\eta}_1 = \boldsymbol{\eta}_1^N(t)$, $\boldsymbol{\eta}_2 = \boldsymbol{\eta}_2^N(t)$, $\boldsymbol{\xi} = \boldsymbol{\xi}^N(t)$, $w = w^N(t)$, $q = q^N(t)$ in (**GF**) and integrate with respect to $t \in (0,T)$.

For a fixed 'N', by the use of weak convergence of the finite-dimensional solution and continuity of the trace operator as $m \to \infty$, we get

$$
(E_{15})\begin{cases}
\int_0^T \Big[d_a(\dot{\mathbf{V}}_1(t),\boldsymbol{\eta}_1^N(t))_{\Omega_1} + 2d_a(\mathbb{D}^f(\mathbf{V}_1(t)),\mathbb{D}^f(\boldsymbol{\eta}_1^N(t)))_{\Omega_1} + \lambda d_a(\nabla\cdot\mathbf{V}_1(t),\nabla\cdot\boldsymbol{\eta}_1^N(t))_{\Omega_1} \\
-\varphi_1^f(P_1(t),\nabla\cdot\boldsymbol{\eta}_1^N(t))_{\Omega_1} + (\mathbf{K}_1\mathbf{V}_1(t),\boldsymbol{\eta}_1^N(t))_{\Omega_1} - (\mathbf{K}_1\dot{\mathbf{U}}_1(t),\boldsymbol{\eta}_1^N(t))_{\Omega_1} \\
+\beta^*(\mathbf{V}_1\cdot\hat{\mathbf{t}},\boldsymbol{\eta}_1^N(t)\cdot\hat{\mathbf{t}})_{\Gamma_I} + d_a\rho_{R_1}\langle\ddot{\mathbf{U}}(t),\boldsymbol{\xi}^N(t)\rangle_{\Omega_1} + 2\gamma_1^s(\mathbb{D}^s(\mathbf{U}(t)),\mathbb{D}^s(\boldsymbol{\xi}^N(t)))_{\Omega_1} \\
+\delta_1^s(\nabla\cdot\mathbf{U}(t),\nabla\cdot\boldsymbol{\xi}^N(t))_{\Omega_1} - \varphi_1^s(P_1(t),\nabla\cdot\boldsymbol{\xi}^N(t))_{\Omega_1} - (\mathbf{K}_1\mathbf{V}_1(t),\boldsymbol{\Psi}^i)_{\Omega_1} \\
+(\mathbf{K}_1\dot{\mathbf{U}}(t),\boldsymbol{\xi}^N(t))_{\Omega_1} + d_a\rho_{R_2}(\ddot{\mathbf{U}}(t),\boldsymbol{\xi}^N(t))_{\Omega_2} + 2\gamma_2^s(\mathbb{D}^s(\mathbf{U}(t)),\mathbb{D}^s(\boldsymbol{\xi}^N(t)))_{\Omega_2} \\
+\delta_2^s(\nabla\cdot\mathbf{U}(t),\nabla\cdot\boldsymbol{\xi}^N(t))_{\Omega_2} - \varphi_2^s(P_2(t),\nabla\cdot\boldsymbol{\xi}^N(t))_{\Omega_2} - (\mathbf{K}_2\mathbf{V}_2(t),\boldsymbol{\xi}^N(t))_{\Omega_2} \\
+(\mathbf{K}_2\dot{\mathbf{U}}(t),\boldsymbol{\xi}^N(t))_{\Omega_2} + d_a(\dot{\mathbf{V}}_2(t),\boldsymbol{\eta}_2^N(t))_{\Omega_2} - \varphi_2^f(P_2(t),\nabla\cdot\boldsymbol{\eta}_2^N(t))_{\Omega_2} \\
+(\mathbf{K}_2\mathbf{V}_2(t),\boldsymbol{\eta}_2^N(t))_{\Omega_2} - (\mathbf{K}_2\dot{\mathbf{U}}_2(t),\boldsymbol{\eta}_2^N(t))_{\Omega_2} + \varphi_1^f(\nabla\cdot\mathbf{V}_1(t),w^N(t))_{\Omega_1} \\
+\varphi_1^s(\nabla\dot{\mathbf{U}}_1(t),w^N(t))_{\Omega_1} + \alpha_1^2(P_1(t),w^N(t))_{\Omega_1} + \varphi_2^f(\nabla\cdot\mathbf{V}_2(t),q^N(t))_{\Omega_2} \\
+\varphi_2^s(\nabla\dot{\mathbf{U}}_2(t),q^N(t))_{\Omega_2} + \alpha_2^2(P_2(t),q^N(t))_{\Omega_2}\Big]\,dt = \int_0^T \Big[(\mathbf{b}_1^f(t),\boldsymbol{\eta}_1^N(t))_{\Omega_1} \\
+(\mathbf{T}_\infty^f(t),\boldsymbol{\eta}_1^N(t))_{\Gamma_1} + (\mathbf{b}_1^s(t),\boldsymbol{\xi}^N(t))_{\Omega_1} + (\mathbf{b}_2^s(t),\boldsymbol{\xi}^N(t))_{\Omega_2} \\
+(\mathbf{b}_2^f(t),\boldsymbol{\eta}_2^N(t))_{\Omega_2} + (\alpha_1^2,w^N(t))_{\Omega_1} + (\alpha_2^2,q^N(t))_{\Omega_2}\Big]\,dt.
\end{cases}
$$

Next letting $N\to\infty$, we obtain the weak formulation (A_w) for a.e. $t\in(0,T)$ and for all $\boldsymbol{\eta}_1(t)\in\mathbf{H}^1(\Omega_1)$, $\boldsymbol{\eta}_2(t)\in\mathbf{H}_{0,\Gamma_2}(\mathrm{div};\Omega_2)$, $\boldsymbol{\xi}(t)\in\mathbf{H}_0^1(\Omega)$, $w(t)\in L^2(\Omega_1)$, and $q(t)\in L^2(\Omega_1)$. Further, passing to the limits in the a priori estimates (43), (E_5), (44), (E_6), (46) and (47), we obtain the bounds (30), (E_1), (31), (E_2), (33) and (34). Passing to the limits in (**GF**) and recovery of initial conditions gives the existence of a solution of (A_w). This completes the proof of Theorem 2. In the next section, we ensure that there is only one solution that satisfies the weak formulation (A_w).

3.6 Continuous Dependence of the Solution on the Given Data

Theorem 4. *Assume that* $\mathbf{b}_i^j\in H^1(0,T;\mathbf{L}^2(\Omega_i))$, $i\in\{1,2\}$, $j\in\{f,s\}$, $\mathbf{T}_\infty^f\in H^1(0,T;\mathbf{L}^2(\Gamma_1))$, *and* $\mathbf{T}_\infty^f(x,0)=0$. *Then, the weak formulation* (A_w) *has a unique solution that depends continuously on the given data.*

Proof of Theorem 4: Define a function of 't',

$$
\Big[G_1^*(t)\Big]^2 = ||\mathbf{b}_{1,1}^f(t)-\mathbf{b}_{1,2}^f(t)||_{\Omega_1}^2 + \frac{\alpha_3\alpha_4}{\min\{2d_a,K_{\min}^1\}}||\mathbf{T}_{\infty,1}^f(t)-\mathbf{T}_{\infty,2}^f(t)||_{\Gamma_1}^2
$$
$$
+\frac{1}{2K_{\min}^1}||\mathbf{b}_{1,1}^s(t)-\mathbf{b}_{1,2}^s(t)||_{\Omega_1}^2 + \frac{1}{\alpha_1^2}||\alpha_{1,1}^2-\alpha_{1,2}^2||_{\Omega_1}^2 + \frac{1}{2K_{\min}^1}||\mathbf{b}_{2,1}^s(t)-\mathbf{b}_{2,2}^s(t)||_{\Omega_2}^2
$$

$$+\frac{1}{2K_{\min}^2}||\mathbf{b}_{2,1}^f(t)-\mathbf{b}_{2,2}^f(t)||_{\Omega_2}^2+\frac{1}{\alpha_2^2}||\alpha_{2,1}^2-\alpha_{2,2}^2||_{\Omega_2}^2.$$

Let $(\mathbf{V}_1^1,\mathbf{V}_2^1,\mathbf{U}^1,P_1^1,P_2^1)$ and $(\mathbf{V}_1^2,\mathbf{V}_2^2,\mathbf{U}^2,P_1^2,P_2^2)$ be two solutions of (A_w) with two sets of data
$(\mathbf{b}_{1,1}^f,\mathbf{b}_{1,1}^s,\mathbf{b}_{2,1}^f,\mathbf{b}_{2,1}^s,\alpha_{1,1}^2,\alpha_{2,1}^2,\mathbf{T}_{\infty,1}^f)$ and $(\mathbf{b}_{1,2}^f,\mathbf{b}_{1,2}^s,\mathbf{b}_{2,2}^f,\mathbf{b}_{2,2}^s,\alpha_{1,2}^2,\alpha_{2,2}^2,\mathbf{T}_{\infty,2}^f)$.
Define the differences

$$(\mathbf{V}_1,\mathbf{V}_2,\mathbf{U},P_1,P_2)=(\mathbf{V}_1^1-\mathbf{V}_1^2,\mathbf{V}_2^1-\mathbf{V}_2^2,\mathbf{U}^1-\mathbf{U}^2,P_1^1-P_1^2,P_2^1-P_2^2)$$

and

$$\mathbf{b}_1^f=\mathbf{b}_{1,1}^f-\mathbf{b}_{1,2}^f,\ \mathbf{b}_1^s=\mathbf{b}_{1,1}^s-\mathbf{b}_{1,2}^s,\ \mathbf{b}_2^f=\mathbf{b}_{2,1}^f-\mathbf{b}_{2,2}^f,\ \mathbf{b}_2^s=\mathbf{b}_{2,1}^s-\mathbf{b}_{2,2}^s,\ \alpha_1^2=\alpha_{1,1}^2-\alpha_{1,2}^2,$$
$$\alpha_2^2=\alpha_{2,1}^2-\alpha_{2,2}^2,\ \mathbf{T}_\infty^f=\mathbf{T}_{\infty,1}^f-\mathbf{T}_{\infty,2}^f.$$

Choosing the test functions $\boldsymbol{\eta}_1=\mathbf{V}_1(t)$, $\boldsymbol{\eta}_2=\mathbf{V}_2(t)$, $\boldsymbol{\xi}=\dot{\mathbf{U}}(t)$, $w=P_1(t)$, $q=P_2(t)$ in the weak formulation (A_w), and using the Cauchy-Schwarz, trace, and Korn's inequalities, and integrating with respect to $t\in(0,\ t)$, we obtain

$$(E_{20})\begin{cases} d_a||\mathbf{V}_1(t)||_{\Omega_1}^2+\min\{2d_a,K_{\min}^1\}\int_0^t\left[||\mathbb{D}^f(\mathbf{V}_1(\zeta))||_{\Omega_1}^2+||\mathbf{V}_1(\zeta)||_{\Omega_1}^2\right]d\zeta \\ +\int_0^t\left[2\lambda d_a||\nabla\cdot\mathbf{V}_1(\zeta)||_{\Omega_1}^2+2\beta^*||\mathbf{V}_1(\zeta)\cdot\hat{\mathbf{t}}||_{\Gamma_I}^2\right]d\zeta+\left[d_a\rho_{R_1}||\dot{\mathbf{U}}(t)||_{\Omega_1}^2\right. \\ \left.+2\gamma_1^s||\mathbb{D}^s(\mathbf{U}(t))||_{\Omega_1}^2+\delta_1^s||\nabla\cdot\mathbf{U}(t)||_{\Omega_1}^2\right]+\left[d_a\rho_{R_2}||\dot{\mathbf{U}}(t)||_{\Omega_2}^2+2\gamma_2^s||\mathbb{D}^s(\mathbf{U}(t))||_{\Omega_2}^2\right. \\ \left.+\delta_2^s||\nabla\cdot\mathbf{U}(t)||_{\Omega_2}^2\right]+d_a||\mathbf{V}_2(t)||_{\Omega_2}^2+\int_0^t\left[\alpha_1^2||P_1(\zeta)||_{\Omega_1}^2+\alpha_2^2||P_2(\zeta)||_{\Omega_2}^2\right]d\zeta \\ \leq\int_0^t[G_1^*(\zeta)]^2\,d\zeta+\int_0^t\left[2K_{\max}^1||\dot{\mathbf{U}}(\zeta)||_{\Omega_1}^2+(1+2K_{\max}^1)||\mathbf{V}_1(\zeta)||_{\Omega_1}^2+2K_{\max}^2||\dot{\mathbf{U}}(\zeta)||_{\Omega_2}^2\right. \\ \left.+2K_{\max}^2||\mathbf{V}_2(\zeta)||_{\Omega_2}^2\right]d\zeta. \end{cases}$$

From (E_{20}) we can extract

$$(E_{21})\begin{cases} ||\mathbf{V}_1(t)||_{\Omega_1}^2+||\dot{\mathbf{U}}(t)||_{\Omega_1}^2+||\dot{\mathbf{U}}(t)||_{\Omega_2}^2+||\mathbf{V}_2(t)||_{\Omega_2}^2\leq\frac{1}{\rho_{\min}d_a}\left[||G_1^*||_{L^2(0,T)}^2\right] \\ +\frac{\mu}{\rho_{\min}d_a}\int_0^t\left[||\dot{\mathbf{U}}(\zeta)||_{\Omega_1}^2+||\mathbf{V}_1(\zeta)||_{\Omega_1}^2+||\dot{\mathbf{U}}(\zeta)||_{\Omega_2}^2+||\mathbf{V}_2(\zeta)||_{\Omega_2}^2\right]d\zeta. \end{cases}$$

Gronwall's integral inequality supplies

$$||\mathbf{V}_1(t)||_{\Omega_1}^2+||\dot{\mathbf{U}}(t)||_{\Omega_1}^2+||\dot{\mathbf{U}}(t)||_{\Omega_2}^2+||\mathbf{V}_2(t)||_{\Omega_2}^2\leq\frac{1}{\rho_{\min}d_a}\left[||G_1^*||_{L^2(0,T)}^2\right]\exp\left(\frac{\mu}{\rho_{\min}d_a}T\right),\tag{60}$$

or,

$$
\begin{aligned}
&||\mathbf{V}_1^1-\mathbf{V}_1^2||^2_{L^\infty(0,T,\mathbf{L}^2(\Omega_1))}+||\dot{\mathbf{U}}^1-\dot{\mathbf{U}}^2||^2_{L^\infty(0,T,\mathbf{L}^2(\Omega))}+||\mathbf{V}_2^1-\mathbf{V}_2^2||^2_{L^\infty(0,T,\mathbf{L}^2(\Omega_2))}\\
&\qquad\leq \beta_0\Big[||\mathbf{b}^f_{1,1}(t)-\mathbf{b}^f_{1,2}(t)||^2_{\Omega_1}+\frac{\alpha_3\alpha_4}{\min\{2d_a,K^1_{\min}\}}||\mathbf{T}^f_{\infty,1}(t)-\mathbf{T}^f_{\infty,2}(t)||^2_{\Gamma_1}\\
&+\frac{1}{2K^1_{\min}}||\mathbf{b}^s_{1,1}(t)-\mathbf{b}^s_{1,2}(t)||^2_{\Omega_1}+\frac{1}{\alpha_1^2}||\alpha^2_{1,1}-\alpha^2_{1,2}||^2_{\Omega_1}+\frac{1}{2K^2_{\min}}||\mathbf{b}^2_{s,1}(t)-\mathbf{b}^2_{s,2}(t)||^2_{\Omega_2}\\
&\qquad+\frac{1}{2K^2_{\min}}||\mathbf{b}^f_{2,1}(t)-\mathbf{b}^f_{2,2}(t)||^2_{\Omega_2}+\frac{1}{\alpha_2^2}||\alpha^2_{2,1}-\alpha^2_{2,2}||^2_{\Omega_2}\Big],
\end{aligned}
\tag{61}
$$

where $\beta_0=\frac{1}{\rho_{\min}d_a}\exp\left(\frac{\mu}{\rho_{\min}\mathbf{d}_a}T\right)$. Further, using (60) and (E_{20}) we obtain

$$
(E_{22})\begin{cases}
\frac{\min\{2d_a,K^1_{\min}\}}{\alpha_3}||\mathbf{V}_1^1-\mathbf{V}_1^2||^2_{L^2(0,T,\mathbf{H}^1(\Omega_1))}+2\gamma_1^s||\mathbb{D}^s(\mathbf{U}^1)-\mathbb{D}^s(\mathbf{U}^2)||^2_{L^\infty(0,T,\mathbf{L}^2(\Omega_1))}\\
+2\gamma_2^s||\mathbb{D}^s(\mathbf{U}^1)-\mathbb{D}^s(\mathbf{U}^2)||^2_{L^\infty(0,T,\mathbf{L}^2(\Omega_2))}+\alpha_1^2||P_1^1-P_1^2||^2_{L^2(0,T,L^2(\Omega_1))}\\
+\alpha_2^2||P_2^1-P_2^2||^2_{L^2(0,T,L^2(\Omega_2))}\leq\beta_1\Big[||\mathbf{b}^f_{1,1}(t)-\mathbf{b}^f_{1,2}(t)||^2_{\Omega_1}\\
+\frac{\alpha_3\alpha_4}{\min\{2d_a,K^1_{\min}\}}||\mathbf{T}^f_{\infty,1}(t)-\mathbf{T}^f_{\infty,2}(t)||^2_{\Gamma_1}+\frac{1}{2K^1_{\min}}||\mathbf{b}^s_{1,1}(t)-\mathbf{b}^s_{1,2}(t)||^2_{\Omega_1}\\
+\frac{1}{\alpha_1^2}||\alpha^2_{1,1}-\alpha^2_{1,2}||^2_{\Omega_1}+\frac{1}{2K^2_{\min}}||\mathbf{b}^s_{2,1}(t)-\mathbf{b}^s_{2,2}(t)||^2_{\Omega_2}\\
+\frac{1}{2K^2_{\min}}||\mathbf{b}^f_{2,1}(t)-\mathbf{b}^f_{2,2}(t)||^2_{\Omega_2}+\frac{1}{\alpha_2^2}||\alpha^2_{2,1}-\alpha^2_{2,2}||^2_{\Omega_2}\Big],
\end{cases}
$$

where $\beta_1=\left\{1+\frac{T}{\rho_{\min}d_a}\left[1+4(K^1_{\max}+K^2_{\max})\right]\exp\left(\frac{\mu}{\rho_{\min}d_a}T\right)\right\}$. Thus, if $(\mathbf{b}^f_{1,1},\mathbf{b}^s_{1,1},\mathbf{b}^f_{2,1},\mathbf{b}^s_{2,1},\alpha^2_{1,1},\alpha^2_{2,1},\mathbf{T}^f_{\infty,1})$ close to $(\mathbf{b}^f_{1,2},\mathbf{b}^s_{1,2},\mathbf{b}^f_{2,2},\mathbf{b}^s_{2,2},\alpha^2_{1,2},\alpha^2_{2,2},\mathbf{T}^f_{\infty,2})$ then left hand side of (61) or (E_{22}) (the difference of solutions) must be small. Hence, the solution continuously depends on the data. This also implies the uniqueness of solutions. This completes the proof of Theorem 4.

Remark 2. *We have shown that* $\mathbf{V}_1\in L^2(0,T;\mathbf{H}^1(\Omega_1))$, $\dot{\mathbf{V}}_1\in L^2(0,T;(\mathbf{H}^1(\Omega_1))^*)$, *implying* $\mathbf{V}_1\in C([0,T];\mathbf{L}^2(\Omega_1))$. *Further, we have shown* $\mathbf{U}\in L^2(0,T;\mathbf{H}^1_0(\Omega))$, $\dot{\mathbf{U}}_s\in L^2(0,T;\mathbf{L}^2(\Omega))$, *and* $\ddot{\mathbf{U}}_s\in L^2(0,T;\mathbf{H}^{-1}(\Omega))$, *implying* $\mathbf{U}\in C([0,T];\mathbf{L}^2(\Omega))$ *and* $\dot{\mathbf{U}}_s\in C([0,T];\mathbf{H}^{-1}(\Omega))$.

Having proven the existence and uniqueness of results, we now wish to take a step toward a realistic scenario. In this direction, we list the parameters involved in the model and use the literature to estimate the range of their values. We then use these data to compute the system energy and estimate its maximum value.

4 Estimates of Parameter Values

A tumour mass can develop within a healthy tissue environment when cells divide uncontrollably due to genetic and epigenetic mutations. Tumours and their surrounding healthy tissue have many structural and functional differences. When we model a tumour and its surrounding host tissue as deformable porous media, the structural and material parameters, such as interstitial hydraulic conductivity, interstitial fluid viscosity, and the elasticity of the solid phase, distinguish them. In Table 1, we list all the poroelastohydrodynamic parameters involved, along with reference values for specific tissues. Based on these values, we compute the ranges of the dimensionless model parameters that appear in the governing equations (see Table 2). Blood perfusion in tumours is significantly lower than the surrounding normal tissue due to several reasons, including the presence of leaky and compressed blood vessels, heterogeneously distributed blood vessels, high interstitial fluid pressure, and dilated and tortuous capillaries [55]. With this view in mind, we consider tumour tissue to be less permeable than its host. We use a Darcy-type momentum equation to describe interstitial fluid flow inside the tumour. By contrast, we use a Brinkman-type momentum equation to describe fluid flow through the surrounding normal host tissue.

Solid tumours are typically stiffer than the surrounding normal tissue, and this increased rigidity is often associated with a higher cancer risk, as well as contributing to tumour invasion and metastasis. This increased stiffness is attributed to the overproduction and cross-linking of extracellular matrix (ECM) proteins, such as collagen, within the tumour microenvironment [53, 54]. Hence, the magnitudes of the Poisson ratio and Young's modulus are considered accordingly. These parameters are often clinically significant when diagnosing, treating, and predicting the malignancy. Young's modulus and Poisson ratio values are considered within a specific range, as described in Table 2 [42]. On the other hand, the magnitudes of K_1 and K_2 vary significantly depending on tumour type and host tissue. We report a broad range of values for K_2 and K_1 in Tables 3 and 4, respectively, covering five tumour types and their corresponding host values.

5 System Energy (SE) Bounds

Establishing the well-posedness of the governing unsteady poro-elastohydrodynamic system for the tumour model considered validates the overall modelling approach. Obtaining relevant stability estimates reveals the solution behaviour in response to various parameters. Implementing Equations (12)-(21) using the Galerkin method would provide a means to understand the behaviour of the present model for arbitrarily shaped tumours in higher dimensions.

To establish the well-posedness of the unsteady tumour poroelastohydrodynamics model, it is necessary to show existence-uniqueness results over the Sobolev space using L^2 and H^1 norms. The L^2 norm of the velocity of a specific phase represents the kinetic energy of that phase. On the other hand, the H^1 norm of a phase velocity represents a higher state of energy where the velocity gradient is involved. Alam et

Parameter	Description	Baseline value	References
R_{I}	Radius of tumour	0.007-0.013 m	[37]
φ_1^s and φ_2^s	Volume fractions of tumour and normal cells	0.6-0.8	[37]
K_d	hydraulic resistivity inside a tumour interior in the absence of deformation	32.28×10^{12} Pa sec m^{-2}	[19, 20]
μ^f	Interstitial fluid viscosity	3.5×10^{-3} $\text{kgm}^{-1}\text{s}^{-1}$	[38, 39]
ρ^f	Interstitial fluid density	1×10^3 kgm^{-3}	[39]
ρ_1^s	Normal tissue density	1.030×10^3 kgm^{-3}	[37]
ρ_2^s	tumour tissue density	1.040×10^3 kgm^{-3}	[37]
$\mathcal{Y}_1^s$	Young's modulus of normal tissue	$0.5 - 30$ kPa (varies among various normal tissues)	[40]
$\mathcal{Y}_2^s$	Young's modulus of tumour tissue	$0.8 - 11,000$ kPa (varies among various tumours)	[40]
P_{F}	Weighted vascular pressure	5 mmHg	[6, 7, 20, 41]

Table 1: Different poroelastohydrodynamics parameters corresponding to the tumour and surrounding healthy tissue with their baseline values

Dimensionless parameter	Description	Range of values	References
d_a	Darcy's number (Dimensionless specific permeability of tumour)	$10^{-4} - 10^{-3}$	[6, 7]
α_1 and α_2	Strength of transvascular solute perfusion inside normal and tumour tissue	$\alpha_1, \alpha_2 \geq 0$	[6, 7]
ϱ_1^s and ϱ_2^s	Dimensionless Young's modulus (YM) corresponding to various soft normal(host) and tumour tissues respectively	$0.001 \leq \varrho_1^s \leq 1$ $0.01 \leq \varrho_2^s \leq 1$	[6, 7]
ν_1^s and ν_2^s	Poisson ratio (PR) corresponding to normal and tumour tissues respectively	$0.45 \leq \nu_1^s, \nu_2^s \leq 0.49$	[6, 7, 42, 43]

Table 2: Different dimensionless poroelastodynamics parameters corresponding to the tumour and surrounding healthy tissue with their value range.

tumour type	**Hydraulic conductivity** ($cm^2 mmHg^{-1} sec^{-1} \times 10^{-8}$)	**Calculated hydraulic resistivity** (Pa sec $m^{-2} \times 10^{12}$) 1 mmHg = 133.322 Pa	**Normalized K_2** ($= K_2/K_d$)	**References**
Fibrosarcoma (Human)	$100 - 1360$	$0.098 - 1.33$	$\sim 0.003 - 0.04$	[40]
Hepatoma (Human)	$3 - 4.1, 28$	$4.76,\ 32.52 - 44.44$	$0.15,\ \sim 1 - 1.377$	[40]
4T1 murine tumour (Human)	$950 - 2300$	$0.058 - 0.14$	$\sim 0.0018 - 0.004$	[40]
U87 tumour (Human)	$65 - 7000$ [40]	$0.019 - 2.05$	$\sim 0.0006 - 0.063$	
MCaIV tumour (Rat)	248	0.5376	~ 0.0167	[40]

Table 3: Estimated values of normalised hydraulic resistivity for different types of tumours.

Tumour tissue type	**Normal Host site**	**Hydraulic conductivity** ($m^2 Pa^{-1} sec^{-1} \times 10^{-12}$)	**Calculated hydraulic resistivity** (Pa sec $m^{-2} \times 10^{12}$)	**Normalized K_1** ($= K_1/K_d$)	References
Fibrosarcoma (Human)	Mesenchyme (fibrous connective tissue)	$0.0021 - 0.0064$, $0.045 - 0.141$	$156.25 - 476.19$, $7.092 - 22.22$	$\sim\ 4.84 - 14.75$ $\sim\ 0.22 - 0.69$	[44, 45] [40, 45]
Hepatoma (Human)	Hepatic sinusoids	6.5	0.154	~ 0.005	[45, 46]
4T1 murine tumour (Human)	mammary gland (primary), lymph nodes, lung, and bone.	$0.025 - 1.5$	$0.67 - 40$	$0.02 - 1.24$	Ch. 31 of [47]
U87 tumour (Human)	Brain tissue	$4 - 1000$ $0.015 - 0.9$	$0.001 - 0.25$ $1.11 - 66.67$	$3.1 \times 10^{-5} - 0.0077$ $0.034 - 2.065$	[48, 49]
MCaIV tumour (Rat)	Rat abdominal muscle	$0.1125 - 0.585$	$1.71 - 8.89$	$0.053 - 0.275$	[40]

Table 4: Estimated values of the normalised hydraulic resistivity for healthy host tissues

al. [3, 4] introduce the term system energy or internal energy, which is calculated using the composite velocity field. We can discuss the system energy behaviour using upper and lower bounds of L^2 and H^1 norms of the composite velocity field inside the tumour.

The L^2 system energy (SE) within a tissue domain Ω is defined as $\| V_2^{\text{com}} \|_{\Omega}^2$. Accordingly, we define

$$\mathcal{E}_{\Omega_2} = \| V_2^{\text{com}} \|_{\Omega_2}^2 = \| \varphi_2^f V_2^f + \varphi_2^s V_2^s \|_{\Omega_2}^2 . \tag{62}$$

We estimate the maximum of $\mathcal{E}_{\Omega_2}$ using the estimate (30) developed in Section 3

$$\begin{aligned} \| V_2^{\text{com}} \|_{\Omega_2} &= \| \varphi_2^f V_2^f + \varphi_2^s V_2^s \|_{\Omega_2} \\ &\leq \varphi_2^f \| V_2^f \|_{\Omega_2} + \varphi_2^s \| V_2^s \|_{\Omega_2}, \\ &= \frac{T}{\rho_{\min} \mathrm{d}_a} \left[\frac{\alpha_3 \alpha_4}{\min\{2\mathrm{d}_a, K_1\}} \left(T_\infty^f\right)^2 + \alpha_1^2 + \alpha_2^2 \right] \exp\left(\frac{\mu \tau}{\rho_{\min} \mathrm{d}_a} \right), \end{aligned} \tag{63}$$

where $\tau > 0$, $\rho_{\min} = \min\{1, \rho_{\mathrm{R}_1}, \rho_{\mathrm{R}_2}\}$, $\mu = \max\{(1 + 2K_1), 2K_2\}$. If we choose $\alpha_1 = 1$, $\alpha_2 = 1$, and $\alpha_3 \alpha_4 \left(T_\infty^f\right)^2 = 1$, the following maximum of the system energy (MASE) is obtained

$$\overline{\mathcal{E}}_{\Omega_2} = \left(\frac{T}{\rho_{\min} \mathrm{d}_a} \right)^2 \left[\frac{1}{\min\{2\mathrm{d}_a, K_1\}} + 2 \right]^2 \exp\left(\frac{2\mu \tau}{\rho_{\min} \mathrm{d}_a} \right), \tag{64}$$

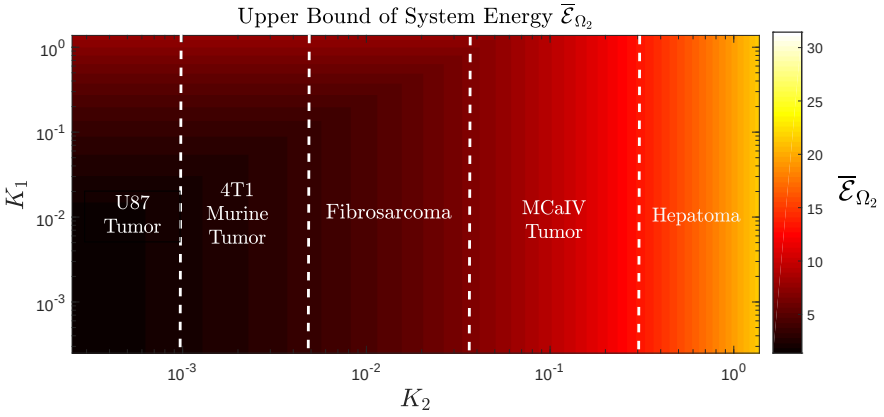

Fig. 2: (Colour online) Maximum of system energy for tumour tissues with different values of K_1 and K_2

Figure 2 shows the variation of $\overline{\mathcal{E}}_{\Omega_2}$, (as defined by equation (64)) as K_1 and K_2, vary between the values associated with different types of tumour. We find that $\overline{\mathcal{E}}_{\Omega_2}$ attains its minimum value for U87 tumours and its maximum value for hepatoma tumours, which evolve within brain tissue and hepatic lobes, respectively.

On the other hand, the minimum of system energy (MISE) can be computed from the 1D closed form solution of the poroelastohydrodynamic equations inside the tumour tissue. We consider the geometry depicted in Figure 3, which represents a simplified form of Figure 1 where the boundary Γ_2 maps to the point $\mathrm{x} = 0$, the tumour boundary Γ_{I} maps to $\mathrm{x} = \mathrm{x}_{\mathrm{I}}$ and the host boundary Γ_1 maps to $\mathrm{x} = \mathrm{x}_{\mathrm{H}}$. Attention is restricted to short timescales for which cell proliferation and death can be neglected.

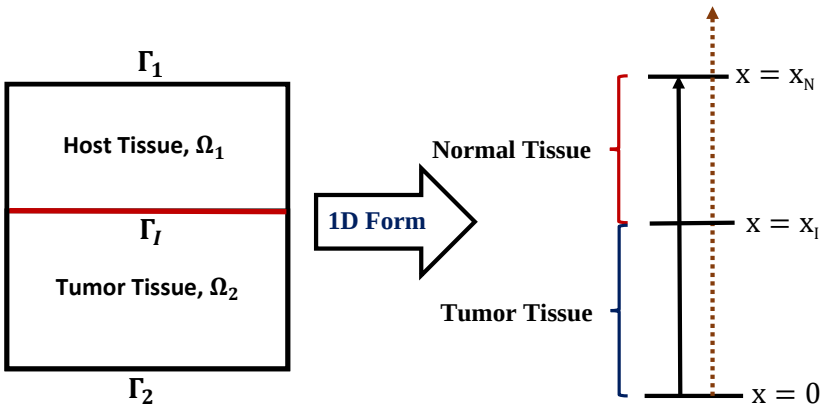

Fig. 3: (Colour online) Schematic of domain for the 1D solution

Now, we seek an analytical solution of Equations $\mathcal{M}_1$: (12)-(14) and $\mathcal{M}_2$: (15)-(17) for a 1D cartesian geometry subject to the boundary conditions (9a) and (9c)-(11). We assume $P_{\mathrm{i}}(\mathbf{x},t) = P_{\mathrm{i}}(\mathrm{x},t)$, $\mathbf{U}^s_{\mathrm{i}}(\mathbf{x},t) = U^s_{\mathrm{i}}(\mathrm{x},t)\hat{\mathbf{e}}_{\mathbf{x}}$ and $\mathbf{V}^f_{\mathrm{i}}(\mathbf{x},t) = V^f_{\mathrm{i}}(\mathrm{x},t)\hat{\mathbf{e}}_{\mathbf{x}}$, for $\mathrm{i} \in \{\mathrm{H},\ \mathrm{T}\}$. The 1D equations are as follows

$$\frac{\partial}{\partial \mathrm{x}}\left(\varphi^f_1 V^f_1\right) = \mathcal{S}_1, \quad \frac{\partial}{\partial \mathrm{x}}\left(\varphi^s_1 \frac{\partial U^s_1}{\partial t}\right) = 0, \tag{65a}$$

and

$$\frac{\partial}{\partial \mathrm{x}}\left(\varphi^f_2 V^f_2\right) = \mathcal{S}_2, \quad \frac{\partial}{\partial \mathrm{x}}\left(\varphi^s_2 \frac{\partial U^s_2}{\partial t}\right) = 0, \tag{65b}$$

$$d_a \frac{\partial V^f_1}{\partial t} + \varphi^f_1 \frac{\partial P_1}{\partial \mathrm{x}} + K_1\left(V^f_1 - \frac{\partial U^s_1}{\partial t}\right) = d_a(\lambda+2)\frac{\partial^2 V^f_1}{\partial \mathrm{x}^2}, \tag{65c}$$

and

$$d_a \frac{\partial V^f_2}{\partial t} + \varphi^f_2 \frac{\partial P_2}{\partial \mathrm{x}} + K_2\left(V^f_2 - \frac{\partial U^s_2}{\partial t}\right) = 0, \tag{65d}$$

$$d_a\rho_{\mathrm{R}_1}\frac{\partial}{\partial t}\left(\frac{\partial U_1^s}{\partial t}\right)+\varphi_1^s\frac{\partial P_1}{\partial \mathrm{x}}+K_1\left(\frac{\partial U_1^s}{\partial t}-V_1^f\right)-\frac{\varrho_1^s(1-\nu_1^s)}{(1+\nu_1^s)(1-2\nu_1^s)}\frac{\partial^2 U_1^s}{\partial \mathrm{x}^2}=0, \quad (65e)$$

and

$$d_a\rho_{\mathrm{R}_2}\frac{\partial}{\partial t}\left(\frac{\partial U_2^s}{\partial t}\right)+\varphi_2^s\frac{\partial P_2}{\partial \mathrm{x}}+K_2\left(\frac{\partial U_2^s}{\partial t}-V_2^f\right)-\frac{\varrho_2^s(1-\nu_2^s)}{(1+\nu_2^s)(1-2\nu_2^s)}\frac{\partial^2 U_2^s}{\partial \mathrm{x}^2}=0. \quad (65f)$$

In Equations (65a) and (65b), we note that

$$\mathcal{S}_i(\mathrm{x},t)=\alpha_i^2\left(1-P_i(\mathrm{x},t)\right), \qquad i\in\{\mathrm{H},\ \mathrm{T}\}. \quad (66)$$

The interstitial fluid source term depends only on the IFP. We note that Equations (65a) and (65b) involve multiple parameters, and simultaneously considering all of them will be challenging. However, certain biological assumptions can be used to simplify the parameter dependency. One can move to Appendix (A.3) for discussions regarding parameter simplification and a detailed description of the analytical solution.

We can compute the minimum system energy (MISE) from the 1D closed-form solution of poroelastohydrodynamics in tumour tissue. For the bounded domain Ω_2 such that in 1D form $V_2^{\mathrm{com}^*}\in L^2([0,\ \mathrm{x_I}])$ and $1\in L^2([0,\ \mathrm{x_I}])$ then using Hölder's inequality we obtain

$$\left|\int_{\mathrm{x}\in\mathcal{I}_{\mathrm{x_I}}} V_2^{\mathrm{com}^*}\mathrm{dx}\right|\leq\int_{\mathrm{x}\in\mathcal{I}_{\mathrm{x_I}}}\left|V_2^{\mathrm{com}^*}\right|\mathrm{dx}\leq\sqrt{\mathrm{x_I}}\left(\int_{\mathrm{x}\in\mathcal{I}_{\mathrm{x_I}}}\left|V_2^{\mathrm{com}^*}\right|^2\mathrm{dx}\right)^{\frac{1}{2}}, \quad (67)$$

where $\mathcal{I}_{\mathrm{x_I}}=[0,\mathrm{x_I}]$. Similarly,

$$\left|\int_{\mathrm{x}\in\mathcal{I}_{\mathrm{x_I}}}\nabla_{\mathrm{x}}V_2^{\mathrm{com}^*}\mathrm{dx}\right|\leq\int_{\mathrm{x}\in\mathcal{I}_{\mathrm{x_I}}}\left|\nabla_{\mathrm{x}}V_2^{\mathrm{com}^*}\right|\mathrm{dx}\leq\sqrt{\mathrm{x_I}}\left(\int_{\mathrm{x}\in\mathcal{I}_{\mathrm{x_I}}}\left|\nabla_{\mathrm{x}}V_2^{\mathrm{com}^*}\right|^2\mathrm{dx}\right)^{\frac{1}{2}}. \quad (68)$$

The corresponding minimum of the system energy based on the lower bounds of L^2 and H^1 norms is respectively given as

$$\underline{\mathcal{E}}_{L^2(\mathcal{I}_{\mathrm{x}_2})}=\left|\int_{\mathrm{x}\in\mathcal{I}_{\mathrm{x_I}}}V_2^{\mathrm{com}^*}\mathrm{dx}\right|\leq\left(\int_{\mathrm{x}\in\mathcal{I}_{\mathrm{x_I}}}\left|V_2^{\mathrm{com}^*}\right|^2\mathrm{dx}\right)^{\frac{1}{2}}=\sqrt{\mathrm{x_I}}\parallel V_2^{\mathrm{com}^*}\parallel_{L^2(\mathcal{I}_{\mathrm{x_I}})}, \quad (69)$$

and

$$\underline{\mathcal{E}}_{H^1(\mathcal{I}_{\mathrm{x_I}})}=\left[\left|\int_{\mathrm{x}\in\mathcal{I}_{\mathrm{x_I}}}V_2^{\mathrm{com}^*}\mathrm{dx}\right|^2+\left|\int_{\mathrm{x}\in\mathcal{I}_{\mathrm{x_I}}}\nabla_{\mathrm{x}}V_2^{\mathrm{com}^*}\mathrm{dx}\right|^2\right]^{\frac{1}{2}}$$

$$\leq \sqrt{\mathrm{x_I}} \left[\left(\int_{\mathrm{x} \in \mathcal{I}_{\mathrm{x_I}}} \left| V_2^{\mathrm{com}^*} \right|^2 \right) + \left(\int_{\mathrm{x} \in \mathcal{I}_{\mathrm{x_I}}} \left| \nabla_{\mathrm{x}} V_2^{\mathrm{com}^*} \right|^2 \right) \right]^{\frac{1}{2}} = \sqrt{\mathrm{x_I}} \parallel V_2^{\mathrm{com}^*} \parallel_{H^1(\mathcal{I}_{\mathrm{x_I}})} \quad (70)$$

which can be further manipulated as

$$\underline{\mathcal{E}}_{H^1(\mathcal{I}_{\mathrm{x_I}})} = \left[\left| \int_{\mathrm{x} \in \mathcal{I}_{\mathrm{x_I}}} V_2^{\mathrm{com}^*} \mathrm{dx} \right|^2 + \left| V_2^{\mathrm{com}^*}(\mathrm{x} = \mathrm{x_I}) - V_2^{\mathrm{com}^*}(\mathrm{x} = 0) \right|^2 \right]^{\frac{1}{2}}, \quad (71)$$

where the first term on the right-hand side represents volumetric flux as above, and the second term represents net velocity gradient within $\mathcal{I}_{\mathrm{x_I}}$. The second term signifies the velocity difference between the periphery and the tumour center. We identify two parameters, dimensionless hydraulic resistivity (K_2) and solute perfusion strength (α_2), through the vasculature that promote the lower limit of system energy ($\underline{\mathcal{E}}_k$).

We show the behavior of $\underline{\mathcal{E}}_k$ changes as K_2 varies for fibrosarcoma in Figure 4, where $\alpha_2 = 5$ and $\ln(t) \in \left[10^{-3},\ 10^{1}\right]$. Our discussion utilizes a logarithmic time interval scale ranging from 10^{-3} to 10^{1}. Based on our observation, it is apparent that for the five tumour types listed in Table 3, $\underline{\mathcal{E}}_{L^2}$ is lower than $\underline{\mathcal{E}}_{H^1}$ within $\mathcal{I}_{\mathrm{x_I}}$. The host mesenchyme parameters are chosen as $K_1 = 0.22$ and α_1 is large (indicating significant fluid (containing nutrients) perfusion through the vasculature). We observe two varied behaviors of $\underline{\mathcal{E}}_k$ in two ranges: (1) $0.003 \leq K_2 \leq 0.01$ and (2) $K_2 > 0.01$.

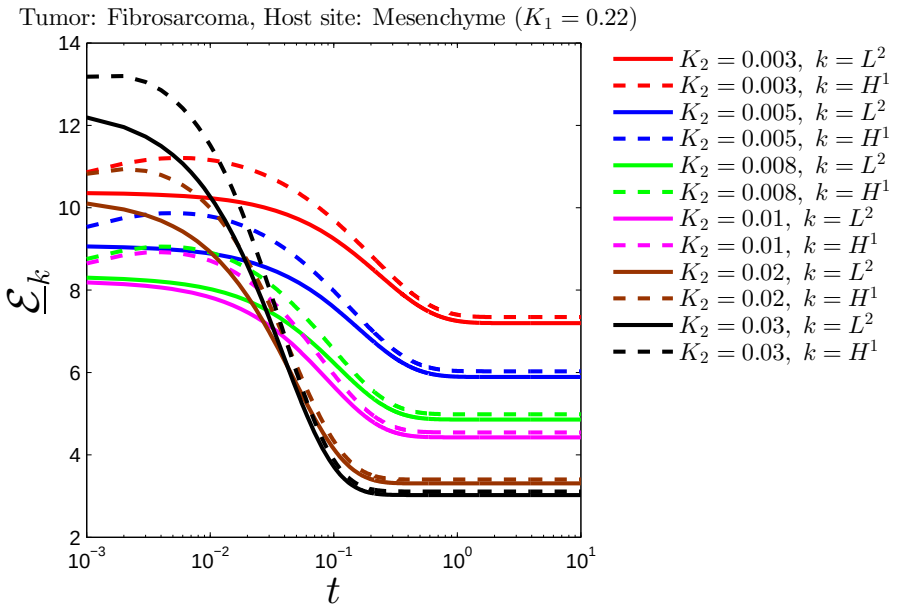

Fig. 4: (Colour online) Minimum of system energies (MISE) ($\underline{\mathcal{E}}_k$) versus dimensionless time (t) corresponding to six fibrosarcoma tumours which differ in terms of their hydraulic resistivity values, i.e., $K_2 = 0.003,\ 0.005,\ 0.008,\ 0.01,\ 0.02,\ 0.03$ within the host mesenchyme tissue having hydraulic resistivity $K_1 = 0.22$ when $\alpha_1 \to \infty,\ \alpha_2 = 5$, $\nu_1 = \nu_2 = 0.45$.

When K_2 is below 0.01, $\underline{\mathcal{E}}_k$ behaves inversely with K_2; however, it becomes directly proportional when K_2 exceeds 0.01. Corresponding to the first range, $\underline{\mathcal{E}}_k$ increases due to decrease in K_2. On the other hand, an increase in K_2 corresponding to the second range results in an increase in $\underline{\mathcal{E}}_k$. In the former case, an increase in the $\underline{\mathcal{E}}_k$ is due to the larger deformation in the solid phase of the tumour. The solid phase velocity dominates the interstitial fluid velocity. In the latter case, higher interstitial hydraulic resistivity opposes the interstitial fluid flow. Specifically, when $K_2 \geq 0.01$, interstitial fluid flow dominates the solid phase velocity with increasing K_2. For a tumour with a larger volume of solid components, the effect of V_2^f on $\underline{\mathcal{E}}_k$ is negligible. In this case, there is a rapid change in the energy profile $\underline{\mathcal{E}}_k$ over time.

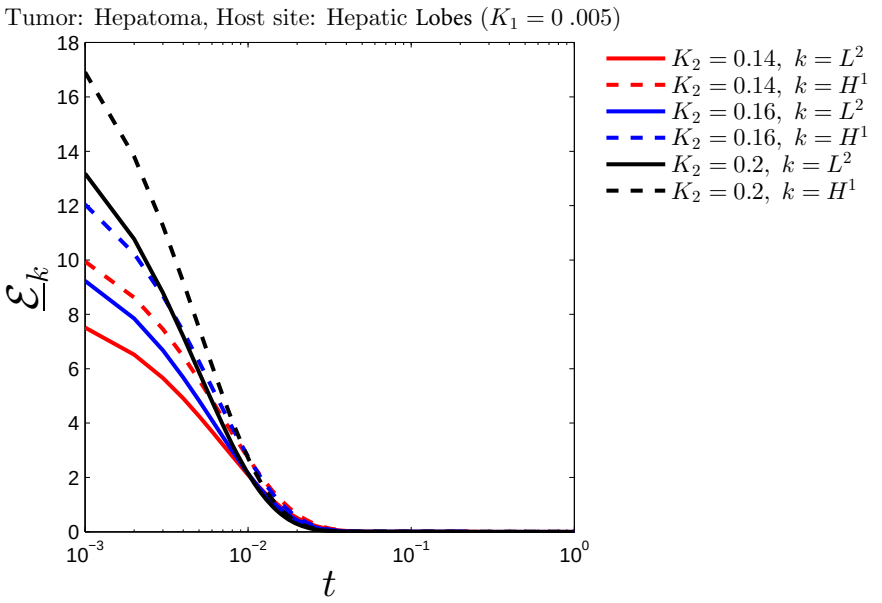

Fig. 5: (Colour online) The minimum of system energy ($\mathcal{E}_k$) versus dimensionless time (t) corresponding to six varieties of Hepatoma tumours differentiated in terms of their hydraulic resistivity values, i.e., $K_2 = 0.14,\ 0.16,\ 0.22$ within hepatic sinusoids (host) having H.R. $K_1 = 0.005$ when $\alpha_1 \to \infty,\ \alpha_2 = 5,\ \nu_1,\ \nu_2 = 0.45$.

Figure 5 illustrates the variation in system energy over a small time interval of $10^{-3} - 10^{-1}$. The MISE profiles consistently behave in relation to K_2. When the hydraulic resistivity value of a hepatic lobe host is set at $K_1 = 0.005$, the SE profile increases with $K_2 \geq 0.14$, which differs from the corresponding changes observed in fibrosarcoma. Generally, hepatoma exhibits higher interstitial hydraulic resistance than its host hepatic lobe and shows a similar level of MISE to fibrosarcoma when K_2 is at least 0.02. In comparison, we can conclude that the likelihood of system energy deficiency is greater in hepatoma than in fibrosarcoma.

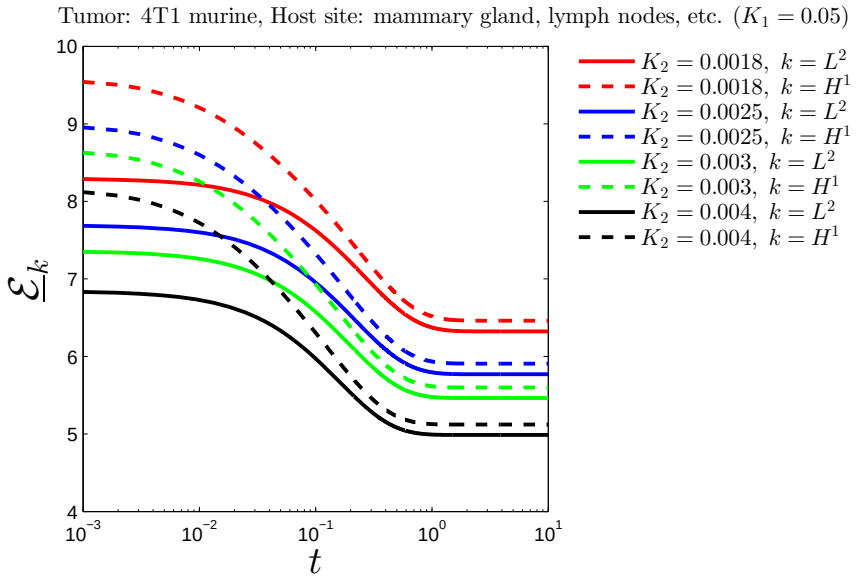

Fig. 6: (Colour online) The minimum of system energies ($\mathcal{E}_k$) versus dimensionless time (t) corresponding to six varieties of 4T1 murine tumours differentiated in terms of their hydraulic resistivity values i.e., $K_2 = 0.0018,\ 0.0025,\ 0.003,\ 0.004$ within the mammary gland, lymph nodes, etc. (hosts) having standard hydraulic resistivity $K_1 = 0.05$ when $\alpha_1 \to \infty,\ \alpha_2 = 5,\ \nu_1,\ \nu_2 = 0.45$.

In this section, we analyse the behaviour of $\underline{\mathcal{E}}_k$ in 4T1 murine tumours concerning K_2 when the tumours are in the mammary gland, lymph nodes, and other similar hosts (see Figure 6). It is worth noting that the 4T1 murine tumour and fibrosarcoma show a similar dependency on K_2. We found that $\underline{\mathcal{E}}_k$ reaches its maximum value when $K_2 = 1.8 \times 10^{-3}$, which is essential for promoting $\underline{\mathcal{E}}_k$. Lastly, when $K_1 > K_2$, it suggests that the host-tumour interface is leaky and that an increase in the difference between $|K_1 - K_2|$ enhances the magnitude of $\underline{\mathcal{E}}_k$.

Figures 7(a)-7(b) illustrate the behavior of $\underline{\mathcal{E}}_k$ over time within a U87 tumor (glioma) for specific K_2 values corresponding to two different host brain tissues, with $K_1 = 5 \times 10^{-2}$ and $K_1 = 8 \times 10^{-4}$, respectively. The average magnitude of $\underline{\mathcal{E}}_k$ is higher for $K_1 = 8 \times 10^{-4}$ compared to $K_1 = 5 \times 10^{-2}$, which indicates that in the former case, the hydraulic resistivity of the glioma tumour is lower than that of the surrounding healthy tissue. In contrast, in the latter case, the internal hydraulic resistivity of the glioma is higher than that of the surrounding healthy tissue. This incident suggests that $\underline{\mathcal{E}}_k$ has a more pronounced effect in the second case. The latter case generally has more MISE.

Figures 8(a) and 8(b) illustrate the temporal changes in $\underline{\mathcal{E}}_k$ for MCaIV tumours located in different abdominal muscles of a rat (host site), with varying values of K_1. The

value of K_2, which represents the rate of interstitial fluid flow, is set at 0.0167 for MCaIV tumours. Despite the wide range of variations in K_1, we observe only minimal changes in $\underline{\mathcal{E}}_k$. We have considered two different ranges for K_1: $0.053 \leq K_1 \leq 0.275$ and $0.22 < K_1 \leq 14$. In these ranges, $K_2 < K_1$, and an increase in K_1 generally results in a decrease in $\underline{\mathcal{E}}_k$. Notably, when $K_1 \geq 0.69$, we observe a slight change in $\underline{\mathcal{E}}_k$, as demonstrated in a zoomed-in plot. These findings suggest that an increase in K_1 reduces the penetration of interstitial fluid from the host to the tumour interstitium. Furthermore, when K_1 is much greater than K_2, the profiles of $\underline{\mathcal{E}}_k$ for two different K_1 values show no significant variations. Thus, when $K_1 = 0.69$ and $K_2 = 0.0167$, we reach a threshold combination beyond which further increases in K_1 do not affect $\underline{\mathcal{E}}_k$.

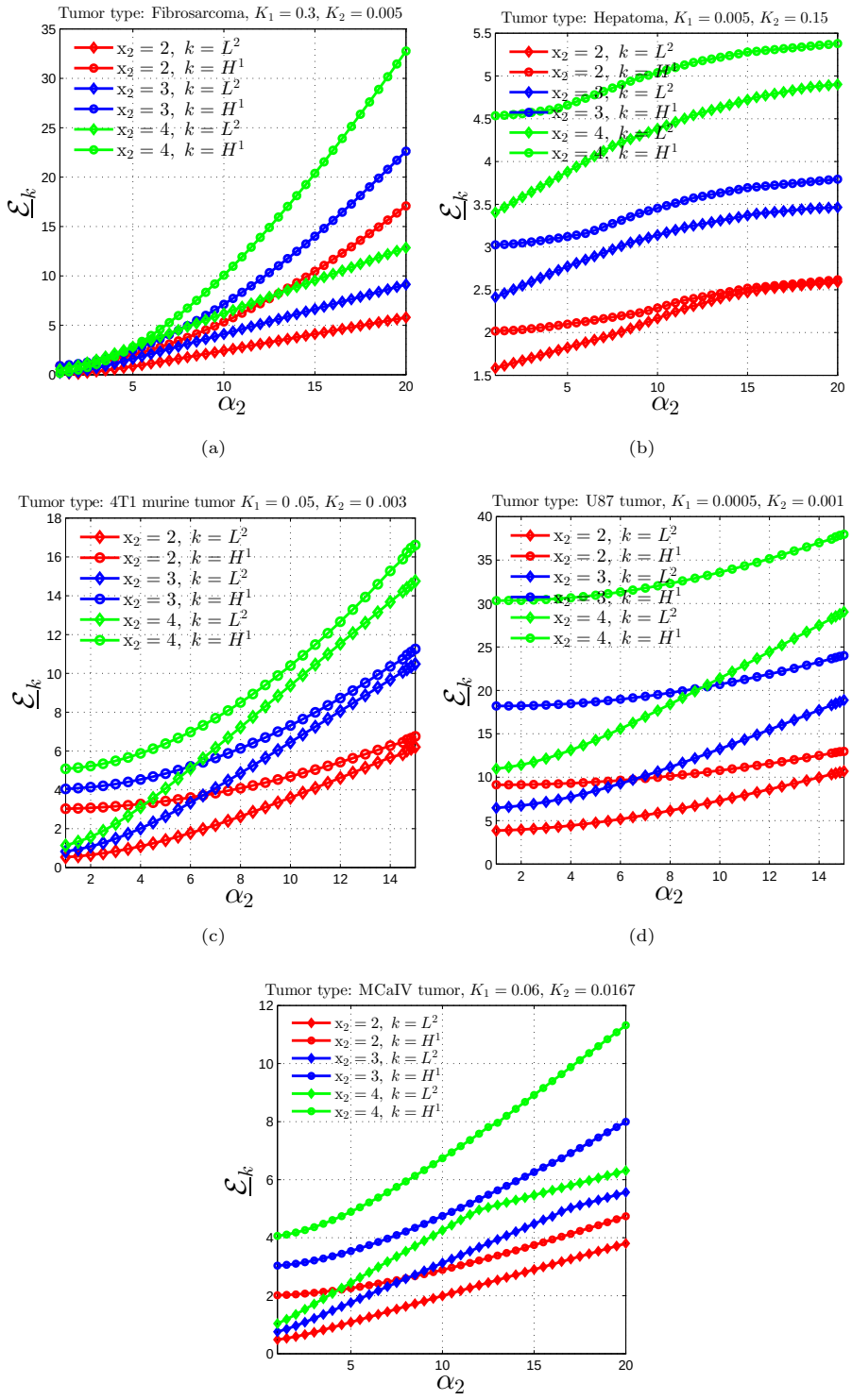

Fig. 9: (Colour online) Variation of the minimum of system energy ($\underline{\mathcal{E}_k}$) with α_2 within the range $0 < \alpha_2 \leq 20$ for (a) a fibrosarcoma with $K_2 = 0.005$ inside mesenchyme $K_1 = 0.3$, (b) a hepatoma with $K_2 = 0.15$ inside normal hepatic lobe $K_1 = 0.005$, (c) a 4T1 murine tumour with $K_2 = 0.003$ inside any of mammary gland, lymph nodes, lungs etc. having a standard hydraulic resistivity $K_1 = 0.05$, (d) a U87 tumour with $K_2 = 0.001$ inside brain tissue with $K_1 = 0.0005$, (e) a MCaIV tumour with $K_2 = 0.0167$ within Rat abdominal muscle with $K_1 = 0.06$ with following tumour sizes $\mathrm{x}_2 = 2,\ 3,\ 4$ when $\alpha_1 \to \infty$, $\nu_1,\ \nu_2 = 0.46$.

Figures 9(a)-9(e) show the variation of $\underline{\mathcal{E}}_k$ for α_2 (strength of perfusion through the vasculature within tumour Ω_2) corresponding to (1) fibrosarcoma, (2) hepatoma, (3) 4T1 murine tumour (4) U87 tumour (glioma) and (5) MCaIV tumour respectively. Highest $\underline{\mathcal{E}}_k$ can be achieved for hepatoma within the given interval $\alpha_2 \geq 0$. We consider three tumour radii $\mathrm{x}_2 = 2,\ 3,\ 4$. Both $\underline{\mathcal{E}}_{k=H^1}$ and $\underline{\mathcal{E}}_{k=L^2}$ increases with the tumour size. Moreover, $\underline{\mathcal{E}}_{k=H^1} > \underline{\mathcal{E}}_{k=L^2}$ in all these cases.

In case of fibrosarcoma, $\underline{\mathcal{E}}_k$ increases with the fluid perfusion strength α_2 for all possible tumour sizes. The internal hydraulic resistivity of a fibrosarcoma is supposed to be less than that of its host mesenchyme. Under these circumstances, the tumour viability becomes higher. On the other hand, Figure 9(b) shows the marginal growth of $\underline{\mathcal{E}}_k$ with increasing α_2 in the case of a hepatoma due to the higher internal hydraulic resistivity. Expect fibrosarcoma, strictly increasing behaviour in $\underline{\mathcal{E}}_k$ is shown with respect to α_2 for 4T1 murine tumour (see Figure 9(c)). At a higher magnitude of α_2 two $\underline{\mathcal{E}}_k$ profiles corresponding to $k = L^2$ and $k = H^1$ tend to coincide. However, at a higher value x_2 (e.g., $\mathrm{x}_2 = 4$), such coincidence may be delayed. Now Figure 9(d) depicts that similar to hepatoma, U87 tumours (glioma) show marginal growth in $\underline{\mathcal{E}}_{k=H^1}$ regarding α_2, but $\underline{\mathcal{E}}_{k=L^2}$ demonstrates significant growth. Therefore, the composite velocity gradient has a marginal impact on $\underline{\mathcal{E}}_{k=H^1}$. There is a similarity between the $\underline{\mathcal{E}}_k$ profiles corresponding to a Hepatoma and U87 tumour, which is due to the similar influence they receive from their respective host environments having low hydraulic resistivity. Finally, in the case of MCaIV tumours, Figure 9(e) shows an increase in $\underline{\mathcal{E}}_k$ profiles with α_2 for two different energy levels.

The overall observation on magnitudes of $\underline{\mathcal{E}}_k$ corresponding to five tumours depicts the following increasing sequence of minimum SE: MISE of hepatoma tumours $<$ MISE of MCaIV tumours $<$ MISE of 4T1 murine tumours $<$ MISE of fibrosarcoma tumours $<$ MISE of U87 tumours. The reciprocal of the MISE is the MASE. Hence, the MASE should obey the increasing relation: MASE of U87 tumours $<$ MASE of fibrosarcoma tumours $<$ MASE of 4T1 murine tumours $<$ MASE of MCaIV tumours $<$ MASE of hepatoma tumours. However, Figure 2 shows a slight variation in the order between 4T1 murine tumours and fibrosarcoma as illustrated through the order mentioned above. Nevertheless, we are in a position to compare these MASEs $\underline{\mathcal{E}}_k$ with $\overline{\mathcal{E}}_{\Omega_2}$. Therefore, among these five tumours, U87 tumours and hepatomas attain the minimum and maximum of the system energy, respectively. In other words, in terms of the system energy, our study highlights that U87 tumours show the least viability, and hepatomas show the most viability towards interstitial fluid percolation and solid phase deformation. However, in terms of magnitude, no significant difference in the system energy is observed between fibrosarcoma and the 4T1 murine tumour. They can be treated as at most equally viable. Moreover, magnitudes of $\underline{\mathcal{E}}_k$ corresponding to U87-tumours and fibrosarcoma are very close. Therefore, in terms of viability, they differ little. Hence, in the viability issue, our system energy analysis indicates that U87-tumours, fibrosarcoma, and 4T1 murine tumours are almost equally viable, with 4T1 murine tumours being slightly more viable. On the other hand, in the issue of viability, the hepatomas and MCaIV tumours are much higher among these five. However, the

system energy analysis is just a theoretical prediction of tumour viability; one must rely on clinical data. Some clinical evidence suggests the U87-tumours or glioblastoma are the most aggressive kind of carcinoma with a low prognosis rate [56]. But the aggressiveness of a cancer and its prognosis always depend on the disease diagnosis, staging, etc., along with several interacting factors.

6 Conclusions

This paper studies poroelastohydrodynamics of a model of *in-vivo* tumour growth on the short timescale for which changes in tumour volume can be neglected. Based on the biphasic mixture models, the corresponding boundary value problem is formulated. We have shown the well-posedness of this problem in a weak sense, including the existence, uniqueness, and continuous dependence of the model on the boundary data. First, the weak/variational formulation is derived, and then the finite-dimensional problem is demonstrated using the semi-discrete Galerkin method.

Our analysis reveals that the upper and lower bounds of tumour system energy are strongly governed by the dimensionless hydraulic resistivity of tumour and host tissues. These regulate the interplay between interstitial fluid percolation and solid-phase deformation across the tumour–host interface. Tumours with lower internal resistivity relative to their host attain higher minimum system energy, indicating enhanced poroelastohydrodynamic viability, whereas highly resistive tumours suppress interstitial perfusion and sustain reduced energy levels. These findings establish hydraulic resistivity as a key mechanobiological parameter linking tissue microstructure to short-time tumour viability in the present framework. Further, it is observed that these energy estimates are sensitive to the model parameters.

It is realized that upper bounds for the system energy are readily available by virtue of the well-posedness results. However, one needs the fluid percolation velocity and the solid-phase displacement explicitly to obtain the lower bounds of the energy. Thanks to the 1D model, which enables us to obtain the closed-form analytical solution and, subsequently, the MISE based on the lower bounds of the L^2 and H^1 norms. The five tumour case studies we have chosen can be sorted in decreasing order of their system energy upper bound as: hepatoma, MCaIV tumour, fibrosarcoma, 4T1 murine, and U87 tumour. On the other hand, a similar sorting based on the lower bound is: hepatoma, MCaIV tumour, 4T1 murine, fibrosarcoma, and U87 tumour. Hence, any characterizations associated with the system energy can provide additional insights into various types of tumours.

In the present model, we investigate short-time-scale fluid percolation and solid-phase deformation within a tumour embedded in a host tissue. However, fluid perfusion through the tumour vasculature network and interstitial percolation occur on a much faster time scale than that required for cell growth. As a result, the growth of the cell population has been neglected. The corresponding model appears more involved and challenging, both in establishing well-posedness results and in numerical simulations.

Accordingly, one may treat tumour cells as a fluid with a viscosity different from that of the interstitial fluid [14, 16, 18]. The source terms in the mass conservation equations would then depend on the nutrient concentration within both the tumour and the host. One may further consider a pseudo–steady-state nutrient transport process in both regions, incorporating a moving interface between the tumour and the host.

Data Availability

The authors declare that the manuscript has no associated data.

Declaration

Conflict of interest

The authors have no conflicts of interest to declare that are relevant to the content of this article.

A Appendix

A.1 Function spaces and useful results

[6] We define below various function spaces, useful inequalities and certain results that we use in the analysis of the weak formulation.

Let $\Omega \subset \mathbb{R}^d$, $d = 2,\ 3$ be a bounded, open, connected domain with a Lipschitz continuous boundary. $L^2(\Omega)$ denotes the space of square-integrable functions equipped with standard norm $||u||_\Omega = (\int_\Omega |u|^2\, d\Omega)^{1/2}$. The corresponding vector and matrix-valued space of square-integrable functions are denoted and defined by

$$\mathbf{L}^2(\Omega) := [L^2(\Omega)]^d, \quad \mathbb{L}^2(\Omega) := [L^2(\Omega)]^{d\times d},$$

and the corresponding norm is $||\cdot||_\Omega$. The symbols $(\ ,\ )_\Omega$, and $(\ ,\ )_{\partial\Omega}$ denote inner products in $L^2(\Omega)$, and in the corresponding trace space $L^2(\partial\Omega)$, respectively.
$L^\infty(\Omega)$: denotes the space of measurable functions which are essentially bounded on Ω and equipped with the norm $||u||_{\infty,\Omega} = \text{esssup}_{x\in\Omega}|u|$. The corresponding vector and matrix-valued space of essentially bounded functions are denoted and defined by

$$\mathbf{L}^\infty(\Omega) := [L^\infty(\Omega)]^d, \quad \mathbb{L}^\infty(\Omega) := [L^\infty(\Omega)]^{d\times d},$$

and the corresponding norm is $||\cdot||_{\infty,\Omega}$.
Further, $H^1(\Omega)$ denotes the standard Sobolev space of order '1' equipped with standard norm
$||u||_{1,\Omega} = \left[\int_\Omega (|u|^2 + |\nabla u|^2)\, d\Omega\right]^{1/2}$. We denote the vector and matrix-valued Sobolev spaces as follows:

$$\mathbf{H}^1(\Omega) := [H^1(\Omega)]^d, \quad \mathbb{H}^1(\Omega) := [H^1(\Omega)]^{d\times d},$$

[6] see [4, 36]

and still write $||\cdot||_{1,\Omega}$ for corresponding norm.
$\mathbf{H}_0^1(\Omega) = \{\mathbf{u} \in \mathbf{H}^1(\Omega) : \ \mathbf{u} = 0 \text{ on } \partial\Omega\}$ and $\mathbf{H}_{0,\Gamma}^1(\Omega) = \{\mathbf{u} \in \mathbf{H}^1(\Omega) : \ \mathbf{u} = 0 \text{ on } \Gamma\}$, where Γ is an open subset of $\partial\Omega$. $(H^1(\Omega))^*$ and $H^{-1}(\Omega)^d$ denote the dual space of $H^1(\Omega)$ and $H_0^1(\Omega)^d$, respectively. The norm on a dual space $\mathbf{X}^*$ is defined as

$$||\mathbf{f}||_{\mathbf{X}^*} = \sup_{0 \neq \mathbf{u} \in \mathbf{X}} \frac{|\langle \mathbf{f}, \mathbf{u} \rangle_\Omega|}{||\mathbf{u}||_{\mathbf{X}}}, \tag{72}$$

where $\langle \cdot \ , \ \cdot \rangle_\Omega$ denotes the duality pairing.
Further, $\mathbf{H}^{1/2}(\partial\Omega) = \{\tau_0 \mathbf{u} | \mathbf{u} \in \mathbf{H}^1(\Omega)\}$, where τ_0 is the trace operator on $\mathbf{H}^1(\Omega)$. A norm on $\mathbf{H}^{1/2}(\partial\Omega)$ defined as

$$||\mathbf{f}||_{1/2,\Omega} = \inf_{\mathbf{v} \in \mathbf{H}^1(\Omega), \tau_0 \mathbf{v} = \mathbf{f}} ||\mathbf{v}||_{1,\Omega}. \tag{73}$$

The space $\mathbf{H}^{1/2}(\partial\Omega)$ is a Hilbert space continuously embedded in $\mathbf{L}^2(\partial\Omega)$.

We define a function space $\mathbf{H}(\text{div}; \Omega) = \{\mathbf{v} \in \mathbf{L}^2(\Omega) | \nabla \cdot \mathbf{v} \in L^2(\Omega)\}$ and its subspace $\mathbf{H}_0(\text{div}; \Omega) = \{\mathbf{v} \in \mathbf{H}(\text{div}; \Omega) | \mathbf{v} \cdot \mathbf{n} = 0 \ \text{ on } \ \partial\Omega\}$. The following relation holds

$$\mathbf{H}_0^1(\Omega) \subset \mathbf{H}_0(\text{div}; \Omega) \subset \mathbf{H}(\text{div}; \Omega).$$

Definition 1. *Let* $\mathbf{X}$ *denote the real Banach space, with the norm* $||\ \ ||_{\mathbf{X}}$. *The space* $L^p(0, T; \mathbf{X})$ *consists of all strongly measurable functions* $u : [0, T] \to \mathbf{X}$ *with*
(i) $1 \leq p < \infty$,

$$||u||_{L^p(0,T;\mathbf{X})} := \left(\int_0^T ||u||_{\mathbf{X}}^p \, dt \right)^{1/p} < \infty$$

and
(ii) $p = \infty$,

$$||u||_{L^\infty(0,T;\mathbf{X})} := ess\ sup_{0 \leq t \leq T} ||u(t)||_{\mathbf{X}} < \infty.$$

Definition 2. *The space* $C([0, T]; \mathbf{X})$ *comprises all continuous functions* $u : [0, T] \to \mathbf{X}$ *with*

$$||u||_{C([0,T];\mathbf{X})} := \max_{0 \leq t \leq T} ||u(t)||_{\mathbf{X}} < \infty.$$

A.2 Coefficient matrices

We refer the system .()... that involve several coefficient matrices. We define these here.

- $\mathbf{A}_1 = (d_a(\mathbf{w}_1^j, \mathbf{w}_1^i)_{\Omega_1})_{1 \leq i,j \leq m}$,
- $\mathbf{A}_2 = (2d_a(\mathbb{D}^f(\mathbf{w}_1^j, \mathbb{D}^f(\mathbf{w}_1^i)_{\Omega_1} + \lambda d_a(\nabla \cdot \mathbf{w}_1^j, \nabla \cdot \mathbf{w}_1^i)_{\Omega_1} + (\mathbf{K}_1 \mathbf{w}_1^j, \mathbf{w}_1^i)_{\Omega_1} + \beta^*(\mathbf{w}_1^j \cdot \hat{\mathbf{t}}, \mathbf{w}_1^i \cdot \hat{\mathbf{t}})_{\Gamma_I})_{1 \leq i,j \leq m}$,
- $\mathbf{A}_3 = (\varphi_1^f(q_1^j, \nabla \cdot \mathbf{w}_1^i)_{\Omega_1})_{1 \leq i,j \leq m}$,
- $\mathbf{A}_4 = ((\mathbf{K}_1 \mathbf{\Psi}^j, \mathbf{w}_1^i)_{\Omega_1})_{1 \leq i,j \leq m}$,
- $\mathbf{A}_5 = (d_a(\mathbf{w}_2^j, \mathbf{w}_2^i)_{\Omega_2})_{1 \leq i,j \leq m}$,
- $\mathbf{A}_6 = (\varphi_2^f(q_2^j, \nabla \cdot \mathbf{w}_2^i)_{\Omega_2})_{1 \leq i,j \leq m}$,
- $\mathbf{A}_7 = ((\mathbf{K}_2 \mathbf{w}_2^j, \mathbf{w}_2^i)_{\Omega_2})_{1 \leq i,j \leq m}$,
- $\mathbf{A}_8 = ((\mathbf{K}_2 \mathbf{\Psi}^j, \mathbf{w}_2^i)_{\Omega_2})_{1 \leq i,j \leq m}$,
- $\mathbf{B}_1 = (d_a \rho_{R_1}(\mathbf{\Psi}^j, \mathbf{\Psi}^i)_{\Omega_1} + d_a \rho_{R_2}(\mathbf{\Psi}^j, \mathbf{\Psi}^i)_{\Omega_2})_{1 \leq i,j \leq m}$,

- $\mathbf{B}_2 = (2\gamma_1^s(\mathbb{D}^s(\mathbf{\Psi}^j), \mathbb{D}^s(\mathbf{\Psi}^i))_{\Omega_1} + \delta_1^s(\nabla \cdot \mathbf{\Psi}^j, \nabla \cdot \mathbf{\Psi}^i)_{\Omega_1} + 2\gamma_2^s(\mathbb{D}^s(\mathbf{\Psi}^j), \mathbb{D}^s(\mathbf{\Psi}^i))_{\Omega_2} + \delta_2^s(\nabla \cdot \mathbf{\Psi}^j, \nabla \cdot \mathbf{\Psi}^i)_{\Omega_2})_{1 \le i,j \le m}$,
- $\mathbf{B}_3 = ((\mathbf{K}_1 \mathbf{\Psi}^j, \mathbf{\Psi}^i)_{\Omega_1} + (\mathbf{K}_2 \dot{\mathbf{U}}_2^m(t), \mathbf{\Psi}^i)_{\Omega_2})_{1 \le i,j \le m}$,
- $\mathbf{B}_4 = ((\mathbf{K}_1 \mathbf{w}_1^j, \mathbf{\Psi}^i)_{\Omega_1})_{1 \le i,j \le m}$,
- $\mathbf{B}_5 = ((\mathbf{K}_2 \mathbf{w}_2^j, \mathbf{\Psi}^i)_{\Omega_2})_{1 \le i,j \le m}$,
- $\mathbf{B}_6 = (\varphi_1^s(q_1^j, \nabla \cdot \mathbf{\Psi}^i)_{\Omega_1})_{1 \le i,j \le m}$,
- $\mathbf{B}_7 = (\varphi_2^s(q_2^j, \nabla \cdot \mathbf{\Psi}^i)_{\Omega_2})_{1 \le i,j \le m}$,
- $\mathbf{Q}_1 = (\alpha_1^2(q_1^j, q_1^i)_{\Omega_1})_{1 \le i,j \le m}$,
- $\mathbf{Q}_2 = (\alpha_2^2(q_2^j, q_2^i)_{\Omega_2})_{1 \le i,j \le m}$.

Expressions for $\mathbf{F}_i$ $(i = 1 \dots 5)$ are:

$$\mathbf{F}_1 = \begin{pmatrix} (\mathbf{b}_1^f(t), \mathbf{w}_1^1)_{\Omega_1} + (\mathbf{T}_\infty^f(t), \mathbf{w}_1^1)_{\Gamma_1} \\ \vdots \\ (\mathbf{b}_1^f(t), \mathbf{w}_1^m)_{\Omega_1} + (\mathbf{T}_\infty^f(t), \mathbf{w}_1^m)_{\Gamma_1} \end{pmatrix}, \quad \mathbf{F}_2 = \begin{pmatrix} (\mathbf{b}_1^s(t), \mathbf{\Psi}^1)_{\Omega_1} + (\mathbf{b}_2^s(t), \mathbf{\Psi}^1)_{\Omega_2} \\ \vdots \\ (\mathbf{b}_1^s(t), \mathbf{\Psi}^m)_{\Omega_1} + (\mathbf{b}_2^s(t), \mathbf{\Psi}^m)_{\Omega_2} \end{pmatrix}$$

$$\mathbf{F}_3 = \begin{pmatrix} (\mathbf{b}_2^f(t), \mathbf{w}_2^1)_{\Omega_2} \\ \vdots \\ (\mathbf{b}_2^f(t), \mathbf{w}_2^m)_{\Omega_2} \end{pmatrix} \mathbf{F}_4 = \begin{pmatrix} (\alpha_1^2, q_1^1)_{\Omega_1} \\ \vdots \\ (\alpha_1^2, q_1^m)_{\Omega_1} \end{pmatrix}, \quad \mathbf{F}_5 = \begin{pmatrix} (\alpha_2^2, q_2^1)_{\Omega_2} \\ \vdots \\ (\alpha_2^2, q_2^m)_{\Omega_2} \end{pmatrix}.$$

A.3 Analytical Solutions corresponding to 1D system

We exploit the relations (65a) and (65b) and perform some algebra to eliminate V_1^f and $\partial U_1^s/\partial t$ from (65c) and V_2^f and $\partial U_2^s/\partial t$ from (65d). This yields the following equations for the corresponding pressure fields

$$\frac{\partial}{\partial t}(P_1 - 1) - \chi_1^2 \frac{\partial^2}{\partial \mathrm{x}^2}(P_1 - 1) + \chi_2^2 (P_1 - 1) = 0, \tag{74a}$$

and

$$\frac{\partial}{\partial t}(P_2 - 1) - \chi_3^2 \frac{\partial^2}{\partial \mathrm{x}^2}(P_2 - 1) + \chi_4^2 (P_2 - 1) = 0, \tag{74b}$$

where

$$\chi_1^2 = (\lambda + 2) + \frac{\left(\varphi_1^f\right)^2}{(d_a \alpha_1^2)}, \qquad \chi_2^2 = \frac{K_1}{d_a}, \qquad \chi_3^2 = \frac{\left(\varphi_2^f\right)^2}{(d_a \alpha_2^2)}, \qquad \text{and} \qquad \chi_4^2 = \frac{K_2}{d_a}.$$

Note that P_1 and P_2 satisfy unsteady Helmholtz equations which decouple from V_1^f, V_2^f, U_1^s and U_2^s. Further, V_1^f and V_2^f can be eliminated from the above equations with the help of Eqs. (65a) and (65b), respectively:

$$\frac{\partial^3 U_1^s}{\partial \mathrm{x}^3} = \mathcal{E}(\nu_1^s) \left[\chi_5^2 \frac{\partial}{\partial t}(P_1 - 1) + \chi_6^2 (P_1 - 1) \right], \quad \mathrm{x_I} \le \mathrm{x} \le \mathrm{x_H}, \tag{75a}$$

and

$$\frac{\partial^3 U_2^s}{\partial \mathrm{x}^3} = \mathcal{E}(\nu_2^s) \left[\chi_7^2 \frac{\partial}{\partial t}(P_2 - 1) + \chi_8^2 (P_2 - 1) \right], \quad 0 \le \mathrm{x} < \mathrm{x_I}, \tag{75b}$$

where

$$\mathcal{E}(\nu_1^s) = \frac{(1+\nu_1^s)}{(1-\nu_1^s)}, \quad \mathcal{E}(\nu_2^s) = \frac{(1+\nu_2^s)}{(1-\nu_2^s)}, \quad \chi_5^2 \approx \frac{1}{\chi_1^2},$$
$$\chi_6^2 \approx \chi_2^2 \left(\frac{1}{\chi_1^2} + \frac{\varphi^f}{\varphi^s}\right), \quad \chi_7^2 \approx \frac{1}{\chi_3^2}, \quad \text{and} \quad \chi_8^2 \approx \frac{1}{\varphi^s}\left(\frac{\chi_4^2}{\chi_3^2}\right).$$

This process leads to equations illustrating the relationships between solid phase displacements and interstitial pressure fields (IPFs) in the two tissue domains. These displacements are further required in Eqs. (65e)-(65f) to obtain IFVs.

Without loss of generality, one may assume $\varphi_1^f = \varphi_2^f = \varphi^f$ that forces $\varphi_1^s = \varphi_2^s = \varphi^s$. Next, we suppose that the host tissue is highly perfused, so α_1^2 is large. Based on the estimates of d_a in Table 2, we anticipate $\alpha_1^2 \sim \left(\varphi_1^f\right)^2/d_a$ such that $\chi_1^2 \approx (\lambda + 3)$. Refereing again to Table 2, for the values of ν_1^s and ν_2^s and ϱ_1^s and ϱ_2^s, we find estimate that $((1-2\nu_1^s)\varphi^s/(\varrho_1^s)) \sim 1$ and $((1-2\nu_2^s)\varphi^s/(\varrho_2^s)) \sim 1$ respectively.

Eqs. (74a)-(74b), Eqs. (65e)-(65f), and Eqs. (75a)-(75b) comprise unsteady, non-homogeneous linear partial differential equations with non-homogeneous boundaries. In order to produce analytical solutions to these equations, it is convenient to propose the following decompositions for the dependent variables, for $i \in [1,\ 2]$:

$$\begin{aligned} P_i(\mathrm{x},t) &= P_i^{(\mathrm{nh})}(\mathrm{x}) + P_i^{(\mathrm{ho})}(\mathrm{x},t), \\ V_i^f(\mathrm{x},t) &= V_i^{f^{(\mathrm{nh})}}(\mathrm{x}) + V_i^{f^{(\mathrm{ho})}}(\mathrm{x},t), \\ U_i^s(\mathrm{x},t) &= U_i^{s^{(\mathrm{nh})}}(\mathrm{x}) + U_i^{s^{(\mathrm{ho})}}(\mathrm{x},t), \end{aligned} \tag{76}$$

where the prefixes "nh" and "ho" denote for nonhomogeneous and homogeneous parts respectively. We substitute the above decomposition into Eqs. (65c)-(75b) to derive nonhomogeneous and homogeneous solutions for each variable. Clearly, the steady part of Eqs. (74a)-(74b) are Helmholtz-type ordinary differential equations and admit explicit solutions. We use the separation of variables technique to obtain the general solution for the simplified domain shown in Fig. 3.

Here, we present analytical solutions to Eqs. (74a)-(74b), Eqs. (65e)-(65f), and Eqs. (75a)-(75b). The general solution of Eqs. (74a)-(74b) can be obtained through any ad-hoc method and written as follows

$$\begin{aligned} P_1(\mathrm{x},t) = 1 &+ \mathcal{N}_1\Theta_1\left(\mathrm{x}-\mathrm{x}_{\mathrm{I}}\right) + \mathcal{N}_2\Theta_2\left(\mathrm{x}-\mathrm{x}_{\mathrm{I}}\right) \\ &+ \sum_{n=1}^{\infty}\left(M_1^{(n)}\xi_1^{(n)}\left(\mathrm{x}-\mathrm{x}_{\mathrm{I}}\right) + M_2^{(n)}\xi_2^{(n)}\left(\mathrm{x}-\mathrm{x}_{\mathrm{I}}\right)\right)\exp\left(-\lambda_{n,1}^2 t\right), \end{aligned} \tag{77a}$$

and

$$P_2(\mathrm{x},t) = 1 + \mathcal{T}_1\Upsilon_1(\mathrm{x}) + \mathcal{T}_2\Upsilon_2(\mathrm{x}) + \sum_{n=1}^{\infty}\left(R_1^{(n)}\zeta_1^{(n)}(\mathrm{x}) + R_2^{(n)}\zeta_2^{(n)}(\mathrm{x})\right)\exp(-\lambda_{n,2}^2 t), \tag{77b}$$

where

$$\begin{aligned}
\Theta_1\left(\mathrm{x}-\mathrm{x_I}\right) &= \cosh\left(\chi_2^*\left(\mathrm{x}-\mathrm{x_I}\right)\right) \quad \text{and} \quad \Theta_2\left(\mathrm{x}-\mathrm{x_I}\right) = \sinh\left(\chi_2^*\left(\mathrm{x}-\mathrm{x_I}\right)\right),\\
\xi_1^{(n)}\left(\mathrm{x}-\mathrm{x_I}\right) &= \cos\left(\mu_{n,1}(\mathrm{x}-\mathrm{x_I})\right) \quad \text{and} \quad \xi_2^{(n)}\left(\mathrm{x}-\mathrm{x_I}\right) = \sin(\mu_{n,1}(\mathrm{x}-\mathrm{x_I})),\\
\Upsilon_1(\mathrm{x}) &= \cosh(\chi_4\mathrm{x}) \quad \text{and} \quad \Upsilon_2(\mathrm{x}) = \sinh(\chi_4\mathrm{x}),\\
\zeta_1^{(n)}(\mathrm{x}) &= \cos(\mu_{n,2}\mathrm{x}) \quad \text{and} \quad \zeta_2^{(n)}(\mathrm{x}) = \sin(\mu_{n,2}\mathrm{x}),\\
\lambda_1^{(n)} &= \sqrt{\chi_1^{*^2}\left\{\left(\mu_1^{(n)}\right)^2 + \chi_2^{*^2}\right\}} \quad \text{and} \quad \lambda_2^{(n)} = \sqrt{\chi_3^2\left\{\left(\mu_1^{(n)}\right)^2 + \chi_4^2\right\}},
\end{aligned}$$

Subsequently, P_1 and P_2 are substituted in (65a) and (65b) respectively, we deduce that the IFVs can be written as

$$\begin{aligned}
V_1^f(\mathrm{x},t) &= \left[\mathcal{N}_3 - \frac{1}{\chi_2^*}\left\{\mathcal{N}_2\Theta_1\left(\mathrm{x}-\mathrm{x_I}\right) + \mathcal{N}_1\Theta_2\left(\mathrm{x}-\mathrm{x_I}\right)\right\}\right]\\
&+ \sum_{n=1}^{\infty}\frac{1}{\mu_{n,1}}\left(M_2^{(n)}\xi_1^{(n)}\left(\mathrm{x}-\mathrm{x_I}\right) - M_1^{(n)}\xi_2^{(n)}\left(\mathrm{x}-\mathrm{x_I}\right)\right)\exp(-\lambda_{n,1}^2 t),
\end{aligned} \tag{78a}$$

and

$$V_2^f(\mathrm{x},t) = \left[\mathcal{T}_3 - \frac{1}{\chi_4}\left\{\mathcal{T}_1\Upsilon_2(\mathrm{x}) + \mathcal{T}_2\Upsilon_1(\mathrm{x})\right\}\right] + \sum_{n=1}^{\infty}\frac{1}{\mu_{n,2}}\left(R_2^{(n)}\zeta_1^{(n)}(\mathrm{x}) - R_1^{(n)}\zeta_2^{(n)}(\mathrm{x})\right)\exp\left(-\lambda_{n,2}^2 t\right). \tag{78b}$$

Eqs. (77a) and (77b) are then used in Eqs. (75a) and (75b) respectively to determine the corresponding solid phase displacements as

$$\begin{aligned}
U_1^s(\mathrm{x},t) &= \left[\left(\frac{\mathcal{N}_4}{2}\mathrm{x}^2 + \mathcal{N}_5\mathrm{x} + \mathcal{N}_6\right) + \mathcal{E}(\nu_1^s)\left(\frac{\chi_6^{*^2}}{\chi_2^{*^3}}\right)\left\{\mathcal{N}_1\Theta_2\left(\mathrm{x}-\mathrm{x_I}\right) + \mathcal{N}_2\Theta_1\left(\mathrm{x}-\mathrm{x_I}\right)\right\}\right]\\
&+ \sum_{n=1}^{\infty}\Xi_1^{(n)}\left(M_2^{(n)}\xi_1^{(n)}\left(\mathrm{x}-\mathrm{x_I}\right) - M_1^{(n)}\xi_2^{(n)}\left(\mathrm{x}-\mathrm{x_I}\right)\right)\exp\left(-\lambda_{n,1}^2 t\right),
\end{aligned} \tag{79a}$$

and

$$\begin{aligned}
U_2^s(\mathrm{x},t) &= \left[\left(\frac{\mathcal{T}_4}{2}\mathrm{x}^2 + \mathcal{T}_5\mathrm{x} + \mathcal{T}_6\right) + \mathcal{E}(\nu_2^s)\left(\frac{\chi_8^{*^2}}{\chi_4^3}\right)\left\{\mathcal{T}_1\Upsilon_2(\mathrm{x}) + \mathcal{T}_2\Upsilon_1(\mathrm{x})\right\}\right]\\
&+ \sum_{n=1}^{\infty}\Xi_2^{(n)}\left(R_2^{(n)}\zeta_1^{(n)}(\mathrm{x}) - R_1^{(n)}\zeta_2^{(n)}(\mathrm{x})\right)\exp\left(-\lambda_{n,2}^2 t\right),
\end{aligned} \tag{79b}$$

where

$$\Xi_1^{(n)} = \frac{1}{\mu_{n,1}^3}\left(\chi_6^{*^2} - \chi_5^{*^2}\lambda_{n,1}^2\right) \quad \text{and} \quad \Xi_2^{(n)} = \frac{1}{\mu_{n,2}^3}\left(\chi_8^{*^2} - \chi_7^{*^2}\lambda_{n,2}^2\right),$$

The arbitrary constants are obtained by imposing the boundary and interface conditions (18)-(21), which are restated in simplified form in the next section.

A.3.1 Restatement of boundary and interface conditions

The boundary and interface conditions for the simplified geometry, shown in Fig. 3, follow from Eqs. (18)-(21). We first rewrite the conditions at the two boundaries $\mathrm{x} = \mathrm{x_H}$ and $\mathrm{x} = 0$ respectively as follows

$$T_1^f(\mathrm{x} = \mathrm{x_H}, t) = -P_1(\mathrm{x} = \mathrm{x_H}, t) + (\lambda + 2)\left.\frac{\partial V_1^{f^*}}{\partial \mathrm{x}}\right|_{\mathrm{x}=\mathrm{x_H}} = 1 \tag{80a}$$

and

$$U_1^s(\mathrm{x} = \mathrm{x_H}, t) = 0, \qquad V_2^f(\mathrm{x} = 0, t) = 0, \qquad U_2^s(\mathrm{x} = 0, t) = 0. \tag{80b}$$

Here $\mathrm{x} = \mathrm{x_I}$ denotes the interface between tumour and host tissue. The ambient fluid stress $T_\infty^f \sim \varphi^f$ can be considered. The physics of the problem guarantees the continuity of 1D velocities and displacements at the host-tumour interface so that, actually, no mass gets transported from one tissue domain to another. Accordingly, we set

$$V_1^{f^*}(\mathrm{x} = \mathrm{x_I}, t) = V_2^{f^*}(\mathrm{x} = \mathrm{x_I}, t), \qquad U_1^s(\mathrm{x} = \mathrm{x_I}, t) = U_2^s(\mathrm{x} = \mathrm{x_I}, t). \tag{80c}$$

In addition, we have the continuity of normal stresses at $\mathrm{x} = \mathrm{x_I}$:

$$(\lambda + 2)\left.\frac{\partial V_1^{f^*}}{\partial x}\right|_{\mathrm{x}=\mathrm{x_I}} = P_1(\mathrm{x} = \mathrm{x_I}, t) - P_2(\mathrm{x} = \mathrm{x_I}, t), \tag{80d}$$

$$\frac{1}{\mathcal{E}(\nu_1^s)}\left.\frac{\partial U_1^s}{\partial \mathrm{x}}\right|_{\mathrm{x}=\mathrm{x_I}} - \frac{1}{\mathcal{E}(\nu_2^s)}\left.\frac{\partial U_2^s}{\partial \mathrm{x}}\right|_{\mathrm{x}=\mathrm{x_I}} = \varphi^s\varphi^f\left\{P_1(\mathrm{x} = \mathrm{x_I}, t) - P_2(\mathrm{x} = \mathrm{x_I}, t)\right\}, \tag{80e}$$

Note that $\mathrm{x} = 0$ represents the boundary Γ_2 here. In order to obtain $P_{\mathrm{i}}(\mathrm{x}, t)$, $V_{\mathrm{i}}^f(\mathrm{x}, t)$, and $U_{\mathrm{i}}^s(\mathrm{x}, t)$ from (74a)-(74b), (65a)-(65b), and (75a)-(75b) respectively, we need to assume additional conditions. Besides $U_1^s(\mathrm{x} = \mathrm{x_H}, t) = 0$, we further assume $T_1^s(\mathrm{x} = \mathrm{x_H}, t) = T_\infty^s$ (ambient stress corresponding to the solid component inside the host tissue) which gives

$$\frac{1}{\mathcal{E}(\nu_1^s)}\left.\frac{\partial U_1^s}{\partial \mathrm{x}}\right|_{\mathrm{x}=\mathrm{x_H}} = 1 + \varphi^s\varphi^f P(\mathrm{x} = \mathrm{x_H}, t), \tag{81}$$

when we consider $T_\infty^s \sim \varphi^s$.

Interface flux balance: In addition to the above conditions, we assume continuity of the composite volumetric flux [6] across the surface Γ_I (interface of tumour and normal host tissue). Therefore, appending to Eqs. (14) and (17), we have:

$$\iint_{\Gamma_I} \mathbf{V}^{\mathrm{H}}_{\mathrm{com}}.\hat{\mathbf{e}}_{\mathrm{x}} d\Gamma_I = \iint_{\Gamma_I} \mathbf{V}^{\mathrm{I}}_{\mathrm{com}}.\hat{\mathbf{e}}_{\mathrm{x}} d\Gamma_I \xrightarrow[\text{theorem}]{\text{Gauss-divergence}} \int_{\mathrm{x}=\mathrm{x_I}}^{\mathrm{x_H}} (P_1 - 1) d\mathrm{x} = \int_{\mathrm{x}=0}^{\mathrm{x_I}} (P_2 - 1) d\mathrm{x}. \tag{82}$$

Note that the right-hand side of (82) is simplified for the 1D case.

A.3.2 Eigenvalues, eigenvectors and the solution space

The derived solutions for $P_1(\mathrm{x},t)$, $V_1^f(\mathrm{x},t)$ and $U_1^s(\mathrm{x},t)$ are used in (80a) and (81) to equate with prescribed stresses due to interstitial fluid $\left(T_1^{f^\infty}\right)$ and solid components of host tissue $\left(T_1^{s^\infty}\right)$ respectively within host tissue at a distance $(\mathrm{x_H} - \mathrm{x_I})$ away from the tumour site. Accordingly, we obtain

$$\begin{aligned} &[\mathcal{N}_1\Theta_1(\mathrm{x_H} - \mathrm{x_I}) \; + \; \mathcal{N}_2\Theta_2(\mathrm{x_H} - \mathrm{x_I}) - \frac{1}{(\lambda - 1)}\Big] \qquad (83a) \\ &\qquad + \sum_{n=1}^{\infty} \left[M_1^{(n)}\xi_1^{(n)}\left(\mathrm{x_H} - \mathrm{x_I}\right) + M_2^{(n)}\xi_2^{(n)}\left(\mathrm{x_H} - \mathrm{x_I}\right)\right] \times \exp(-\lambda_{n,1}^2 t) = 0, \end{aligned}$$

and

$$\begin{aligned} &\frac{1}{\mathcal{E}(\nu_1^s)}(\mathrm{x_H}\mathcal{N}_4 + \mathcal{N}_5) \qquad (83b) \\ &+ \left[\left\{\left(\frac{\chi_6^*}{\chi_2^*}\right)^2 - \varphi^s\varphi^f\right\}\left(\mathcal{N}_1\Theta_1(\mathrm{x_H} - \mathrm{x_I}) + \mathcal{N}_2\Theta_2(\mathrm{x_H} - \mathrm{x_I})\right) - \left(1 + \varphi^s\varphi^f\right)\right] \\ &= \sum_{n=1}^{\infty}\left(\varphi^s\varphi^f + \Xi_1^{(n)}\mu_{n,1}\right)\left\{M_1^{(n)}\xi_1^{(n)}\left(\mathrm{x_H} - \mathrm{x_I}\right) + M_2^{(n)}\xi_2^{(n)}\left(\mathrm{x_H} - \mathrm{x_I}\right)\right\}\exp(-\lambda_{n,1}^2 t). \end{aligned}$$

Corresponding to

$$M_1^{(n)}\xi_1^{(n)}\left(\mathrm{x_H} - \mathrm{x_I}\right) + M_2^{(n)}\xi_2^{(n)}\left(\mathrm{x_H} - \mathrm{x_I}\right) = 0, \qquad \forall n \in \mathbf{N}, \tag{84}$$

when

$$\left(\varphi^s\varphi^f + \Xi_1^{(n)}\mu_{n,1}\right) \neq 0 \qquad \forall n \in \mathbb{N}. \tag{85}$$

Consequently, we obtain

$$\mathcal{N}_1\Theta_1(\mathrm{x_H} - \mathrm{x_I}) + \mathcal{N}_2\Theta_2(\mathrm{x_H} - \mathrm{x_I}) - \frac{1}{(\lambda - 1)} = 0, \tag{86a}$$

and

$$\frac{1}{\mathcal{E}(\nu_1^s)}(\mathrm{x_H}\mathcal{N}_4+\mathcal{N}_5) \tag{86b}$$
$$+\left[\left\{\left(\frac{\chi_6^*}{\chi_2^*}\right)^2-\varphi^s\varphi^f\right\}(\mathcal{N}_1\Theta_1(\mathrm{x_H}-\mathrm{x_I})+\mathcal{N}_2\Theta_2(\mathrm{x_H}-\mathrm{x_I}))-\left(1+\varphi^s\varphi^f\right)\right]=0.$$

Now, we use Eq. (82), which shows the interfacial continuity of fluxes corresponding to the composite velocity fields for two tissue domains, which leads to

$$\begin{aligned}&\frac{1}{\chi_2^*}\left[\mathcal{N}_1\Theta_2(\mathrm{x_H}-\mathrm{x_I})+\mathcal{N}_2\left\{\Theta_1(\mathrm{x_H}-\mathrm{x_I})-1\right\}\right]-\frac{1}{\chi_4}\left[\mathcal{T}_1\Upsilon_2(\mathrm{x_I})+\mathcal{T}_2\left\{\Upsilon_1(\mathrm{x_I})-1\right\}\right]\\&+\sum_{n=1}^{\infty}\frac{1}{\mu_{n,1}}\left[M_1^{(n)}\xi_2^{(n)}\left(\mathrm{x_H}-\mathrm{x_I}\right)+M_2^{(n)}\left(1-\xi_2^{(n)}\left(\mathrm{x_H}-\mathrm{x_I}\right)\right)\right]\exp(-\lambda_{n,1}^2t),\\&=\sum_{n=1}^{\infty}\frac{1}{\mu_{n,2}}\left\{R_1^{(n)}\zeta_2^{(n)}(\mathrm{x_I})+R_2^{(n)}\left(1-\zeta_1^{(n)}(\mathrm{x_I})\right)\right\}\exp(-\lambda_{n,2}^2t)\end{aligned} \tag{87}$$

For all $n\in\mathbf{N}$,

$$M_1^{(n)}\xi_2^{(n)}\left(\mathrm{x_H}-\mathrm{x_I}\right)+M_2^{(n)}\left(1-\xi_1^{(n)}\left(\mathrm{x_H}-\mathrm{x_I}\right)\right)=0, \tag{88}$$

and

$$R_1^{(n)}\zeta_2^{(n)}(\mathrm{x_I})+R_2^{(n)}\left(1-\zeta_1^{(n)}(\mathrm{x_I})\right)=0, \tag{89}$$

Eq. (87) gives

$$\frac{1}{\chi_2^*}\left[\mathcal{N}_1\Theta_2(\mathrm{x_H}-\mathrm{x_I})+\mathcal{N}_2\left\{\Theta_1(\mathrm{x_H}-\mathrm{x_I})-1\right\}\right]-\frac{1}{\chi_4}\left[\mathcal{T}_1\Upsilon_2(\mathrm{x_I})+\mathcal{T}_2\left\{\Upsilon_1(\mathrm{x_I})-1\right\}\right]=0. \tag{90}$$

For nontrivial solution in $M_1^{(n)}$ and $M_2^{(n)}$ from Eq. (84) and Eq. (88), we have

$$\begin{vmatrix}\xi_1^{(n)}\left(\mathrm{x_H}-\mathrm{x_I}\right) & \xi_2^{(n)}\left(\mathrm{x_H}-\mathrm{x_I}\right)\\ \xi_2^{(n)}\left(\mathrm{x_H}-\mathrm{x_I}\right) & 1-\xi_1^{(n)}\left(\mathrm{x_H}-\mathrm{x_I}\right)\end{vmatrix}=0, \tag{91}$$

Therefore, Eq. (91) obtains $\xi_1^{(n)}\left(\mathrm{x_H}-\mathrm{x_I}\right)=1$ and consequently, $\mu_{n,1}=2n\pi/(\mathrm{x_H}-\mathrm{x_I})$ are the eigenvalues. Next Eqs. (80d) and (80e) correspond to interfacial continuity between the interstitial fluid and solid stresses. Subsequently, we obtain

$$\begin{aligned}&\left[(\mathcal{N}_1-\frac{1}{(\lambda+3)}(\mathcal{T}_1\Upsilon_1(\mathrm{x_I})+\mathcal{T}_2\Upsilon_2(\mathrm{x_I}))\right]+\sum_{n=1}^{\infty}M_1^{(n)}\exp(-\lambda_{n,1}^2t)\\&\qquad+\sum_{n=1}^{\infty}\left\{R_1^{(n)}\zeta_1^{(n)}(\mathrm{x_I})+R_2^{(n)}\zeta_2^{(n)}(\mathrm{x_I})\right\}\exp(-\lambda_{n,2}^2t)=0,\end{aligned} \tag{92a}$$

and

$$\begin{aligned}
&\frac{1}{\mathcal{E}(\nu_1^s)}\left(\mathrm{x_I}\mathcal{N}_4+\mathcal{N}_5\right)-\frac{1}{\mathcal{E}(\nu_2^s)}\left(\mathrm{x_I}\mathcal{T}_4+\mathcal{T}_5\right) \qquad (92b)\\
&+\left\{\left(\frac{\chi_8^*}{\chi_4}\right)^2+\varphi^s\varphi^f\right\}\left\{\mathcal{T}_1\Upsilon_1(\mathrm{x_I})+\mathcal{T}_2\Upsilon_2(\mathrm{x_I})\right\}+\left\{\left(\frac{\chi_6^*}{\chi_2^*}\right)^2-\varphi^s\varphi^f\right\}\mathcal{N}_1\\
&+\sum_{n=1}^{\infty}\left(\frac{1}{\mathcal{E}(\nu_2^s)}\Xi_2^{(n)}\mu_{n,2}+\varphi^s\varphi^f\right)\left\{R_1^{(n)}\zeta_1^{(n)}(\mathrm{x_I})+R_2^{(n)}\zeta_2^{(n)}(\mathrm{x_I})\right\}\exp(-\lambda_{n,2}^2t)\\
&=\sum_{n=1}^{\infty}\left(\frac{1}{\mathcal{E}(\nu_1^s)}\Xi_1^{(n)}\mu_{n,1}+\varphi^s\varphi^f\right)M_1^{(n)}\exp(-\lambda_{n,1}^2t)
\end{aligned}$$

For $\forall n\in\mathbb{N}$ we consider

$$R_1^{(n)}\zeta_1^{(n)}(\mathrm{x_I})+R_2^{(n)}\zeta_2^{(n)}(\mathrm{x_I})=0, \qquad (93a)$$

consequently Eqs. (92a) and (92b) result

$$\mathcal{N}_1-\frac{1}{(\lambda+3)}(\mathcal{T}_1\Upsilon_1(\mathrm{x_I})+\mathcal{T}_2\Upsilon_2(\mathrm{x_I}))+\sum_{n=1}^{\infty}M_1^{(n)}\exp(-\lambda_{n,1}^2t)=0, \qquad (93b)$$

and

$$\begin{aligned}
&\frac{1}{\mathcal{E}(\nu_1^s)}\left(\mathrm{x_I}\mathcal{N}_4+\mathcal{N}_5\right)-\frac{1}{\mathcal{E}(\nu_2^s)}\left(\mathrm{x_I}\mathcal{T}_4+\mathcal{T}_5\right)\\
&+\left\{\left(\frac{\chi_8^*}{\chi_4}\right)^2+\varphi^s\varphi^f\right\}\left\{\mathcal{T}_1\Upsilon_1(\mathrm{x_I})+\mathcal{T}_2\Upsilon_2(\mathrm{x_I})\right\}+\left\{\left(\frac{\chi_6^*}{\chi_2^*}\right)^2-\varphi^s\varphi^f\right\}\mathcal{N}_1\\
&=\sum_{n=1}^{\infty}\left(\frac{1}{\mathcal{E}(\nu_1^s)}\Xi_1^{(n)}\mu_{n,1}+\varphi^s\varphi^f\right)M_1^{(n)}\exp(-\lambda_{n,1}^2t) \qquad (93c)
\end{aligned}$$

respectively. For non-trivial solution in $R_1^{(n)}$ and $R_2^{(n)}$ corresponding to Eqs. (93a) and (89):

$$\begin{vmatrix}\zeta_1^{(n)}(\mathrm{x_I}) & \zeta_2^{(n)}(\mathrm{x_I})\\ \zeta_2^{(n)}(\mathrm{x_I}) & 1-\zeta_1^{(n)}(\mathrm{x_I})\end{vmatrix}=0. \qquad (94)$$

This gives $\mu_{n,2}=2n\pi/\mathrm{x_I}$ as eigenvalues. Now last two conditions of (80b) produce

$$\mathcal{T}_3-\frac{1}{\chi_4}\mathcal{T}_2+\sum_{n=1}^{\infty}\frac{1}{\mu_{n,2}}R_2^{(n)}\exp\left(-\lambda_{n,2}^2t\right)=0, \qquad (95a)$$

and

$$\mathcal{T}_6+\mathcal{E}(\nu_2^s)\left(\frac{\chi_8^{*^2}}{\chi_4^3}\right)\mathcal{T}_2+\sum_{n=1}^{\infty}\Xi_2^{(n)}R_2^{(n)}\exp\left(-\lambda_{n,2}^2t\right)=0, \qquad (95b)$$

if we consider $R_2^{(n)}=0$ for all $n\in\mathbf{N}$, we obtain

$$\mathcal{T}_3-e_1\mathcal{T}_2=0\qquad\text{and}\qquad\mathcal{T}_6+e_3\mathcal{T}_2=0. \tag{96}$$

Eq. (80c), which shows the continuity of IFVs and DSPs at the tumour-host interface, produces

$$\begin{aligned}&\left[(\mathcal{N}_3-\mathcal{T}_3)-\frac{1}{\chi_2^*}\mathcal{N}_2+\frac{1}{\chi_4}\left\{\mathcal{T}_1\Upsilon_2(\mathrm{x_I})+\mathcal{T}_2\Upsilon_1(\mathrm{x_I})\right\}\right]+\sum_{n=1}^{\infty}M_2^{(n)}\exp\left(-\lambda_{n,1}^2t\right)\\&=\sum_{n=1}^{\infty}\frac{1}{\mu_{n,2}}\left(R_2^{(n)}\zeta_1^{(n)}(\mathrm{x_I})-R_1^{(n)}\zeta_2^{(n)}(\mathrm{x_I})\right)\exp\left(-\lambda_{n,2}^2t\right)\end{aligned} \tag{97a}$$

and

$$\begin{aligned}&\frac{\mathrm{x_I}^2}{2}(\mathcal{N}_4-\mathcal{T}_4)+\mathrm{x_I}(\mathcal{N}_5-\mathcal{T}_5)+(\mathcal{N}_6-\mathcal{T}_6)\\&+\mathcal{E}(\nu_1^s)\left(\frac{{\chi_6^*}^2}{{\chi_2^*}^3}\right)\mathcal{N}_2-\mathcal{E}(\nu_2^s)\left(\frac{{\chi_8^*}^2}{\chi_4^3}\right)\left\{\mathcal{T}_1\Upsilon_2(\mathrm{x_I})+\mathcal{T}_2\Upsilon_1(\mathrm{x_I})\right\}\\&+\sum_{n=1}^{\infty}\Xi_1^{(n)}M_2^{(n)}\exp\left(-\lambda_{n,1}^2t\right)=\sum_{n=1}^{\infty}\Xi_2^{(n)}\left(R_2^{(n)}\zeta_1^{(n)}(\mathrm{x_I})-R_1^{(n)}\zeta_2^{(n)}(\mathrm{x_I})\right)\exp\left(-\lambda_{n,2}^2t\right)\end{aligned} \tag{97b}$$

Beside $R_2^{(n)}=0$ we now consider $M_2^{(n)}=0$. Consequently,

$$\left[(\mathcal{N}_3-\mathcal{T}_3)-\frac{1}{\chi_2^*}\mathcal{N}_2+\frac{1}{\chi_4}\left\{\mathcal{T}_1\Upsilon_2(\mathrm{x_I})+\mathcal{T}_2\Upsilon_1(\mathrm{x_I})\right\}\right]=0, \tag{98a}$$

and

$$\begin{aligned}&\frac{\mathrm{x_I}^2}{2}(\mathcal{N}_4-\mathcal{T}_4)+\mathrm{x_I}(\mathcal{N}_5-\mathcal{T}_5)+(\mathcal{N}_6-\mathcal{T}_6)\\&+\mathcal{E}(\nu_1^s)\left(\frac{{\chi_6^*}^2}{{\chi_2^*}^3}\right)\mathcal{N}_2-\mathcal{E}(\nu_2^s)\left(\frac{{\chi_8^*}^2}{\chi_4^3}\right)\left\{\mathcal{T}_1\Upsilon_2(\mathrm{x_I})+\mathcal{T}_2\Upsilon_1(\mathrm{x_I})\right\}=0.\end{aligned} \tag{98b}$$

$\mathcal{T}_3-\mathcal{N}_3=0$ and $\mathcal{N}_6-\mathcal{T}_6=0$ are assumed within (98a) and (98b) respectively to reduce number of arbitrary constants. Lastly, the first boundary condition in (80b) results

$$\begin{aligned}&\left[\left(\frac{\mathcal{N}_4}{2}\mathrm{x_H}^2+\mathcal{N}_5\mathrm{x_H}+\mathcal{N}_6\right)+\mathcal{E}(\nu_1^s)\left(\frac{{\chi_6^*}^2}{{\chi_2^*}^3}\right)\left\{\mathcal{N}_1\Theta_2(\mathrm{x_H}-\mathrm{x_I})+\mathcal{N}_2\Theta_1(\mathrm{x_H}-\mathrm{x_I})\right\}\right]\\&+\sum_{n=1}^{\infty}\Xi_1^{(n)}\left(M_2^{(n)}\xi_1^{(n)}\left(\mathrm{x_H}-\mathrm{x_I}\right)-M_1^{(n)}\xi_2^{(n)}\left(\mathrm{x_H}-\mathrm{x_I}\right)\right)\exp\left(-\lambda_{n,1}^2t\right)=0.\end{aligned} \tag{99}$$

In the above expression, the term within the summation vanishes once we force the values of $M_2^{(n)}$ and $\mu_{n,1}$. Consequently, we have left with

$$\left(\frac{\mathcal{N}_4}{2}\mathrm{x_H^2}+\mathcal{N}_5\mathrm{x_H}+\mathcal{N}_6\right)+\mathcal{E}(\nu_1^s)\left(\frac{\chi_6^{*^2}}{\chi_2^{*^3}}\right)\left(\mathcal{N}_1\Theta_2(\mathrm{x_H}-\mathrm{x_I})+\mathcal{N}_2\Theta_2(\mathrm{x_H}-\mathrm{x_I})\right)=0. \quad (100)$$

Finally, our task is to solve Eqs. (86a)-(86b), Eqs. (93b)-(93c), Eqs. (90) and (96), Eqs. (98a)-(98b) and (100) for the arbitrary constants $\mathcal{N}_i$ and $\mathcal{T}_i$ $(i=1,..,5)$.

A.4 Evaluation of $M_1^{(n)}$ and $R_1^{(n)}$ using the condition at $t=0$

In order to evaluate $M_1^{(n)}$ and $R_1^{(n)}$, we have to use initial condition on IFPs, we try to obtain these from mass conservation equations (9c) and (9e) with the help of initial conditions (19) on them. If $P_{1,0}$ and $P_{2,0}$ are initial IFPs, they are found as

$$P_{1,0}=1-\frac{1}{\alpha_1^2}\left[\frac{\partial}{\partial \mathrm{x}}\left(\varphi_1^f V_{1,0}^f+\varphi_1^s V_{1,0}^s\right)\right] \quad \text{and} \quad P_{2,0}=1-\frac{1}{\alpha_2^2}\left[\frac{\partial}{\partial \mathrm{x}}\left(\varphi_2^f V_{2,0}^f+\varphi_2^s V_{2,0}^s\right)\right]. \quad (101)$$

Note that corresponding to sets of eigenvalues $\mu_{n,1}$ and $\mu_{n,2}$, we have $\cos(\mu_{n,1}(\mathrm{x}-\mathrm{x_I}))$ and $\cos(\mu_{n,2}\mathrm{x})$ as respective eigenvectors in $P_{1,0}(\mathrm{x},t)$ and $P_{2,0}(\mathrm{x},t)$ respectively. Therefore,

$$M_1^{(m)}=\frac{2\chi_2\left(\mathrm{x_1}-\mathrm{x_2}\right)}{\left(\chi_2^2\left(\mathrm{x_1}-\mathrm{x_2}\right)^2+4m^2\pi^2\right)}\left[N_2\left\{1-\Theta_1(\mathrm{x_H}-\mathrm{x_I})\right\}-N_1\Theta_2(\mathrm{x_H}-\mathrm{x_I})\right], \quad (102a)$$

and

$$R_1^{(m)}=\frac{2\chi_2\mathrm{x_2}}{(\chi_2^2\mathrm{x_2^2}+4m^2\pi^2)}\left[T_2\left\{1-\Upsilon_1(\mathrm{x_I})\right\}-T_1\Upsilon_2(\mathrm{x_I})\right]. \quad (102b)$$

References

[1] Kenyon D E (1976) The theory of an incompressible solid–fluid mixture. *Arch Ration Mech Anal* **62**(2):131–147

[2] Mow V C, Holmes M H, Lai W M (1984) Fluid transport and mechanical properties of articular cartilage: a review. *J Biomech* **17**(5):377–394

[3] Alam M, Dey B, Raja Sekhar GP (2018) Mathematical analysis of hydrodynamics and tissue deformation inside an isolated solid tumour. *Theor Appl Mech* **45**(2):253–278

[4] Alam M, Dey B, Raja Sekhar G P (2019) Mathematical modeling and analysis of hydroelastodynamics inside a solid tumour containing deformable tissue. *Z Angew Math Mech* **99**(5):e201800223.

[5] Dey B, Raja Sekhar G P (2016) Hydrodynamics and convection enhanced macromolecular fluid transport in soft biological tissues: application to solid tumour. *J Theor Biol* **395**:62–86.

[6] Dey B, Raja Sekhar G P, Mukhopadhyay S K (2018) In vivo mimicking model for solid tumour towards hydromechanics of tissue deformation and creation of necrosis. *J Biol Phys* **44**(3):361–400.

[7] Dey B, Raja Sekhar G P (2016) Analytical study on hydrodynamics of an unsteady flow and mass transfer through a channel asymmetrically lined with deformable porous layer. *Eur J Mech B Fluids* **55**:71–87.

[8] Barry SI, Aldis GK (1990) Comparison of models for flow induced deformation of soft biological tissue. *J Biomech* **23**(7):647–654.

[9] Barry SI, Parker KH, Aldis GK (1991) Fluid flow over a thin deformable porous layer. *ZAMP* **42**(5):633–648.

[10] Kumar P, Dey B, Raja Sekhar GP (2018) Nutrient transport through deformable cylindrical scaffold inside a bioreactor: an application to tissue engineering. *Int J Eng Sci* **127**:201–216.

[11] Lu XL, Wan LQ, Guo XE, Mow VC (2010) Linearized formulation of triphasic mixture theory for articular cartilage and its application to indentation analysis. *J Biomech* **43**(4):673–679.

[12] Preziosi L (2003) *Cancer modelling and simulation*. CRC Press.

[13] Ambrosi D, Preziosi L (2002) On the closure of mass balance models for tumour growth. *Math Models Methods Appl Sci* **12**(5):737–754.

[14] Byrne HM, Preziosi L (2003) Modelling solid tumour growth using the theory of mixtures. *Math Med Biol* **20**(4):341–366.

[15] Graziano L, Preziosi L (2007) Mechanics in tumor growth. In: Preziosi L (ed) *Modeling of biological materials*. Birkhäuser, pp 263–321.

[16] Preziosi L, Tosin A (2009) Multiphase modelling of tumour growth and extracellular matrix interaction. *J Math Biol* **58**(4):625–656.

[17] Breward CJW, Byrne HM, Lewis CE (2002) The role of cell–cell interactions in a two-phase model for avascular tumour growth. *J Math Biol* **45**(2):125–152.

[18] Byrne HM, King JR, McElwain DLS, Preziosi L (2003) A two-phase model of solid tumour growth. *Appl Math Lett* **16**(4):567–573.

[19] Netti PA, Baxter LT, Boucher Y, Skalak R, Jain RK (1997) Macro- and microscopic fluid transport in living tissues. *AIChE J* **43**(3):818–834.

[20] Baxter LT, Jain RK (1989) Transport of fluid and macromolecules in tumours. *Microvasc Res* **37**(1):77–104.

[21] Girault V, Rivière B (2009) DG approximation of coupled Navier–Stokes and Darcy equations by Beaver–Joseph–Saffman interface condition. *SIAM J Numer Anal* **47**(3):2052–2089.

[22] Cesmelioglu A, Girault V, Rivière B (2013) Time-dependent coupling of Navier–Stokes and Darcy flows. *ESAIM Math Model Numer Anal* **47**(2):539–554.

[23] Muha B, Čanić S (2014) Existence of a solution to a fluid–multi-layered-structure interaction problem. *J Differ Equ* **256**(2):658–706.

[24] Badia S, Quaini A, Quarteroni A (2009) Coupling Biot and Navier–Stokes equations for modelling fluid–poroelastic media interaction. *J Comput Phys* **228**(21):7986–8014.

[25] Bukač M, Yotov I, Zakerzadeh R, Zunino P (2015) Partitioning strategies for the interaction of a fluid with a poroelastic material based on a Nitsche coupling approach. *Comput Methods Appl Mech Eng* **292**:138–170.

[26] Cesmelioglu A (2017) Analysis of the coupled Navier–Stokes/Biot problem. *J Math Anal Appl* **456**(2):970–991.

[27] Alam M, Byrne HM, Raja Sekhar GP (2022) Existence and uniqueness results on biphasic mixture model for an in-vivo tumour. *Appl Anal* **101**(15):5442–5468.

[28] Alam M, Muntean A, Raja Sekhar GP (2025) Non-linear biphasic mixture model: existence and uniqueness results. *Eur J Appl Math* **36**:161–185.

[29] Holmes MH, Mow VC (1990) Nonlinear characteristics of soft gels and hydrated connective tissues in ultrafiltration. *J Biomech* **23**(11):1145–1156.

[30] Ateshian GA, Weiss JA (2010) Anisotropic hydraulic permeability under finite deformation. *J Biomech Eng* **132**(11):111004.

[31] Federico S, Herzog W (2008) On the anisotropy and inhomogeneity of permeability in articular cartilage. *Biomech Model Mechanobiol* **7**(5):367–378.

[32] Wang W, Parker KH (1995) Effect of deformable porous surface layers on the motion of a sphere in a narrow cylindrical tube. *J Fluid Mech* **283**:287–305.

[33] Hou JS, Holmes MH, Lai WM, Mow VC (1989) Boundary conditions at the cartilage–synovial fluid interface. *J Biomech Eng* **111**(1):78–87.

[34] Young YN, Mori Y, Miksis MJ (2019) Slightly deformable Darcy drop in linear flows. *Phys Rev Fluids* **4**(6):063601.

[35] Quarteroni A, Valli A (2008) *Numerical approximation of partial differential equations*. Springer.

[36] Salsa S (2016) *Partial differential equations in action*. Springer.

[37] Keangin P, Rattanadecho P (2018) Numerical investigation of microwave ablation on porous liver tissue. *Adv Mech Eng* **10**(8):1687814017734133.

[38] Chen CT, Malkus DS, Vanderby R (1998) Fiber matrix model for interstitial fluid flow in ligaments and tendons. *Biorheology* **35**(2):103–118.

[39] Yao W, Li Y, Ding G (2012) Interstitial fluid flow. *Evid Based Complement Alternat Med* 2012:1–9.

[40] Swartz MA, Fleury ME (2007) Interstitial flow and its effects in soft tissues. *Annu Rev Biomed Eng* **9**:229–256.

[41] Guyton AC, Hall JE (1986) *Textbook of medical physiology*. Saunders, Philadelphia.

[42] Islam MT, Tang S, Liverani C, Tasciotti E, Righetti R (2020) Non-invasive imaging of Young's modulus and Poisson's ratio in cancers in vivo. *Sci Rep* **10**:7266.

[43] Roose T, Chapman SJ, Maini PK (2007) Mathematical models of avascular tumour growth. *SIAM Rev* **49**(2):179–208.

[44] Swabb EA, Wei J, Gullino PM (1974) Diffusion and convection in normal and neoplastic tissues. *Cancer Res* **34**(10):2814–2822.

[45] Levick JR (1987) Flow through interstitium and fibrous matrices. *Q J Exp Physiol* **72**(4):409–437.

[46] Siggers JH, Leungchavaphongse K, Ho CH, Repetto R (2014) Mathematical model of blood and interstitial flow in the liver. *Biomech Model Mechanobiol* **13**(2):363–378.

[47] Barrett KE, Barman SM, Boitano S, Brooks HL (2016) *Ganong's review of medical physiology*. McGraw-Hill, New York.

[48] McGarry MDJ et al (2015) Suitability of poroelastic and viscoelastic mechanical models for MR elastography. *Med Phys* **42**(2):947–957.

[49] Ray LA, Heys JJ (2019) Fluid flow and mass transport in brain tissue. *Fluids* **4**(4):196.

[50] Stylianopoulos T, Jain RK (2013) Combining two strategies to improve perfusion and drug delivery in solid tumors. *Proc Natl Acad Sci USA* **110**(46):18632–18637.

[51] Gillies RJ, Schomack PA, Secomb TW, Raghunand N (1999) Causes and effects of heterogeneous perfusion in tumors. *Neoplasia* **1**(3):197–207.

[52] Forster JC, Harriss-Phillips WM, Douglass MJJ, Bezak E (2017) Review of development of tumor vasculature. *Hypoxia* **5**:21–32.

[53] Deng B, Zhao Z, Kong W, Han C, Shen X, Zhou C (2022) Biological role of matrix stiffness in tumor growth. *J Transl Med* **20**(1):540.

[54] Fuhs T et al (2022) Rigid tumours contain soft cancer cells. *Nat Phys* **18**:1510–1519.

[55] Jain RK, Martin J D, Stylianopoulos T (2014) Role of mechanical forces in tumor growth and therapy. *Annu Rev Biomed Eng* **16**:321–346.

[56] Sipos D, Raposa BL, Freihat O, Simon M, Mekis N, Cornacchione P, Kovács Á (2025) Glioblastoma: clinical presentation, multidisciplinary management, and long-term outcomes. *Cancers* **17**(1):146.

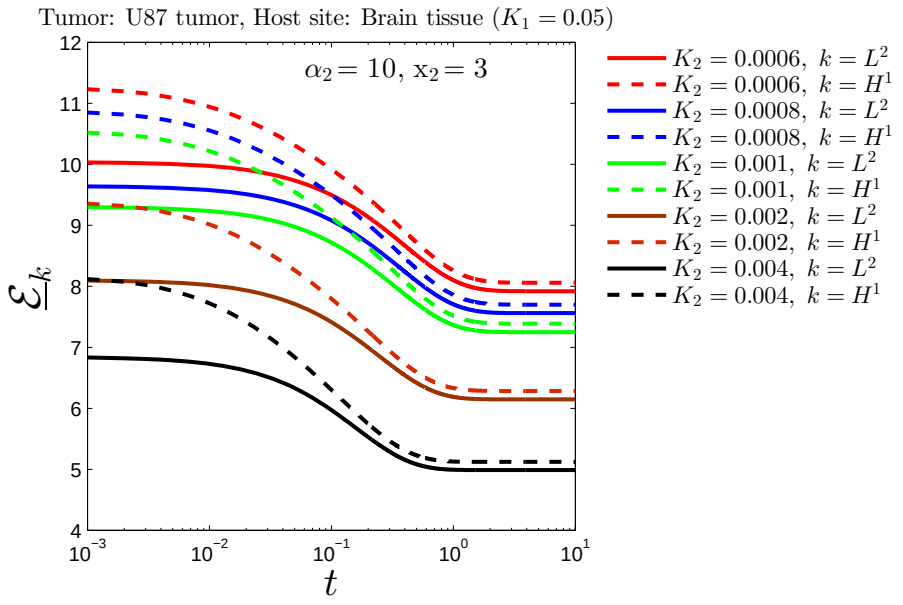

(a)

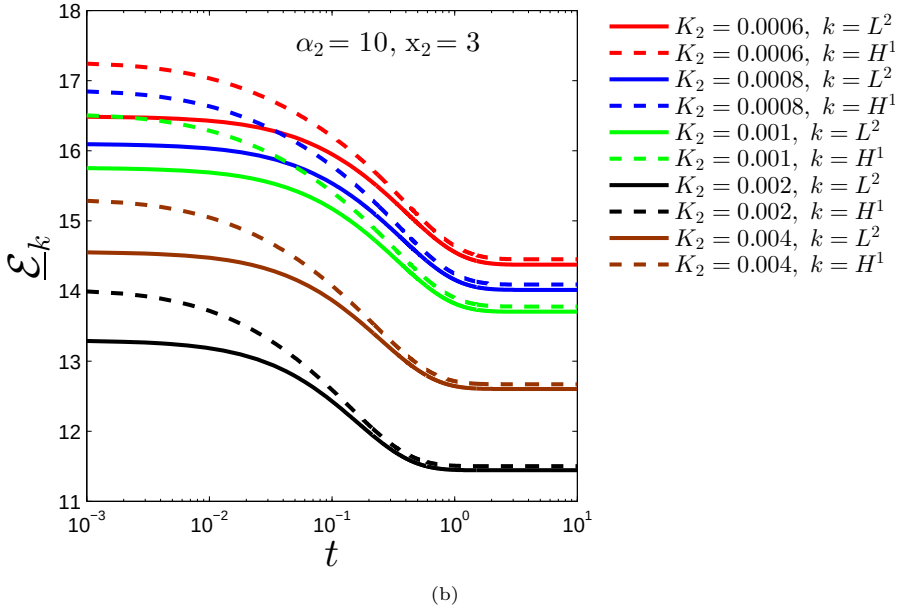

(b)

Fig. 7: (Colour online) The minimum of system energy ($\underline{\mathcal{E}}_k$) versus dimensionless time (t) corresponding to five varieties of U87 tumour (differentiated in term of their hydraulic resistivity values $K_2 = 6,\ 8,\ 10,\ 20,\ 40 \times 10^{-4}$) within brain tissue having hydraulic resistivity either (a) $K_1 = 5 \times 10^{-2}$ or (b) $K_1 = 8 \times 10^{-4}$ when $\alpha_1 \to \infty,\ \alpha_2 = 5,\ \nu_1,\ \nu_2 = 0.45$.

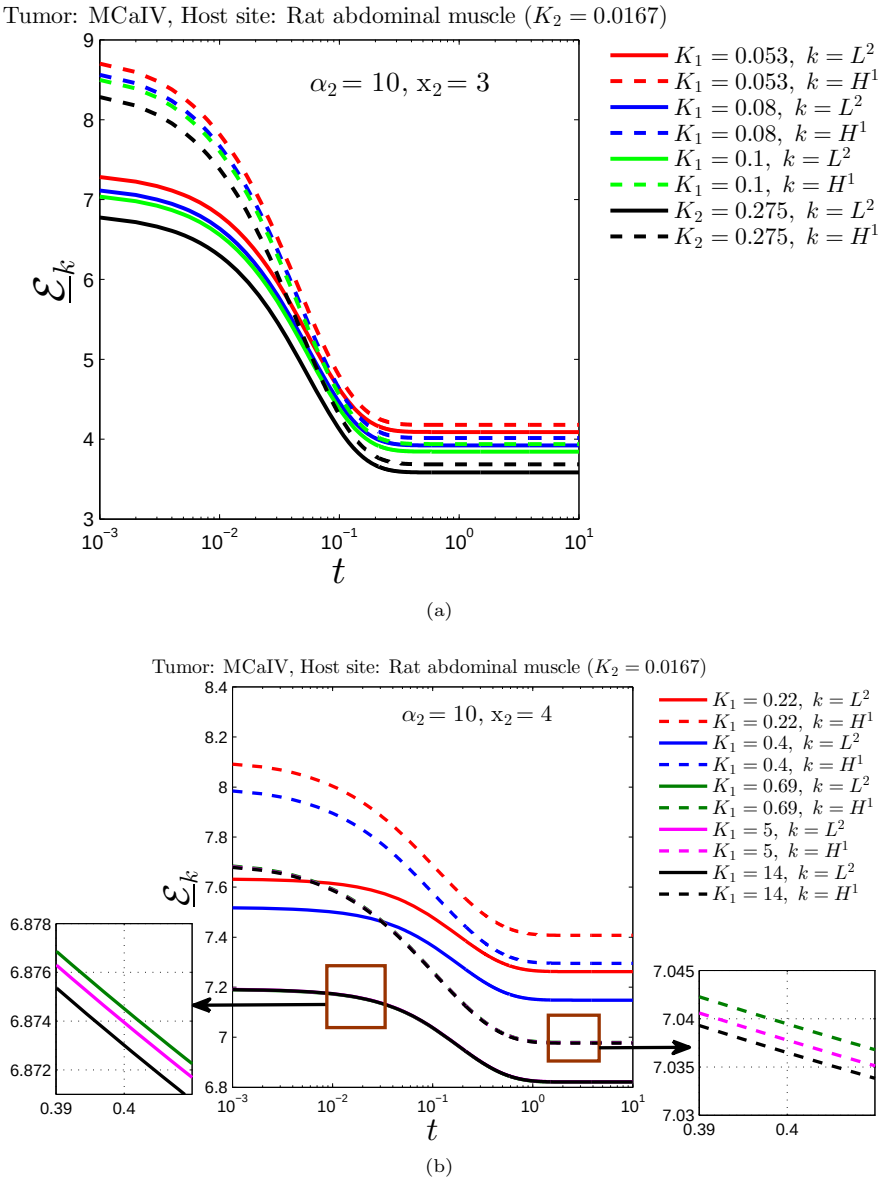

Fig. 8: (Colour online) The minimum of system energy ($\underline{\mathcal{E}}_k$) versus dimensionless time (t) corresponding to an MCaIV tumour with hydraulic resistivity $K_2 = 0.0167$ within Rat abdominal tissue (muscle) having either of the possible hydraulic resistivity combinations (a) $K_1 = 0.053,\ 0.08,\ 0.1,\ 0.275$ and (b) $K_1 = 0.22,\ 0.4,\ 0.69,\ 5,\ 14$ when $\alpha_1 \to \infty,\ \alpha_2 = 5,\ \nu_1,\ \nu_2 = 0.45$.